UCRL 3817

UNIVERSITY OF CALIFORNIA

Radiation Laboratory

TWO-WEEK LOAN COPY

This is a Library Circulating Copy which may be borrowed for two weeks. For a personal retention copy, call Tech. Info. Division, Ext. 5545

A THEORY FOR INDUSTRIAL GAS-LIQUID CHROMATOGRAPHIC COLUMNS

BERKELEY, CALIFORNIA

DISCLAIMER

This document was prepared as an account of work sponsored by the United States Government. While this document is believed to contain correct information, neither the United States Government nor any agency thereof, nor the Regents of the University of California, nor any of their employees, makes any warranty, express or implied, or assumes any legal responsibility for the accuracy, completeness, or usefulness of any information, apparatus, product, or process disclosed, or represents that its use would not infringe privately owned rights. Reference herein to any specific commercial product, process, or service by its trade name, trademark, manufacturer, or otherwise, does not necessarily constitute or imply its endorsement, recommendation, or favoring by the United States Government or any agency thereof, or the Regents of the University of California. The views and opinions of authors expressed herein do not necessarily state or reflect those of the United States Government or any agency thereof or the Regents of the University of California.

UCRL-3817

UNIVERSITY OF CALIFORNIA

Radiation Laboratory
Berkeley, California

Contract No. W-7405-eng-48

A THEORY FOR INDUSTRIAL GAS-LIQUID CHROMATOGRAPHIC COLUMNS

Robert Henry Houston

(Master's Thesis)

April 1958

Printed for the U. S. Atomic Energy Commission

This report was prepared as an account of Government sponsored work. Neither the United States, nor the Commission, nor any person acting on behalf of the Commission:

A. Makes any warranty or representation, express or implied, with respect to the accuracy, completeness, or usefulness of the information contained in this report, or that the use of any information, apparatus, method, or process disclosed in this report may not infringe privately owned rights; or

B. Assumes any liabilities with respect to the use of, or for damages resulting from the use of any information, apparatus, method, or process disclosed in this report.

As used in the above, "person acting on behalf of the Commission" includes any employee or contractor of the Commission to the extent that such employee or contractor prepares, handles or distributes, or provides access to, any information pursuant to his employment or contract with the Commission.

A THEORY FOR INDUSTRIAL GAS-LIQUID CHROMATOGRAPHIC COLUMNS

Contents

Abstract 3

I. Introduction 4

II. Chromatographic Theory 7

III. Apparatus 24

IV. Experimental Procedure 44

V. Data Processing 47

VI. Discussion 77

VII. Conclusion 95

Acknowledgments 98

Appendices 99

- Appendix I. Properties of Experimental Materials 99
- Appendix II. Solution of the Differential Equation of the Chromatographic Model 101
- Appendix III. Thermal-Conductivity-Cell Calibration 109
- Appendix IV. Equilibrium Coefficient Measurements 114
- Appendix V. Sample Calculation for Run Number 116 127
- Appendix VI. G.L.C. Design Problem 132

Nomenclature 162

List of Tables 166

List of Figures 168

Bibliography 170

A THEORY FOR INDUSTRIAL GAS-LIQUID CHROMATOGRAPHIC COLUMNS

Robert Henry Houston

Radiation Laboratory and Department of Chemical Engineering
University of California, Berkeley, California

September 1957

ABSTRACT

A theory of elution chromatography is proposed for the design of large-size chromatographic columns. In this theory, an equilibrium linear isotherm is assumed to be the mass-transfer mechanism, and dispersion of the solute band is attributed to longitudinal diffusion.

The theory was tested with a small-size gas-liquid chromatographic column. The tests were conducted with a column pressure of approximately 100 psig, at various temperatures, and the Reynolds number was varied from 0.2 to 1.8. Results showed that the solute isotherms were dependent chiefly on temperature and slightly on concentration. The isotherms were independent of flow rate.

The effective longitudinal diffusivity was dependent on the flow rate and size of solute sample. The Peclet number decreased from 0.11 to 0.06 with increasing flow (using benzene) and also decreased from 0.16 to 0.06 when sample size was varied from 0.6 to 6.3 micromoles of solute (using toluene).

A THEORY FOR INDUSTRIAL GAS-LIQUID CHROMATOGRAPHIC COLUMNS

I. INTRODUCTION

Origin

Chromatography was originated in method and name by Tswett[1] in 1906. He found that an extract of plant pigments, if placed on a column of solid adsorbent and then eluted or washed into the column with more solvent, would be separated into distinct colored bands. This method of "color writing" Tswett named chromatography. This name is now firmly established even though most current applications of chromatography involve colorless materials.

The work of Tswett went almost unnoticed for 25 years and was then rediscovered by Kuhn, Winterstein, and Lederer.[2] Different modes of operation were developed for this liquid-solid adsorption chromatography in the following year by Tiselius[3] and others. Gas-solid adsorption chromatography was originated by Turner[4] in 1943 and has been extensively developed since then.

Keulmans[5] has given this general definition: "Chromatography is a physical method of separation in which the components to be separated are distributed between two phases, one of these phases constituting a bed of large surface area, the other being a fluid that percolates through the stationary bed."

Partition Chromatography

A new form of chromatography was reported by Martin and Synge[6] in 1941. This process, called liquid-liquid partition chromatography, made use of the distributing or partitioning action of solutes between two immiscible solvents to effect their separation. Briefly, this chromatogram consisted of a stationary aqueous phase uniformly dispersed over a porous solica-gel support, which, in turn, was packed into a glass tube. A moving organic phase was allowed to percolate through the porous solid

bed. The mixture of solutes to be separated was fed to the chromatogram in the mobile phase. The solutes move through the column at different rates because of the different values of their partition coefficients. The order of their emergence at the end of the column and their degrees of purity are dependent to a considerable extent on the relative values of their partition coefficients.

In this same writing, Martin and Synge proposed a gas-liquid partition chromatogram which would consist of a nonvolatile stationary liquid phase and a moving gaseous phase.

In spite of this clear proposal, it was not until 1952 that work with gas-liquid partition chromatography (G.L.C.) was reported. James and Martin[7] had constructed a chromatogram which used as its stationary phase a nonvolatile silicone oil dispersed on kieselguhr. The moving phase was nitrogen gas which transported the solutes through the porous stationway phase. This chromatogram was used to separate a mixture of volatile fatty acids (C_1 to C_{11}) into its components. Detection and quantitative estimation of the solutes leaving the column was accomplished with an automatic recording burette.

Since its inception, G.L.C. has received intense investigation.[8] Its chief attractions and uses are shown in Table I. Application of it to continuous cyclic analysis of process streams in industrial plants has been reported.[9] Commercial units for the separation and purification of gram-size quantities of solutes are now available.

Table I

Features and Common Uses of Gas-Liquid Partition-Chromatography Equipment

Features

1. Simplicity of equipment construction and operation.
2. Easy achievement of very refined separations.
3. Small sample-size requirements.

Uses

1. Identification of components of a volatile liquid or gas mixture.
2. Quantitative estimation of amounts of each solute present.
3. Purification, on a small scale, of volatile organic compounds.

Scope

The purpose of this work is to develop a theory of elution chromatography, using available data on partition coefficients and the flow properties of packed columns, which will make possible the design and prediction of the performance of chromatographic processes on an industrial scale. Because very little has been published on the use and performance of large G.L.C. equipment suitable for industrial application, this writing will use nomenclature and units commonly found in industrial-design practice.

In this work, a chromatographic model is proposed and described mathematically. A solution is obtained for the solute concentration at the column exit, as a function of the volume of the moving phase passed through the column. The model is tested with a laboratory G.L.C. unit. A design method is proposed and illustrated. Also economic factors of the industrial application of G.L.C. are briefly considered.

II. CHROMATOGRAPHIC THEORY

Through the recent years, two basic treatments of the theory of chromatography have been developed. The first considers the chromatographic column as a number of distinct equilibrium stages or plates and leads to the "Plate" theory. The second treats the column as a continuous medium and leads to the "Continuous Column" theory. Though there are three basic modes of operation of chromatograms -- elution development, frontal analysis, and displacement development -- this work will be concerned only with the elution development of the column. In this case, a small quantity of a mixture of solutes is charged to the inlet of the column. The solutes are selectively moved through the column by the mobile phase or eluent. The primary requirement of the eluent is that it be insoluble in the stationary phase, or in any case, be less soluble in the stationary phase than any solute charged to the column.

The Plate Theory

This theory of the chromatographic column was originally developed by Martin and Synge.[6] They reasoned that a chromatographic separation was similar to distillation or extraction and that the chromatographic column could be treated with the methods applied to plate distillation columns. They considered that the column was made up of stages or plates and that a certain height (or length) of column was equivalent to a theoretical plate. This height was named the H.E.T.P. and was defined as a length of the column in which the mean concentration of the solute in the stationary phase is in equilibrium with the solute concentration in the effluent mobile phase. They assumed that the "plate-to-plate" diffusion was negligible and that the partition coefficient was independent of solute concentration and of the presence of other solutes.

Martin and Synge then showed that when a unit mass of solute was placed in the first plate of the column and was eluted by small increments of the mobile phase, the solute concentration in any plate could be expressed by a term of the binomial expansion. With a large number of

plates, i.e. > 100, the binomial distribution closely approximates the Gaussian distribution, and is a function of:

1. The amount of eluant used.
2. The number of theoretical plates.
3. The effective plate volume available to the solute (i.e. equal to the plate's mobile-phase volume plus its stationary-phase volume times the partition coefficient).

Experimental observation showed the interesting fact that the H.E.T.P. of their liquid-liquid partition chromatogram was about 1/500 as large as that of the best distillation or extraction equipment.

The plate theory was amended by James and Martin[7] for its application to gas-liquid partition chromatograms. This modification was necessary to compensate for the expansion of the mobile gas phase as it flows through the column. Two methods were presented for the calculation of the number of plates from experimental elution diagrams, which are plots of solute concentration in the mobile phase at the column exit against the volume of mobile phase used to elute the solute. In their work, 4-ft columns were reported as having 700 to 1200 theoretical plates and an 11-ft column as having 2000 plates.

Glueckauf[10] subsequently revised and elaborated on the mathematical treatment of the plate theory. Where the theory of Martin and Synge described the movement of mobile phase by intermittent flow, Glueckauf used expressions for continuous or uninterrupted flow. The solution obtained in this case expressed the solute concentration as a Poisson distribution, which also approximated a Gaussian distribution in a column with many plates. He also developed an expression for the fractional impurity of one solute in a second after their separation by chromatographic equipment. The fractional impurity is a function of:

1. The molar amounts of solutes being separated.
2. The ratio of their partition coefficients (the separation factor or relative volatility).
3. The number of plates in the column.

Porter, Deal, and Stross[11] have used the plate theory of Martin and Synge to study the influence of solute sample injection on the shape of the elution diagram. The first case that they studied was the injection of a plug of solute having a constant concentration over a definite charging time. The second case was the injection of a certain quantity of solute of a specified initial concentration, but here the concentration fell off exponentially to zero over a certain period of charging time. The first case is often called "plug flow" and the second, "perfect mixing" of the solute with the eluent. Comparison of experimental and theoretical elution diagrams showed that the perfect-mixing solution closely approximated the actual column performance. In their work, the solutes were vaporized in a special chamber of small volume and were then charged to the column when the mobile-phase flow was bypassed through this chamber.

Van Deemter, Zuiderweg, and Klinkenberg[12] have extended the plate theory for the case of a finite volume of feed. Using this volume of feed, the effective volume of a theoretical plate and the square root of the number of plates, they developed expressions for the prediction of the height and width* of the elution diagram. If the volume of feed is gradually reduced to zero, their theory predicts that the width of the peak becomes independent of the feed volume and depends only on the number of plates and the effective plate volume. Other portions of this work will be considered later.

The plate theory, from the above discussion, is seen to be useful in describing the performance of chromatographic columns. The H.E.T.P. is a measure of the efficiency of these columns and is a basis for comparing their performance with that of other separatory methods. The chief shortcoming of the plate theory is that it does not contain within itself

---

*Peak width is defined by these authors as the width, measured at the base of the peak, between tangents constructed through the points of inflection of the elution diagram. See Fig. 15, page 49.

any way of predicting the H.E.T.P. The H.E.T.P. must be evaluated empirically. This fact has led others to find better ways of describing column behavior and of analyzing the factors that influence it.

The Continuous-Column Theory

This theory considers the chromatographic column as a continuous medium and attempts, in principle, to describe the phenomena of chromatography by differential equations. It includes the effects of molecular diffusion, disturbances caused by the bed packing, convective flow, and the rate of mass transfer between the two phases. The prime difficulty of this theory is in describing quantitatively some of these phenomena, especially those connected with the movement of a solute in and around the particles of the bed. This problem has been approached by many authors, each one proposing certain idealizations and simplifications of the physical picture. Some of the factors that must be considered are as follows:

The hydrodynamic velocity gradient. The mobile-phase velocity gradient usually varies over the column section as a result of packing irregularities and the influence of the column wall. Concentration variations result from the uneven velocity distribution. However, mathematical description of the velocity variation is virtually impossible, so a uniform velocity is assumed.

Variation of longitudinal velocity. The chromatographic separations that use a gas or vapor mobile phase, the longitudinal velocity of the moving phase varies along the length of the column. This variation is a result of the expansion of the gas as it traverses the column and may be large if the ratio of inlet pressure to outlet pressure is much different from unity. Most theoretical treatments consider that the velocity gradient affects all molecules, and the assumption of an average velocity is considered permissible.

Constant partition coefficient. The equilibrium relationship of the solute in the two phases is often described adequately by a linear isotherm or a partition coefficient that is independent of solute concentration. However, in some types of chromatography, particularly adsorption chromatography, the nonlinearity is very pronounced. The assumption of linearity simplifies the mathematical treatment considerably.

Axial molecular diffusion. The axial component of molecular diffusion is assumed to be superimposed on the convective flow of the solute and tends to either increase or decrease the rate of solute movement. This effect contributes to the spreading of the band of solute charged to the column and eluted by the moving phase. At low mobile phase velocities, the molecular diffusion may greatly reduce the efficiency of a column, while at high flow rates its influence is negligible.

Eddy diffusion. Dispersion of the solute band, caused by the effects of the column packing, is usually called eddy diffusion. The solute molecules follow a random path through the interparticle spaces. Three effects that contribute to eddy diffusion are:

1. Variations in the legnth of the path followed by the individual solute molecules in their transit of the column.

2. Orientation of portions of this path in other than an axial direction.

3. Variation in molecular velocity which results from changing dimensions of the flow channel (i.e., its expansions and contractions).

These effects cause a variation in the time that solute molecules spend in the column. Because of their nature, they may be treated statistically and are analogous to the eddy diffusion observed in pipes under turbulent flow conditions.

Rate of mass transfer. The rate of mass transfer between the two phases may vary from a very large value at equilibrium conditions to

low-values at nonequilibrium conditions. Here, particularly, description of the phenomena taking place is difficult. Van Deemter et al. have reviewed some of the methods used for analyzing the physical picture.[12] In G.L.C. columns, the dispersion of the liquid phase as a very thin film over the large surface area aids in the attainment of a dynamic equilibrium. Low flow rates also help in the attainment of equilibrium. As the flow rate increases, some of the molecules either fail to enter the stationary phase, thus leading the solute band, or delay in leaving the stationary phase, thus trailing the band. This departure from the ideal, infinite rate of transfer is seen to be a cause of band spreading.

Wilson presented the first continuous column theory of chromatography.[13] He assumed uniform velocities and neglected diffusion and mass-transfer effects. Solutions were presented for both linear and nonlinear isotherms. DeVault gave a more exact solution for the case of the nonlinear isotherm.[14]

Lapidus and Amundson also assumed uniform velocities and included the dispersive effect of longitudinal diffusion on the solute band.[15] Using a linear isotherm, they presented solutions for both the case of infinite rate of mass transfer (equilibrium) and the case of a finite rate of mass transfer (nonequilibrium). Though the mathematics of this latter case are quite involved, this solution represents the most general case for the linear isotherm.

Giddings and Eyring have presented a similar solution except that they neglect longitudinal diffusion.[16] Van Deemter et al. have simplified the nonequilibrium solution of Lapidus and Amundson to a Gaussian expression and have obtained a relation between the diffusion and mass transfer terms of the continuous-column theory and the H.E.T.P. of the plate theory.[12]

The complex problem involving nonlinear isotherms and finite rates of mass transfer has been studies by Thonas,[17] Amundson,[18] Goldstein,[19] Hiester and Vermeulen,[20] and others.

Description of the Chromatographic Model

The chromatographic model, to be developed now, uses certain portions of the equilibrium solution given by Lapidus and Amundson.[15] In their theoretical development, they consider a column of infinite length for which they obtain a solution that describes the solute concentration in the mobile phase at any time or place in the column. Their general solution is for a column feed, the composition of which is a known function of time.

The mathematical model, used for the chromatographic theory here, differs from the above as seen from the following.

Dimensions. The model consists of a column of length L and of circular cross-sectional area A. It is assumed to be uniformly packed with particles, whose average size is d_p and whose fractional void volume is α. (For a G.L.C. column, the solid particles are assumed to be uniformly impregnated with the stationary liquid phase.)

Velocity profile. The hydrodynamic interstitial velocity is assumed to be a constant value, V. The empty-column superficial velocity, V_o, is the product of the void-volume fraction and the interstitial velocity.

Equilibrium relationship. The concentration profile over any cross-section is uniform in either phase. The stationary-phase concentration, n, and the mobile-phase concentration, c, are assumed to be in equilibrium at all times and places through the relationship $n = kc$, where k is the partition coefficient and is a constant.

Longitudinal diffusion. In this model, the spreading of the solute band is assumed to be caused only by the longitudinal diffusion. As was shown earlier, the diffusivity is of two types, molecular and eddy, and both decrease the sharpness of the band by varying the residence times of the solute molecules.

1. The molecular diffusivity, D_M, of the solute molecule in the mobile phase is estimated from the methods summarized by Wilke and Lee.[21] It is independent of the interstitial velocity. The effect of molecular diffusion of the solute will be significant only at low velocities.

2. The eddy diffusivity, E, will be defined by use of the dimensionless Peclet group,

$$Pe \equiv \frac{Vd_p}{E} .$$

Studies of the value of the Peclet group in recent years have shown that it is approximately 1 to 2 in the turbulent flow region -- and about 0.5 for laminar flow. These values were obtained for liquids flowing through regular packings.

In their recent work, van Deemter et al. report that the values of the Peclet number for G.L.C. columns vary from 0.1 to 1 and larger.[12] This variation seems dependent upon regularity of the packing material. The lower values of the Peclet number were observed in beds having the smaller average particle sizes (i.e. Pe = 0.125 for $d_p \cong 30$ microns) and, usually, larger void-volume fractions.

The longitudinal diffusivity, D, is then assumed to be the sum of the molecular and eddy diffusivities:

$$D = D_M + \frac{Vd_p}{Pe} .$$

This assumption has been substantiated by the work of Klinkenberg and Sjenitzer.[22]

Initial bed conditions. The column is assumed to be initially free of solute with the mobile-phase flow established.

Solute injection. At an arbitrary time, t = 0, a unit mass of solute is assumed to be charged uniformly to the initial surface of the column packing. The time interval required for this charging is considered to be, in the limit, of zero duration, and the resulting volumetric concentration of the two phases at the plane containing the solute is infinitely large. This method of solute charging is analogous to the impulsive

function of mechanics or electricity. For this model, the charging function is defined

$$\int_0^\infty \delta\ (t)\ dt \equiv 1$$

for a unit molar mass being fed to a column of unit cross section. This charging function is simulated to a good degree in G.L.C. apparatus where a small quantity of solute is charged either directly on the column packing with a syringe, or is carrier into the column by a small volume of the mobile phase.

Material balance. A material balance of the solute, taken over an incremental length of the column, yields the equation

$$\alpha V \frac{\partial c}{\partial z} - \alpha D \frac{\partial^2 c}{\partial z^2} + \alpha \frac{\partial c}{\partial t} + \frac{\partial n}{\partial t} = 0 , \qquad (1)$$

where z is the distance into the bed. From the equilibrium relationship

$$n = kc$$

and with algebraic manipulations, Eq. (1) may be simplified to

$$D \frac{\partial^2 c}{\partial z^2} = V \frac{\partial c}{\partial z} + \frac{\partial c}{\partial \tau} , \qquad (2)$$

where $\tau = t/\gamma$

and $\gamma = 1 + k/\alpha$.

Boundary conditions. The model of Lapidus and Amundson was an infinite column with only the initial conditions specified. The inlet and outlet conditions for a finite column have been discussed by several writers. The conditions used for the solution of Eq. (2) are those proposed by Danckwerts[23] and elaborated upon by Wehner and Wilhelm.[24] At the column inlet, (z = 0), for $\tau > 0$, we have

$$\delta\ (\tau) = Vc - D \frac{\partial c}{\partial z} , \qquad (3)$$

where $\delta(\tau)$ has the units of lb-mole/ft^2-min by definition. At the column exit, $(z = L)$, for $\tau > 0$, we have

$$\frac{\partial c}{\partial z} = 0 . \tag{4}$$

The initial $(\tau = 0)$ solute-free condition of the bed is described for $0 \leq z \leq L$ by

$$c = 0 . \tag{5}$$

<u>Solution of the differential equation.</u> The detailed solution of Eqs. (2) to (5) is given in Appendix II. If we use the dimensionless parameters

$$s \equiv \frac{VL}{D}$$

and

$$\eta \equiv \frac{t}{\gamma} \frac{D}{L^2} = \frac{\tau D}{L^2} ,$$

the solution for the mobile-phase concentration at the column exit, C, is

$$CL = \frac{4}{\sqrt{\pi\eta}} \left(\frac{s^2\eta}{4} + \frac{1}{2}\right) e^{-\frac{(1-s\eta)^2}{4\eta}} - 2\left(\frac{s^3\eta}{4} + s + \frac{s^2}{4}\right) e^{s} \operatorname{erfc}\left(\frac{1 + s\eta}{2\sqrt{\eta}}\right). \tag{6}$$

The quantity CL is also dimensionless by definition. If the quantity of solute fed to the column or the column cross-sectional area differ from their arbitrarily assigned unit value, the left hand of Eq. (6) should be

$$\frac{CLA}{\omega}$$

where ω is the number of moles fed to the column of area A.

Equation (6) is easily evaluated numerically by the use of the parameters s and $s\eta$ where

$$s\eta = \frac{t}{\gamma} \frac{V}{L} = \frac{t}{(\alpha + k)} \frac{V_o}{L} .$$

A value is assigned to s and then $s\eta$ is varied from 0 through 1.0 to the value were CL becomes negligible. The plot of a CL ordinate and an $s\eta$

abscissa represents the column-elution diagram. The experimental counterpart is seen to be a concentration or millivolt ordinate and a time abscissa. A family of theoretical curves, for various s values, is shown in Figs. 1 and 2. Because the theoretical volumetric concentration of the feed is infinite, the value of CL will increase to infinity as s approaches infinity. The theoretical elution diagrams may be normalized by use of the peak maximum concentration, $(CL)_{max}$, to give the ratio

$$\frac{CL}{(CL)_{max}} = \frac{C}{C_{max}} .$$

Families of normalized elution diagrams are shown in Figs. 3 and 4.

<u>The s parameter</u>. The dimensionless s parameter (VL/D) may be considered as a measure of column efficiency. The larger the s value for a given column operation, the more highly resolved are the solute peaks emerging at the column exit. If the molecular diffusivity is neglected, the s parameter may be written

$$s \cong Pe \frac{L}{d_p} . \qquad (7)$$

From this expression, it would seem that the s value could be increased in two ways, namely, by increasing the length of the column and by decreasing the average particle size. The first effect is usually observed but in G.L.C., where long columns are very feasible, the increase in the s value is not necessarily linear with L because the lengthening of the bed produces other effects such as increased pressure drop and the resulting velocity variation along the bed length.

The variation of column efficiency with average particle size has been studies by Keulmans.[5] He reports that, with the irregular packing materials in common G.L.C. use, a decrease in the particle size results in approximately an equivalent decrease in the Peclet number.

One of the most effective ways to increase the resolution of the column is to increase its length. Fredricks and Brooks report the use of a 50-foot G.L.C. column packed with a crushed, diatomaceous-earth firebrick.[25]

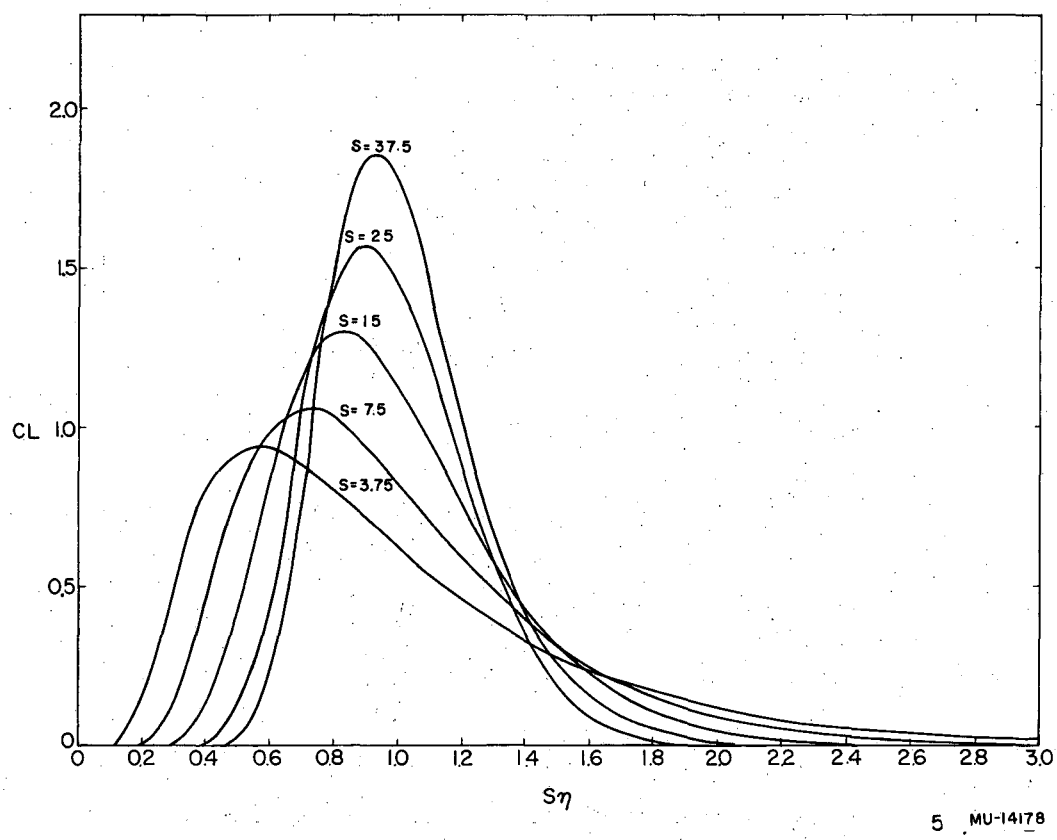

Fig. 1. Theoretical elution diagram for low values of the s-parameter.

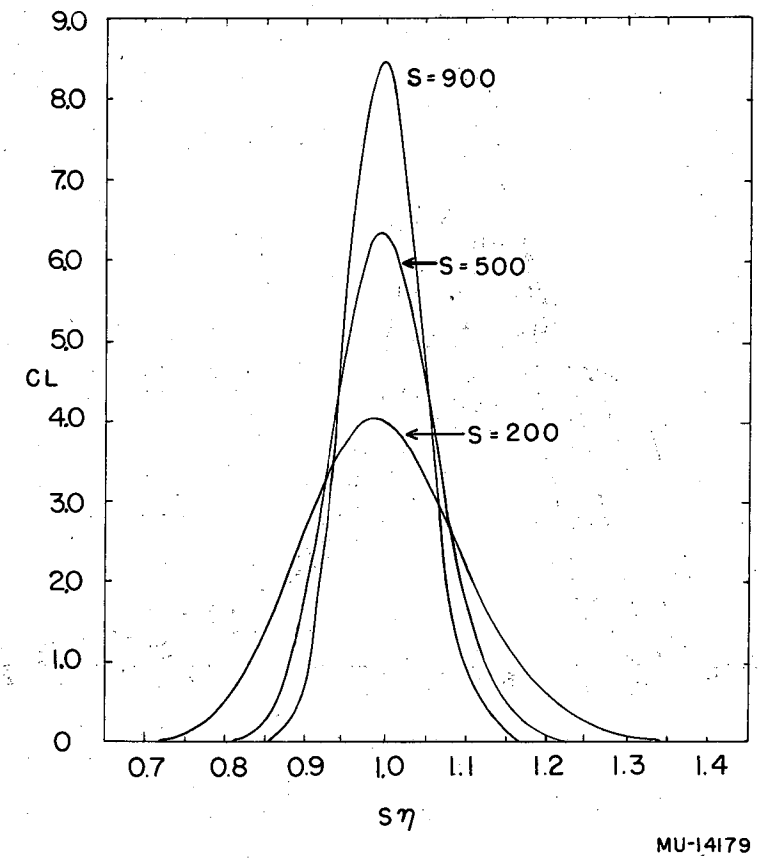

Fig. 2. Theoretical elution diagrams for high values of the s-parameter.

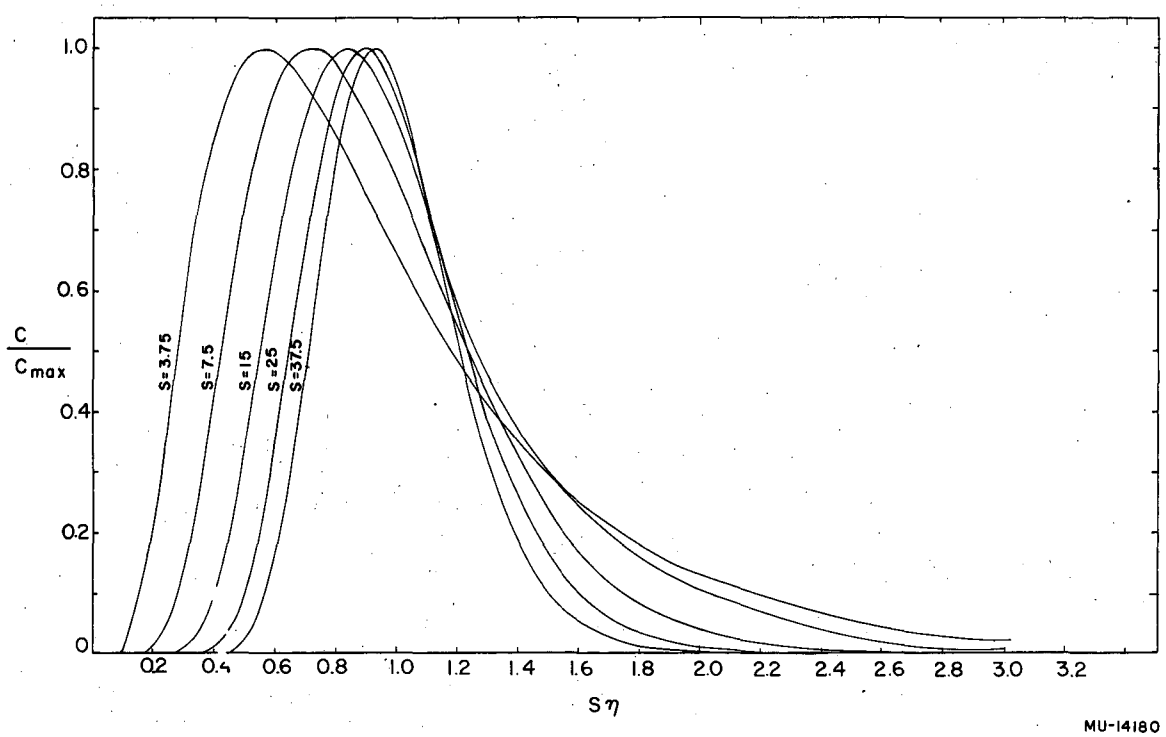

Fig. 3. Theoretical elution diagrams (normalized) for low values of the s-parameter.

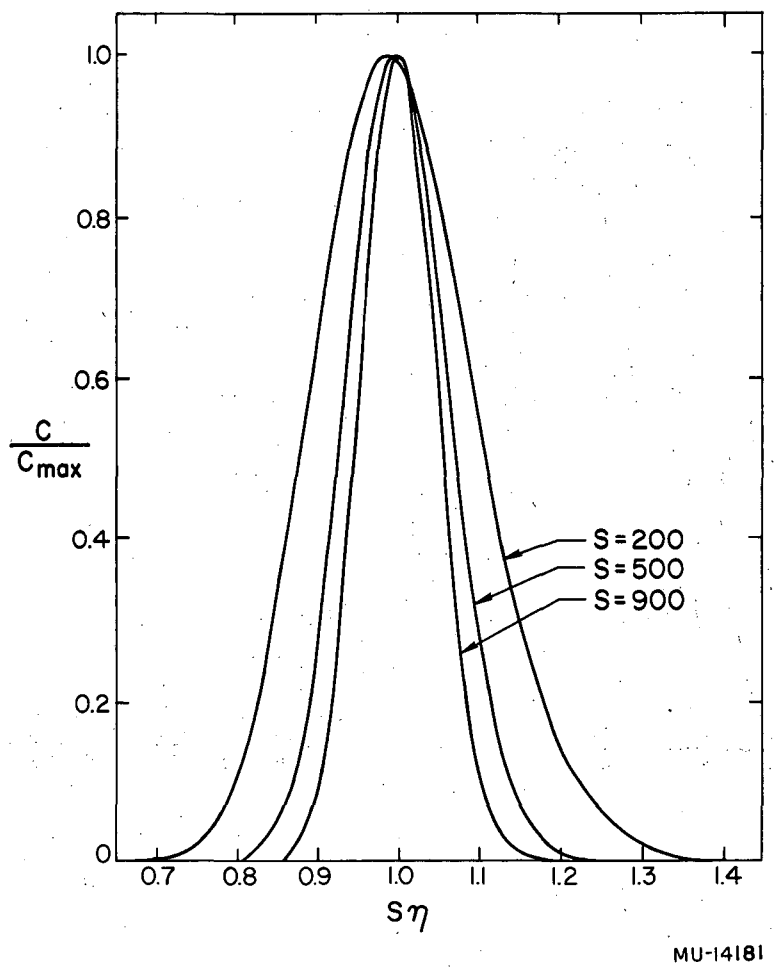

Fig. 4. Theoretical elution diagrams (normalized) for high values of the s-parameter.

The $s\eta$ parameter. The dimensionless $s\eta$ parameter $[tV_o/(\alpha+k)L]$ may be considered as a measure of the solute residence time. For a given solute and column operation, $s\eta$ is dependent only on the time. In most chromatographic work, where $s > 100$, the solute peak emerges when the value of $s\eta$ is approximately 1 (i.e. for $s = 100$, $[s\eta]_p = 0.97$). So the time of peak emergence is essentially independent of the s parameter.

Then it follows that if we know the dimensions and the operating conditions of the column, the times of peak emergence may be calculated from the partition coefficients.

From thermodynamic considerations discussed later, the partition coefficient is shown to be dependent upon the nature of the solute-solvent system and the temperature of column operation. As the temperature increases, the value of the partition coefficient will decrease.

Test Program for the Chromatographic Model

Because the chromatographic model assumes a constant partition coefficient or linear isotherm, a type of chromatography that approaches this ideality was needed for the testing program. Because the basic mechanism of partition chromatography, the distribution of the solute between the two phases, is a solution effect and is not dependent on the number of adsorption sites etc., the partition coefficient is often almost linear. Gas-liquid partition chromatography was chosen over its liquid-liquid counterpart because of:

1. The current interest in G.L.C.
2. The higher mobile-phase velocities which speed up the time of analysis.
3. The need for evaluation of this process for industrial application.

A test program, using G.L.C. equipment, was established to compare the actual column performance with that predicted by the chromatographic theory.

The partition coefficient. The $s\eta$ parameter embodies the partition coefficient and should be free from the influence of the longitudinal diffusivity in G.L.C. equipment as mentioned earlier. The partition coefficient should also be independent of the mobile-phase flow rate and of the nature of the packing. It is sensitive to temperature change and is, of course, a property of the solute-solvent system. For a given solute and column length, the product of the peak time (t_p) and superficial velocity (V_o) should be a constant. If this constant is multiplied by the column area and corrected for pressure effects, the retention volume of the solute is obtained. This method is used extensively as a means of reporting the partition coefficient in the literature. The retention volume also will vary from solute to solute, will decrease with a temperature rise, and should be independent of the quantity of solute charged to the column, if, of course, the equilibrium equation is to be truly linear.

The longitudinal diffusivity. The s parameter contains the longitudinal diffusivity term. As shown in Eq. (7), for a given packing and length of column, the s value should be approximately constant, except at low values of the moving-phase velocity. Also, the s value should be independent of changes in column temperature, pressure, and the solutes in the column. The quantity of solute charged to the column should not influence the s value, either.

The experimental program. The experimental program, of necessity, was limited to the testing of the most important aspects of the theory and included the following studies:

1. Flow variation over a 7-fold variation of the Reynolds number.
2. Temperature variation over a 19°C range, from 87°C to 106°C.
3. Solute variation using acetone, benzene, and toluene.
4. Solute charge variation over an 8-fold range of sample size, using toluene.

III. APPARATUS

The schematic diagram of the G.L.C. apparatus is shown in Fig. 5. The overall arrangement, shown in Fig. 6, is typical of most G.L.C. equipment in its component parts. The usual laboratory G.L.C. unit, however, is much more compact and often portable.

The G.L.C. unit used in this work was constructed to operate at a column-inlet pressure of 100 psig, rather than at lower pressures, in order to minimize the relative pressure drop and, therefore, the variation of the longitudinal velocity along the length of the column. Description and construction detail of the component parts of the G.L.C. unit follow.

Column

The G.L.C. column was made of 3/8-in. o.d. copper tubing, the wall thickness of which was 0.035 in. Fig. 7 shows the detail of the column construction. The column was attached to the sample-injection valve assembly, Fig. 8, with 1/2-in. R-L fittings.* Neoprene rubber gaskets were used in these fittings.

Three copper-constantan thermocouples (No. 24 gage) were inserted into the column by means of modified R-L fittings. A cylindrical molding of Epon was cast about the wires. When the resin had hardened, it was machined to fit into an enlarged 3/8-in. R-L fitting, as shown in Fig. 9. The thermocouples were inserted into the empty column and, after they were centered, the column was packed.

Column Packing

Solid support. The porous solid support for the stationary phase was crushed insulation brick, Johns-Manville Sil-O-Cel C-22. The bricks were

---

*University of California Radiation Laboratory standard tubing fittings for pressure and vacuum uses.

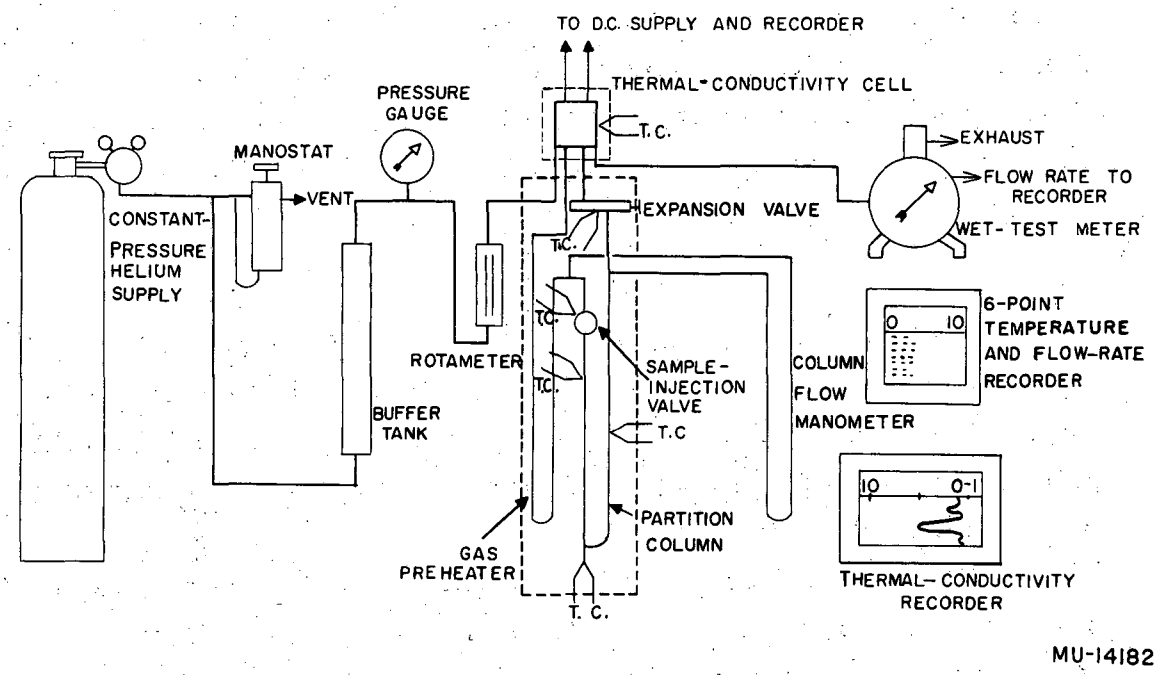

Fig. 5. Over-all G.L.C. equipment schematic diagram.

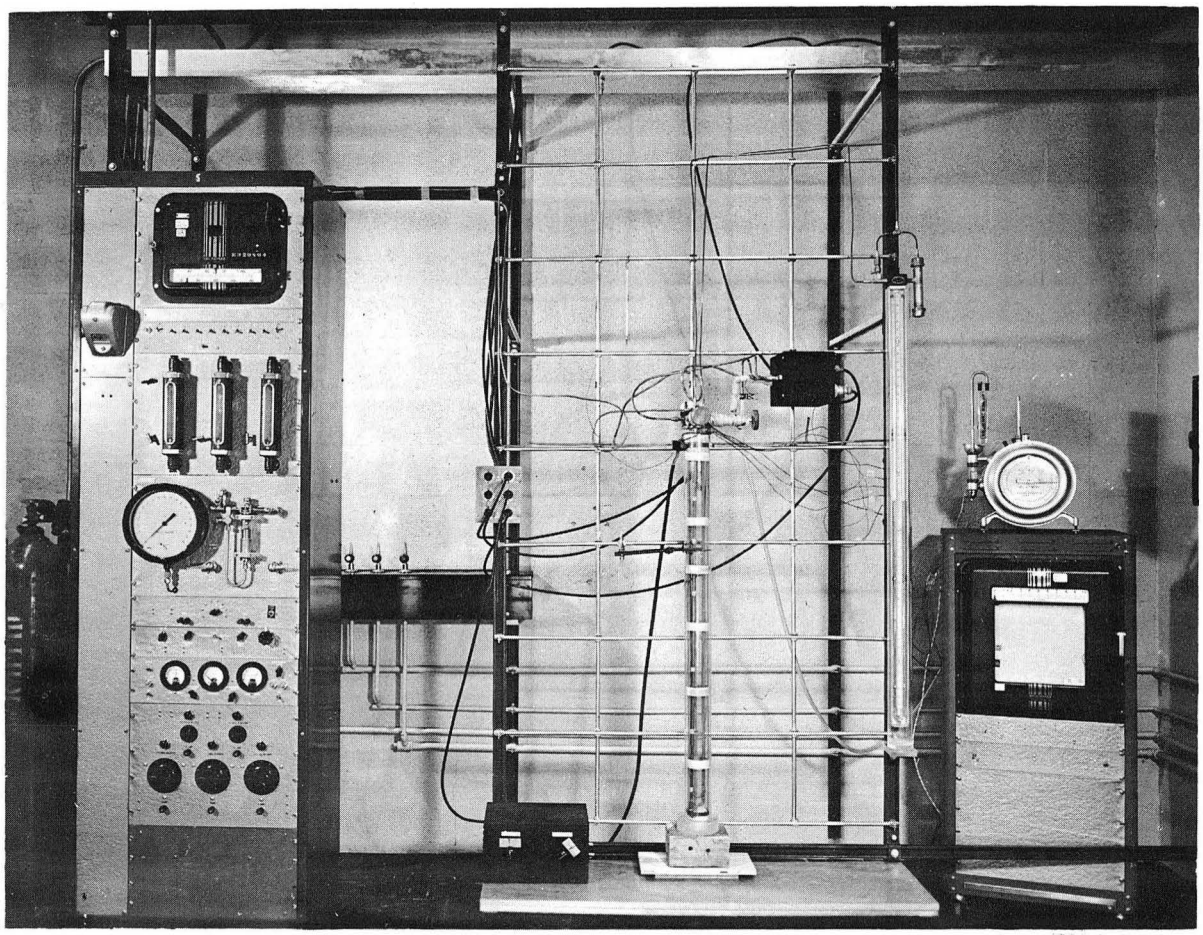

ZN-1783

Fig. 6. G.L.C. equipment arrangement.

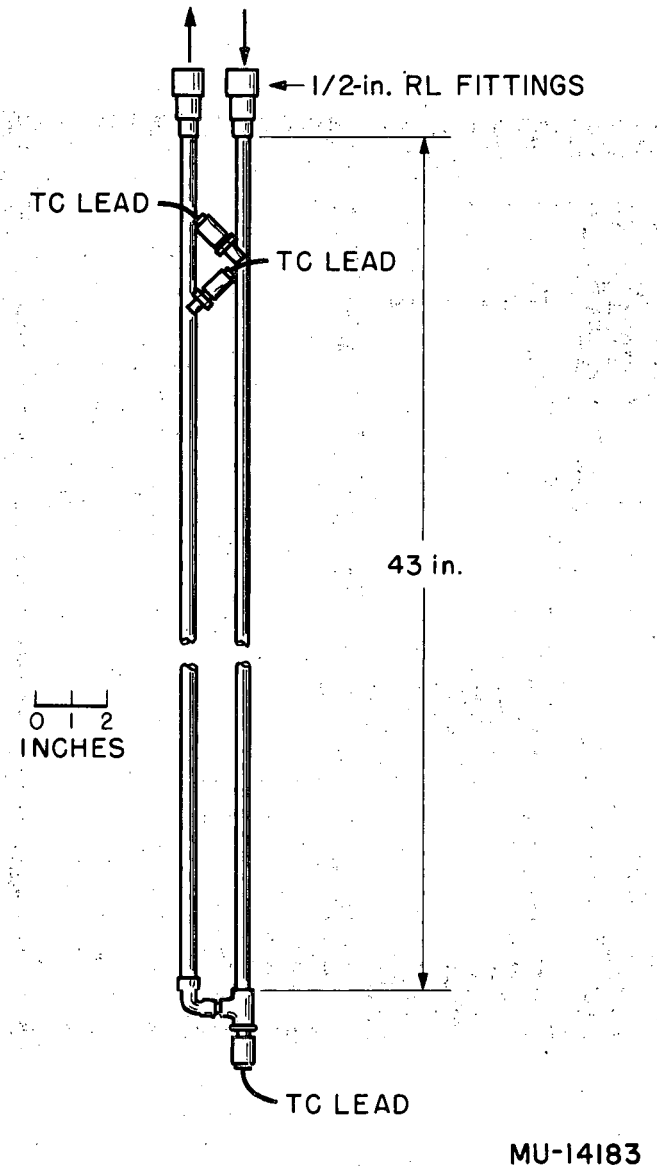

Fig. 7. Construction detail of G.L.C. column.

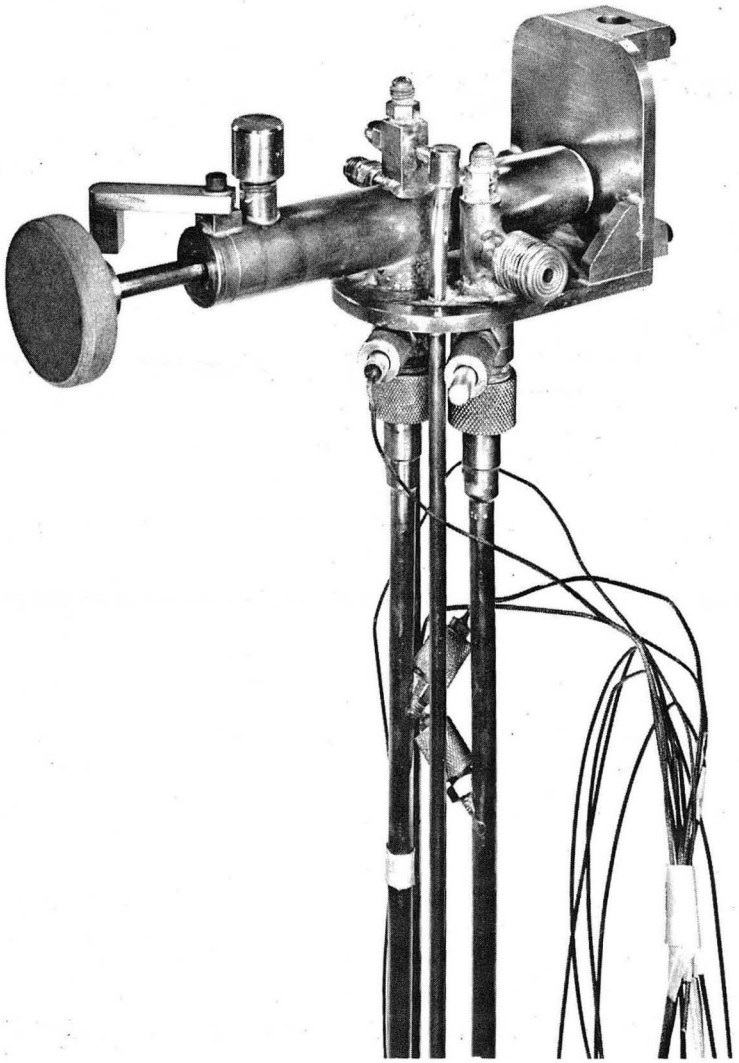

ZN-1781

Fig. 8. Sample-injection valve and upper column assembly.

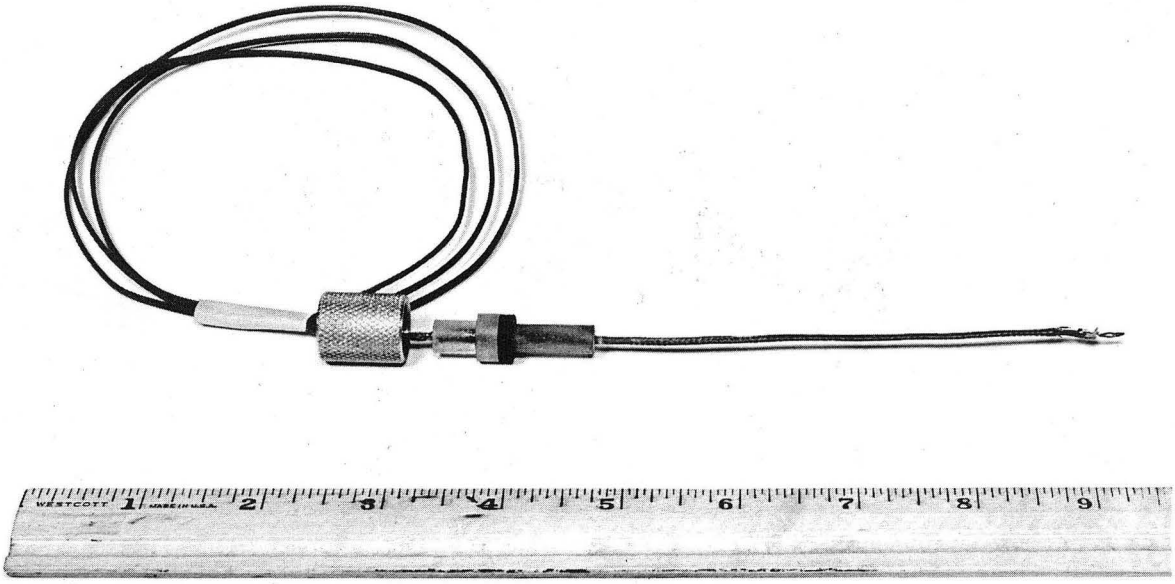

ZN-1780

Fig. 9. Internal thermocouple construction for G.L.C. column.

pulverized in a laboratory jaw crusher and then sized on a series of vibrating sieves. Portions of 30 to 40 mesh, 40 to 50 mesh, and 50 to 60 mesh (U.S. Standard Sieve Series) screenings were blended together into the packing mixture. The weight ratios of these portions were 2:2:1 respectively. The brick was treated with 6 N HCl and washed with distilled water. The water washing removed some fines adhering to the larger particles. The support was removed from the final washing by filtration and dried at 130°C.

Solvent phase. The stationary solvent phase used for this work was a methyl-phenyl silicone oil, Dow Corning DC-550. It was selected as a typical G.L.C. solvent because it has excellent thermal stability, low volatility, and a viscosity of 18 centipoises at 100°C. The manufacturer reports* a calculated molecular weight of 1756. The volatility of DC-550 is expressed as an evaporation loss rate. Approximately 3% by weight is lost over a 24-hr period when the solvent is held at 250°C. Various physical properties of this solvent and other materials used in this work are summarized in Appendix I.

Mixing of solvent and support. The column packing was prepared by mixing 35.5 g of DC-550 dissolved in 300 ml of acetone with 87.5 g of the sized solid support to form a slurry. The acetone was evaporated over a steam plate under continuous stirring. The last traces of acetone were removed by drying at 130°C. The packing material was a free-flowing powder, which was blended with 9.5 g of a similar material prepared at an earlier time. The final composition of the packing material was

Stationary liquid phase	28.8 wt %
Solid support	71.2 wt % ,

which corresponds to 40.5 parts liquid per 100 parts solid.

The mean particle size, calculated from the range of sieve sizes, was 0.0165 in. (420μ).

---

* Private communication

Packing operation. The column was packed by slowly feeding the powder to the column while vibrating it with an eccentric cam on the shaft of an electric motor. The material was free-flowing and packed easily to a density of 37.2 lbs/ft^3 or 0.597 g/cc. The volumes occupied by the various phases are shown in Table II.

Table II

Properties of DC-550--C-22 Firebrick Packing

Volume of empty column	108	cc
Weight of solid support	46	g
True density of solid support*	2.07	g/cc
True volume of solid support	22.2	cc
Weight of solvent liquid	18.6	g
Density of solvent liquid	1.07	g/cc
Volume of solvent liquid	17.3	cc
Volume of voids (by difference)	68.5	cc
Volume fraction - support	0.205	
Volume fraction - solvent	0.160	
Volume fraction - void	0.635	

* Determined by P-V measurements.

Mobile Gas Phase

Hydrogen, helium, and nitrogen are the gases most generally used for the G.L.C. mobile phase. Where a thermal conductivity cell is used for solute detection, either hydrogen or helium is preferred to nitrogen because their high thermal conductivities simplify calibration and interpretation of the detector data. Helium was favored over hydrogen because of its inertness. Though the molecular diffusivities of the volatile solutes are much higher in helium (and hydrogen) than in nitrogen, use of high column pressures and avoidance of very low interstitial velocities nullified this effect.

Grade A helium, which is oil- and moisture-free and has a purity of about 99.9%, was used for this work. It was supplied in cylinders pressurized to 2000 psig.

Sample-Injection Valve

The sample-injection valve was designed to receive solute samples at room temperature and pressure and to charge these samples into the mobile gas phase entering the column at 100 psig. Figure 8 shows the sample-injection valve with its bracket for mounting it on the lattice work.

The sample-injection valve was constructed of brass stock. The interior detail of the valve and the method of charging are shown in Fig. 10. With the valve in the LOADING position, the solute sample was placed on the bed section. The bed section consisted of a 1/2-in-diam. hole in the 1-in. cylindrical valve block that was filled to a depth of about 5/8-in. with column-packing material. This packing was retained in the valve by a 100-mesh screen support soldered to the valve block as shown. Micropipettes were used to measure the quantity of solute charged to the bed section.

As soon as the solute had been ejected from the micropipette, the valve was moved to the EQUILIBRATING position for solute heating and equilibration with the bed section. After a 2 to 5 min period, depending on the size of sample and the solute volatility, the valve was then moved to the CHARGING position, placing the bed section in the flow of the mobile phase.

Pressure differences between the column and the bed section caused a minor flow fluctuation when the bed section was moved into the gas-flow path. This fluctuation was sensed by the reference side of the thermal-conductivity cell, making a "start" mark or initiating pulse on the elution diagram of the recorder.

When the solute was placed in the bed section, a small volume of air would also "contaminate" the bed section. This air, when charged to

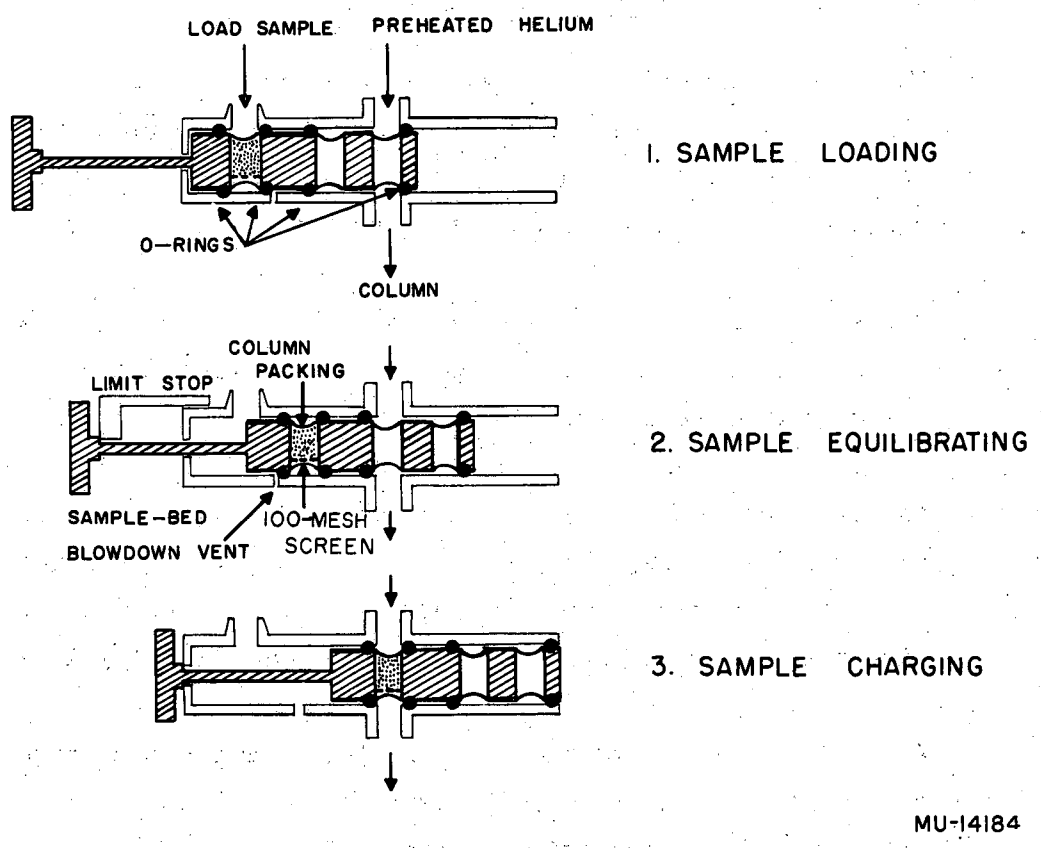

Fig. 10. Sample-injection valve.

the column, was only slightly, if at all, retained by the stationary phase, so it moved through the column at approximately the same velocity as that of the mobile phase. This air was sensed by the thermal-conductivity cell upon emergence from the column. The time of its emergence was used to calculate a measured void fraction.

Silicone-rubber O-rings were used for pressure seals in the sample-injection valve. A small hole was drilled in the side* of the valve outer cylinder to vent the pressure of the bed section as it is moved to the LOADING position. This early "blowdown" prevented upset of the sample bed as it was moved under the injection port on top of the valve.

The EQUILIBRATING stop was manually positioned to limit the travel of the valve as it moved into the EQUILIBRATING position. This stop prevented premature charging of the solute.

The sample-injection valve was heated with a glass-fiber, electric heating tape which was 1/2 in. wide and 2 ft long. The tape was wrapped around the outer cylinder of the valve. Current was supplied to the tape from a Variac at the control panel.

Gas Preheater

The helium gas, from the reference side of the thermal conductivity cell, was heated to column temperature by passing through a preheater tube inside the column heater. This tube was made from 1/4-in. o.d. copper tubing having a 0.030-in. wall thickness. The length of the preheater tube was 90-in. The gas, on leaving the preheater, passed directly into the sample-injection valve. A portion of the preheater tube is seen in Fig. 8.

---

* The "blowdown" hole is shown in Fig. 10 on the bottom of the valve only to illustrate its relative location.

Thermal-Conductivity Cell

A thermal conductivity (T.C.) cell was used to detect the presence of solutes in the mobile phase leaving the column. A Gow Mac* model 9285 T.C. cell, used in this work, was mounted in a 6-in. cubic equipment box. The box was fitted with the necessary gas inlet and outlet connections. Electrical connections for the T.C. cell and the heater were mounted on the opposite side of the box. The T.C. cell is shown in Fig. 11 with the heating tape, normally wrapped around the cell block, removed. The box was insulated with glass-fiber pads and was mounted on the lattice framework. The cell was connected to the expansion valve with a short length of 1/4-in. o.d. insulated tubing.

The flow channel through the T.C. cell was designed so that the cell would rapidly detect changes in the thermal conductivity of the gas flowing through it. Details of the cell's construction are shown in Fig. 12. The filaments, reported by the manufacturer to be tungsten helices, are located between the two legs of the flow channel to reduce the cell's sensitivity to flow changes. Flow sensitivity has been considered by Dimbat et al.[26] and Keulmans[5] and was measured for this cell as reported in Appendix III.

As seen in Fig. 12, this T.C. cell has four filaments, two in each flow channel. These filaments constitute the four resistances in the T.C.-cell bridge circuit shown in Fig. 13. One of the flow channels served as the pure-helium reference cell, R. High pressure helium from the control panel passed through this channel to the gas preheater. The other channel was the sampling cell, S, which monitored the thermal conductivity of the effluent gas from the column. The unbalance output of the bridge circuit, caused by solutes in the sample cell, was fed through a voltage-divider circuit to a Brown self-balancing, recording potentiometer. This instrument has a range of -1 to +10 mv.

The filaments of the T.C. cell were heated by a 120 ma current supplied to the bridge circuit by the 6 v dc battery.

Calibration of the T.C. cell is reported in Appendix III.

---

* Gow Mac Instrument Company, Madison, New Jersey.

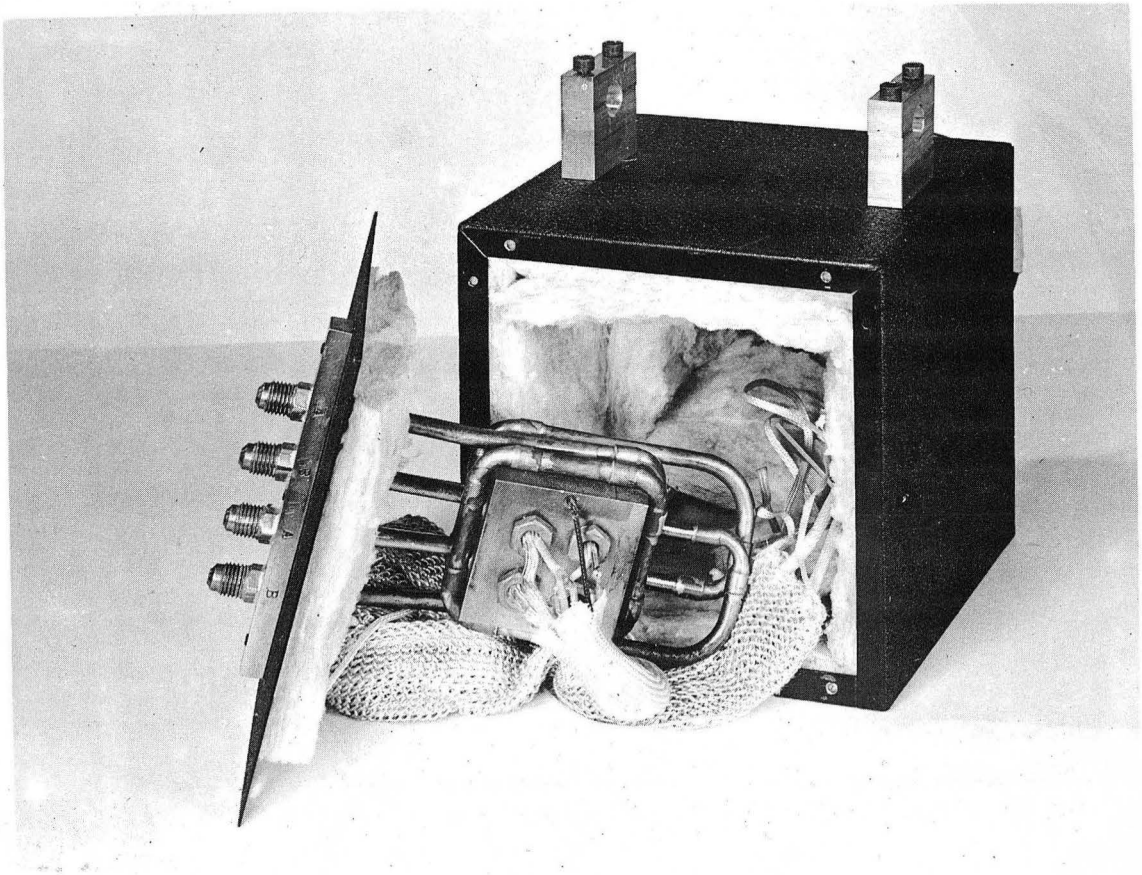

ZN-1778

Fig. 11. Thermal conductivity cell and controlled temperature box.

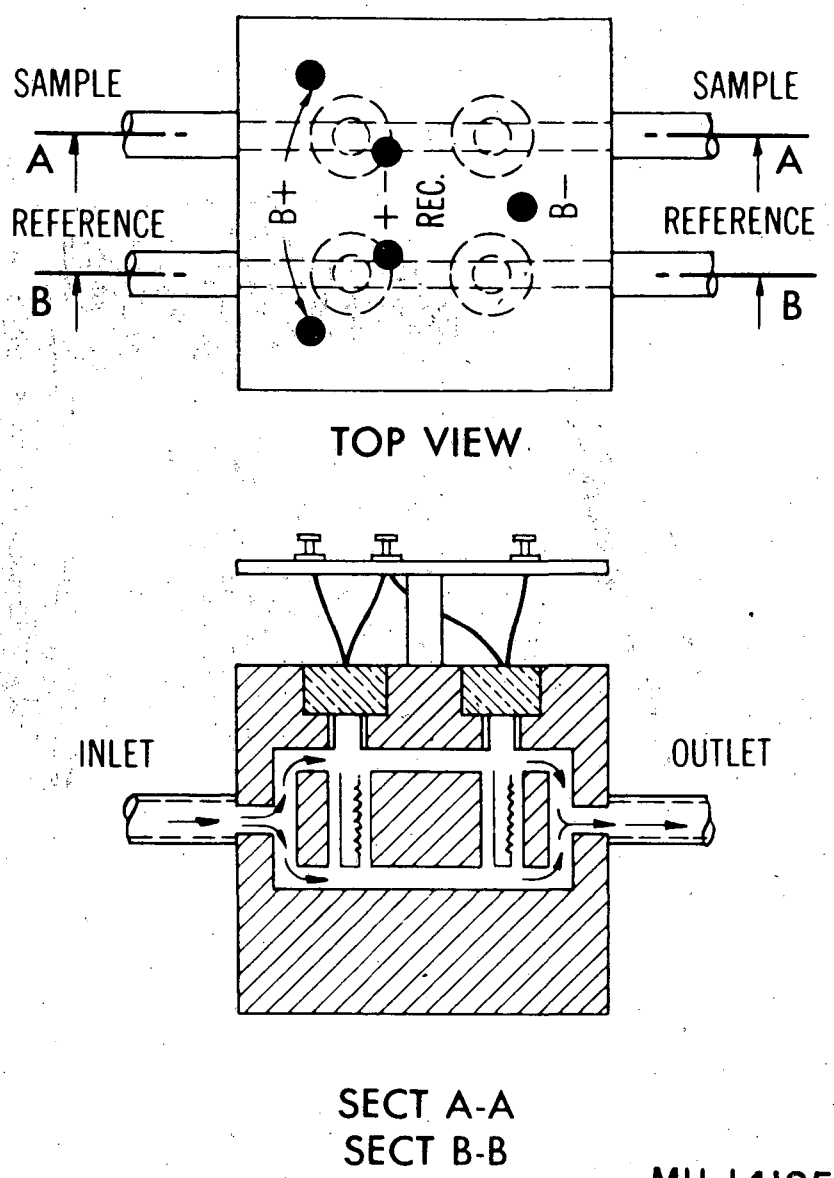

Fig. 12. Internal construction of the T.C. cell.

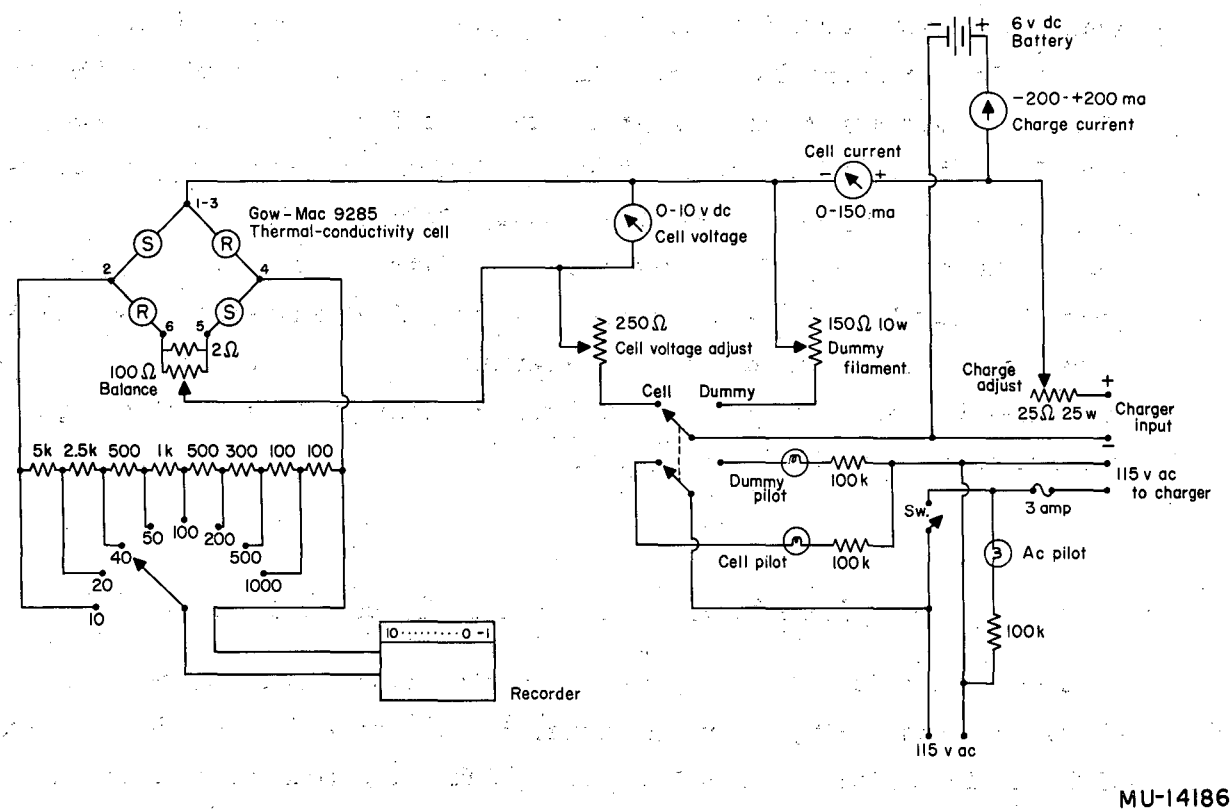

Fig. 13. Thermal-conductivity cell schematic diagram.

Pressure Regulation and Measurement

High-pressure helium was expanded with a 2-stage regulator to a pressure a few pounds greater than the column-inlet pressure. A Manostat Corporation No. 6 manostat was used to maintain a constant column-inlet pressure. An Ascroft No. 1082A laboratory test gauge measured the inlet pressure. This precision bourdon-tube gage had a range of 0 to 100 psig.

The pressure drop across the column was measured with a Meriam 50-in. mercury manometer. The pressure taps for this U-tube manometer were located at the column inlet and outlet on the sample-injection valve. Connections to the manometer were through 3/16-in. o.d. copper tubing. The low pressure leg of the manometer was fitted with a mercury trap to prevent contamination of the column in case of a manometer blowout. A bypass valve was mounted across the manometer lines for use during rapid pressure changes of the G.L.C. system. A Lucite tube served as a protective shield around the manometer.

Heaters, Temperature Measurement, and Control

Column. The column was electrically heated with a Corning E-C coated glass tube (No. 9340). This 2.56-in. i.d., 4-ft.-long tube was coated with an electrically conducting film which had a room temperature resistance of approximately 60 ohms. The coating was subdivided into 3 sections by 4 metallic electrodes. Electrical connections were made with copper bands fastened around the tube at the electrodes. The column heater was connected to the controlled voltage supply at the control panel. Two variable resistors were placed in parallel with the two lower sections of the heating tube to obtain a uniform temperature along the length of the heated section. The maximum allowable operating temperature of the tube is 350°C.

An iron-constantan thermocouple was attached to the midpoint of the upper section of the heating tube with adhesive glass tape. A strip of this tape was also used to insulate the thermocouple from direct

contact with the surface of the tube. The thermocouple was connected to a Leeds and Northrup Micromax temperature indicator-controller which had a temperature range of 0 to 200°C. The desired temperature was manually set on this instrument, which, in turn, would apply one or the other of two voltages. The values of these voltages were set by Variacs on the control panel. One voltage was of high enough value to cause rapid heating of the column to and above the desired temperature. The second voltage was low enough that the column would cool below the set temperature. This system would control the column temperature to ± 0.5°C at 100°C.

The column-heating tube was enclosed in a 3-in. i.d. Pyrex tube 4 ft. long. The outer tube was wrapped with glass-fiber insulation and asbestos paper.

Other units. The T.C. cell, the sample-injection valve, and the expansion valve (described below) were all heated with glass-fiber electric tapes, which received their heating currents from Variacs mounted on the control panel. Fairly constant temperatures were maintained by thermal equilibrium of these units with their surroundings. Minor temperature fluctuations resulted from variation of the mobile-phase flow rate, the ambient temperature, and the line voltage.

Temperature recordings. Temperatures were measured at six points with copper-constantan thermocouples. The voltages of the thermocouple circuits were measured and recorded by a Leeds and Northrup 6-point recording potentiometer. This self-balancing recorder printed one point every 4 sec. The reference junctions of the thermocouple circuits were immersed in an ice bath.

Three thermocouples measured the inlet, midpoint, and outlet temperatures of the G.L.C. column. Approximate locations of these thermocouples are shown in Fig. 7. The thermocouple junction was about 3 inches beyond the resin-plug fitting. A fourth thermocouple measured the sample-injection valve temperature and was located just below the valve (see Fig. 8). The fifth and sixth thermocouples measured the temperatures of the T.C. cell and the expansion valve.

Expansion Valve

A needle valve was used to regulate the mobile-phase flow rate and expand the gas to approximately atmospheric pressure. Originally, a Hoke brass needle valve (No. 304) was tried but found unsuitable for close control of the mobile-phase flow rate. A needle valve with a long, tapered valve stem (Ohio Chemical and Surgical Equipment Company No. 304-5208-800) was found to give very precise flow control.

Two locations of the expansion valve were tried. The first and preferred location was at the exit of the column as shown in Figs. 5 and 14. After leaving the column, the mobile phase was expanded and then passed through the T.C. cell and wet-test meter. The second location was at the exit of the T.C. cell. The height, shape, and time of emergence of the solute peaks were not significantly affected by the location of the expansion valve. However, condensation of the solute in an unheated expansion valve did distort the shape of the solute peak. An electric, glass-fiber heating tape was wrapped around the valve to heat it, thus preventing solute condensation in the valve.

Flow Rate Measurement

In this G.L.C. equipment, there were three methods whereby the flow rate of the mobile gas phase could be measured. Three Fisher-Porter flow meters (Tri-Flat Tubes No. 08-F 1/16-12-4/70, 02-F 1/8-12-5/70, and 02-F 1/8-25-5/70) were mounted on the control panel to give an approximate measure of the helium flow rate. The meters were manifolded to be used separately or in parallel and had a flow-rate range of 12 to 2500 cc/min of air at one atmosphere and 70°F when used separately.

The 50-in. mercury manometer measured the pressure difference between the column inlet and outlet. This pressure drop was an excellent indicator of the flow rate and was quantity observed when setting the gas flow rate with the expansion valve.

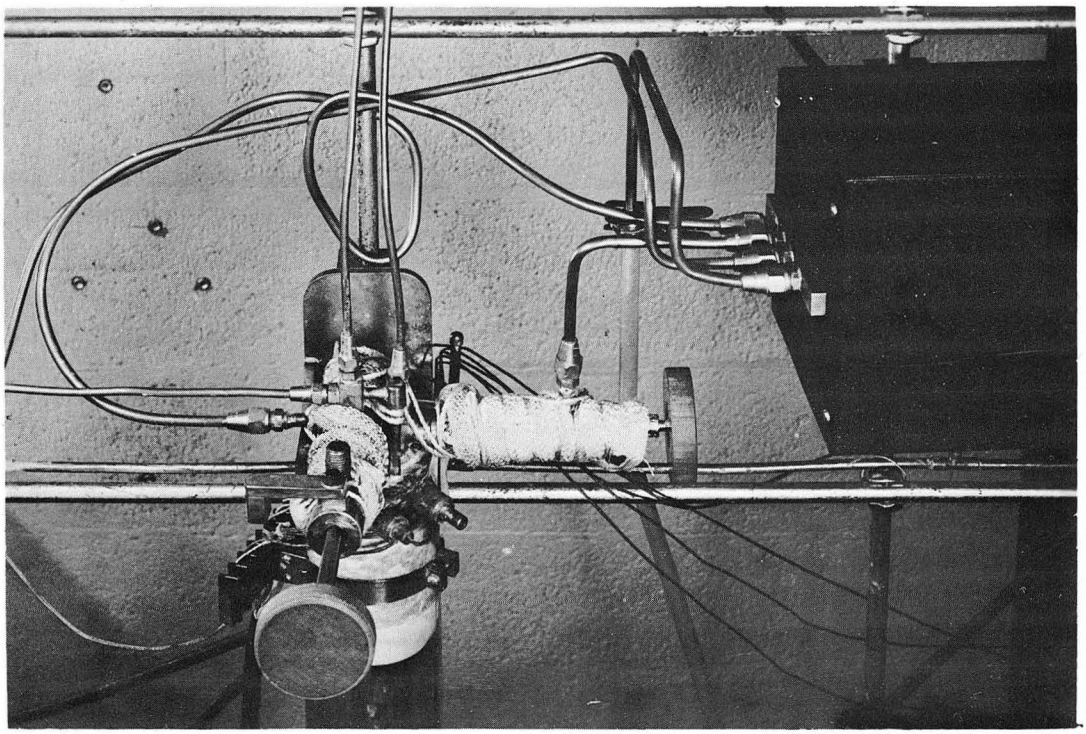

ZN-1785

Fig. 14. Operational arrangement of sample-injection valve, expansion valve, and T.C. cell. (Fiberglass insulation removed.)

A 0.1 cubic-foot wet test meter (W.T.M.) of the Precision Scientific Company (Model 3110) was used to measure the mobile-phase flow rate. The W.T.M. was fitted with an electric contactor at the zero index of the dial. As the dial pointer passed the index, the contact was closed, activating a solenoid pen mounted on the 6-point recorder. This pen drew a continuous trace on the recorder chart and made a pulse along this trace line for each 0.1 ft^3 of mobile phase passing through the W.T.M. The conditions of measurement were approximately room temperature and atmospheric pressure.

Buffer Vessel

A 0.29-ft^3 buffer vessel was placed on the high-pressure side of the column, as shown in Fig. 5, to improve the base-line stability of the T.C. cell circuit. Minor flow fluctuations from the rotameters and the manostat were damped by the presence of this vessel in the gas system. It was constructed from a 45-in. section of 4-in. brass tube.

IV. EXPERIMENTAL PROCEDURE

The G.L.C. apparatus was simply operated. The basic procedure used in the experimental work was as follows:

Preliminary Steps

Temperature equilibration. Prior to operation, the column and the auxiliary components had to be heated to the desired operating temperature and, with the T.C. cell, expansion valve, and sample injection valve, the Variacs had to be set to maintain a thermal equilibrium at these temperatures. Temperatures of the various units were continuously available from the 6-point recorder.

Mobile-phase flow. As the equipment approached operating temperatures, the helium flow was started. The cylinder regulator was set to supply gas at a few pounds pressure higher than the operating inlet pressure. The manostat was adjusted to give fine pressure regulation at the desired column-inlet pressure. The flow rate through the column was regulated with the expansion valve and the pressure drop through the column was used as the approximate measure of the flow while the expansion valve was adjusted. The contactor circuit on the wet-test meter was energized to record the actual flow rate on the 6-point recorder chart.

Thermal-conductivity cell. The 6-v dc supply was applied to the T.C. cell circuit and the cell current adjusted to 120 ma. As the filaments reached operating temperatures small adjustments of the cell current were necessary. The T.C. cell recorder was energized and the chart motor started. The bridge circuit was then balanced to give a zero reading on the recorder.

Operation

Final adjustments. Just prior to charging the solutes, the flow rate, temperatures, cell current, and T. C. bridge circuit were checked and adjusted, if necessary. Barometric pressure, room temperature, etc. were recorded.

Sample charging. The solutes were charged to the column in the manner described under the Sample-Injection Valve in the preceding chapter.

Run operation. Once the solute is charged, the operation of the run continued without any further participation of the operator unless:

1. The attenuation of the bridge circuit has to be varied to give a good display of the solute-elution diagrams.
2. The operational program calls for variation of flow or temperature as the run progresses, in order to expedite the run.

As the solutes are eluted from the column, they pass through the T.C. cell which detects their "contamination" of the helium mobile phase. The unbalance of the bridge circuit is displayed on the recorder chart and from this, the progress of the run is known if the components of the sample charged to the column are known.

The effluent from the column may either be passed directly to the wet-test meter for flow measurement or diverted through a cold trap in order to separate the solute from the mobile phase and then passed on to the wet-test meter.

Variations

Operating conditions. At the completion of a run, changes in the flow rate are easily made by adjustment of the expansion valve. Temperature changes require a longer period for equilibration. As a rule, the temperature of the T.C. cell and the expansion valve are set higher than

the column temperature. Then, the column temperature may be varied without changing the temperatures of the T. C. cell or expansion valve.

Repetitive operation. The column may be charged again as soon as the last solute is eluted from the column. Where the nature of the sample is known, sample charging may precede the elution of all the solutes if it is timed so as to preclude overlapping of the elution diagrams of the two runs.

Shut-down Operations

The G.L.C. apparatus is removed from operation in the reverse of its preparation for operation. The bridge supply voltage is shut off, the flow is stopped, and the heaters are turned off. The system pressure is rapidly vented by opening the manometer bypass valve and the expansion valve.

For continued day to day operation, the column pressure is not vented and the heater units are left in operation.

During shut-down periods, the 6 v dc battery was connected to the charger and received a small amount of current, i.e. 150 to 200 ma, to sustain the charge of the battery.

V. DATA PROCESSING

Data Collection

During the course of the experimental program, some 135 G.L.C. runs were made. The data acquired from 123 of these runs were used to analyze the performance of the G.L.C. unit. Distributions of these 123 runs among the different solutes, column temperatures, and flow rates is shown in Table III. The experimental data were obtained from the traces of the thermal-conductivity-cell recorder and the temperature-flow-rate recorder.

Thermal Conductivity Trace

During the progress of the chromatographic run, the unbalance of the T.C. cell circuit was recorded by the -1 to 10 mv recorder as a function of time. The time base, in turn, was a function of the volume of eluting gas passed through the column. For each run, the following events were displayed along the time base.

"Start" mark or initiating pulse. This mark was recorded at the instant the sample-injection valve was moved to the CHARGING position. It indicated the zero time of each run, and the time of each subsequent event was obtained by measurement from this reference.

Air peak. When a solute sample was loaded on the bed section of the sample valve, a small quantity of air was captured in this section. This air contaminant would be charged with the solute sample. Because air is not significantly soluble in the stationary solvent phase, it would pass through the column at the same rate as the helium gas and would be the first material detected by the T.C. cell. The time of emergence of the point of maximum air concentration was designated the air peak time, t_{pa}.

Table III

Solute, temperature and flow-rate distribution of G.L.C. experimental runs

Solute	Approx. temp. (°C)	Approximate pressure drop through column In. Hg (inlet pressure of 100 psig)								
		40	35	30	25	20	15	10	5	Total
	88	2	-	2	-	2	1	1	1	9
Benzene	98	6	3	3	3	2	2	2	1	22
	105	2	-	3	-	2	2	1	1	11
	88	1	-	2	-	1	1	1	-	6
Toluene	98	4	3	3	2	9*	2	1	1	25
	105	2	-	2	-	2	1	1	-	8
	88	2	-	2	-	2	1	1	1	9
Acetone	98	2	3	3	2	3	2	3	2	20
	105	2	-	2	-	4	2	2	1	13

*Includes 7 runs with sample size variation.

Solute peak. For a run with only one solute, the next and final event that was obtained was emergence of the solute from the column. The time of maximum solute concentration, the peak time, t_p, was used to calculate the partition coefficient. The width of the solute, relative to the peak time, was used to calculate the longitudinal diffusivity. The shape of the peak served as a qualitative indication of the linearity of the partition coefficient.

The method of van Deemter et al.[12] was adopted for the measurement of peak width, (Fig. 15). Tangents were drawn through the points of inflection of the leading and trailing edges of the peak. The initial time, t_i, and the final time, t_f, were at the points where the leading edge and trailing tangents, respectively, intersect the recorder base line (usually zero mv). The peak width, t_w, measured in time units, was the difference between the final and initial times.

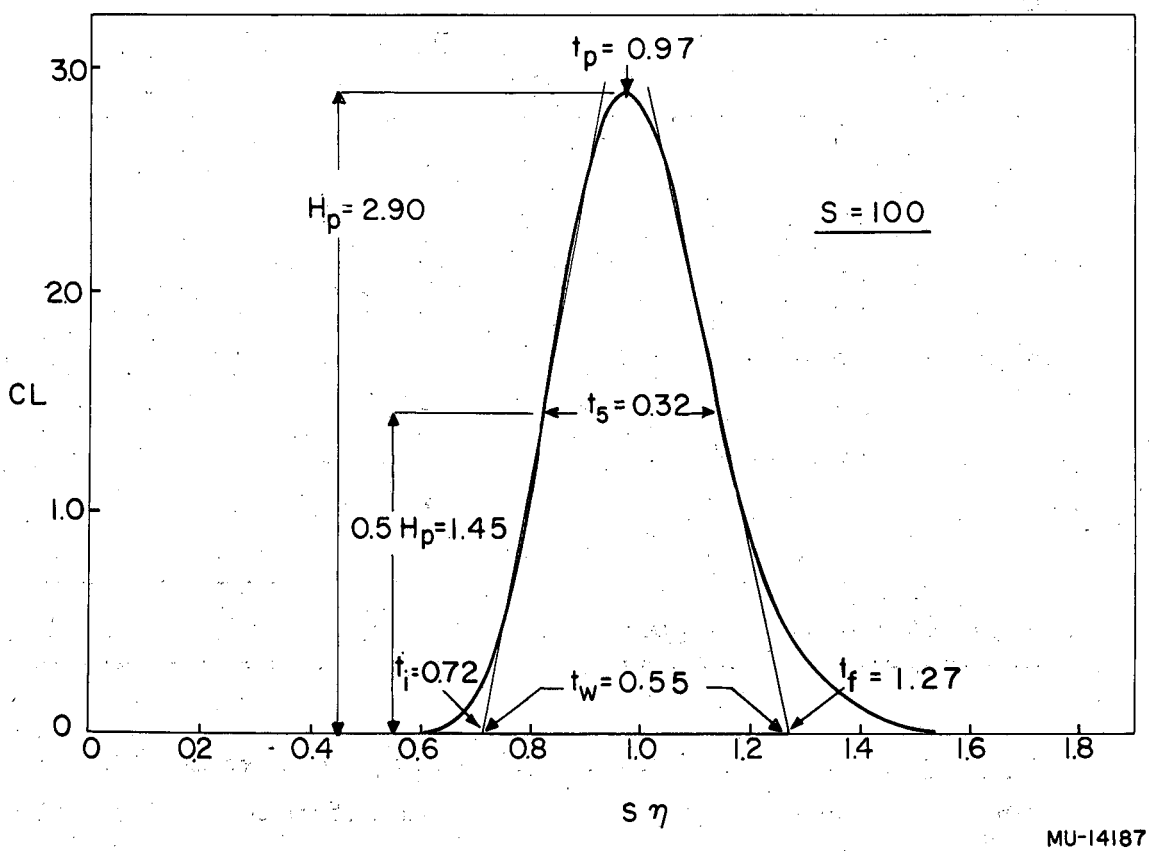

Fig. 15. Method of elution-peak characterization.

The maximum solute concentration, observed on the elution diagram, was termed the peak height, H_p, and was used to calculate the maximum solute mobile-phase concentration observed at the column exit as well as the approximate molar quantity of solute emerging from the column. For this latter calculation, the product of the peak height, H_p, and the peak width at half the value of maximum concentration, t_5, was an approximate value of the peak area. This area was multiplied by the T.C. cell and flow coefficients to give the approximate number of micromoles in the solute peak. Figure 15a shows a superposition of experimental elution diagrams for the three solutes on a common timebase. Also, Fig. 15a shows the equivalent theoretical elution diagrams for each of the solutes as determined from the experimental partition coefficients and values of the s parameter. The asymmetry of the peaks is apparent in this figure.

Temperature and Flow Rate Trace

The voltages of the thermocouple circuits and the marks for the 0.1 ft^3 volumes of eluting gas were recorded on the chart of the 6-point recorder as a function of time. Utilization of these experimental data was as follows:

Column temperatures. The voltages of the three column thermocouples were converted to their equivalent temperatures. As shown earlier in Fig. 7, the thermocouples were located in the packed section of the column near the entrance, at the midpoint and near the exit. The measured temperatures -- i.e. the inlet, T_i; the midpoint, T_m; and the outlet, T_o -- were averaged to yield a column temperature, T_{col}, which was used in calculating the column gas flow rate and other properties. The spread in the three column temperatures was usually about 1 to 2°C. Occasionally it was greater than 3°C.

Miscellaneous temperatures. The temperatures indicated by the three other thermocouples were used to ascertain when the T.C. cell, the sample-

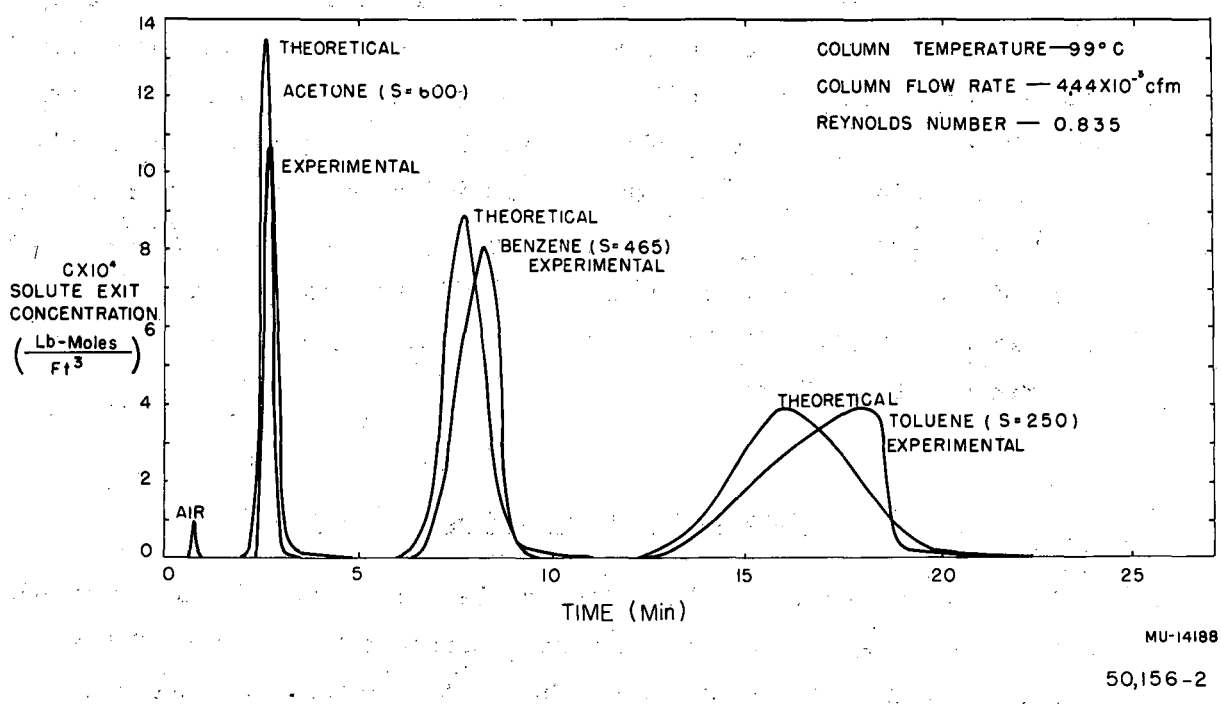

Fig. 15a. Superimposed experimental and theoretical elution diagrams.

injection valve, and the expansion valve were in thermal equilibrium with their surroundings. These units were held at an approximately constant temperature during all the runs. These measured temperatures were not used in the analysis of the data.

Mobile-phase flow rate. The marks recorded by the solenoid pen on the 6-point recorder gave an indication of the time required for the flow of 0.1 ft^3 of helium through the W.T.M. The measured volume of helium was assumed to be saturated with water vapor and to be at the temperature of the water in the W.T.M. The pressure in the W.T.M. during these measurements was the prevailing barometric pressure. This flow rate, Q, was calculated for a time unit of one minute.

Miscellaneous Operating Data

Most other data, used in this work, did not vary significantly with time but were pertinent to column operation. These quantities, their units of measure, and the frequency of observations are shown in Table IV.

Table IV

Miscellaneous Experimental Data

Quantity	Unit	Remarks
Barometric pressure	in. Hg	Recorded once or twice a day.
W.T.M. temperature Room temperature	°F °C	Recorded once or twice a day from mercury thermometers.
T.C. cell current	ma	Manually set to 120 ma and checked every 2 to 3 runs.
Column inlet pressure (p_i)	psig	Manually set to 100 psig and checked every 2 to 3 runs.
Column pressure drop (Δ_p)	in. Hg	Measured at start, peak time (when possible), and at end of each run.
Rotameter (F_1, F_2, or F_3)	Arbitrary scale units	Recorded for each run.
Solute and sample size	λ (0.001 ml)	Recorded at each run. Sample sizes for each solute were usually constant.

Data Correlation

In order to test the ability of the chromatographic theory to predict actual column performance, methods were developed for correlating theoretical predictions with experimental observations. The longitudinal diffusivity parameter, s, and the partition coefficient parameter, $s\eta$, are correlated to the peak width and the peak time in the following manner:

The s Correlation

Fig. 15 illustrates the method used in this work for characterizing the solute peaks. The peak width, t_w, or $(s\eta)_w$, is divided into the peak time, t_p or $(s\eta)_p$, to give a dimensionless ratio which is an expression of the relative peak width. This ratio, for the theoretical elution diagrams, is proportional to the square root of the s value. The s value, conversely, may be written

$$s = 2 \left[4 \frac{(s\eta)_p}{(s\eta)_w} \right]^2 \tag{8}$$

for $s > 100$. The s parameter is likewise related to the initial and final $s\eta$ values

$$s = 2 \left[4 \frac{(s\eta)_i}{(s\eta)_w} + 2 \right]^2 = 2 \left[4 \frac{(s\eta)_f}{(s\eta)_{N_w}} - 2 \right]^2 . \tag{9}$$

These relationships follow from the fact that at the higher s values the theoretical elution diagrams closely approximate the normal-error curve.

When experimental data are applied to Eq. (8) or (9), it is possible to assign an s value to the peaks. Because the experimental elution diagrams seldom have exactly the same shape as the theoretical curves, two s values may be assigned. The first is obtained from the measured peak time and width,

$$s \doteq 2 \left[4 \frac{t_p}{t_w} \right]^2 . \tag{10}$$

The second s value is obtained from the peak's initial or final time and its width,

$$s_i \equiv 2\left[4\frac{t_i}{t_w} + 2\right]^2$$

and

$$s_f \equiv 2\left[4\frac{t_f}{t_w} - 2\right]^2 . \qquad (11)$$

Because of the way they are defined, s_i and s_f are always equal to the same value, which will be designated as s'. The designation of this s' value as an initial or final value will be discussed later.

The $(s\eta)_p$ Correlation

We have seen in the theoretical development that the $s\eta$ value for the maximum concentration of the elution diagram, $(s\eta)_p$, is approximately 1 for values of $s > 100$. From the numerical calculations of the theoretical elution diagrams, the values of $(s\eta)_p$ were determined for various values of the s parameter. From these values, a power series in s was calculated by electronic computer for evaluation of $(s\eta)_p$ at experimentally determined s values. The series is

$$(s\eta)_p = 1.0000720 - \frac{2.9925346}{s} + \frac{4.3187708}{s^2} . \qquad (12)$$

The accuracy of the experimental work does not justify use of this refinement, but it was easily included in the program for correlating the experimental data and it may be of use in future continuations of this work.

Peak-Height Correlation

The solution to the equation of the chromatographic model, Eq. (6), is used to calculate the maximum value of the solute concentration at the exit of the column. Before Eq. (6) can be applied to an actual column operation, it must be modified in three ways.

First, because the column area and the quantity of solute usually differ from their arbitrarily assigned unit values, the left-hand term of Eq. (6) is modified, as noted earlier, to CLA/ω. Second, the impulsive feed function that charges the column was defined in time units of τ. If the time unit t is used, where $t = \gamma\tau$, the left-hand term of Eq. (6) must also be multiplied by γ. And third, because the T.C. cell is not located in the packed portion of the column, the void fraction, α, must be included in the left-hand term of Eq. (6).

The expression then, to be used for calculating the solute mobile-phase concentration at the exit of the column, for the given s value, is

$$c_{max} = \frac{\omega}{\alpha\gamma AL} \left[\begin{array}{c} \text{maximum ordinate} \\ \text{of Eq. (6) for} \\ \text{given s value} \end{array} \right]_{(s\eta)_p} . \tag{13}$$

From the plots of Eq. (6) in Figs. 1 and 2, the values of $(CL)_{max}$ were found to vary with the s parameter by the relation

$$(CL)_{max} \cong \frac{1}{2\sqrt{\pi}} \sqrt{s} \tag{14}$$

for $s > 100$. From Eq. (14), the final expression for the predicted maximum in solute concentration at the column exit is then

$$c_{max} = \frac{\omega\sqrt{s}}{2\sqrt{\pi}\ \alpha\gamma AL} . \tag{15}$$

Calculations

An IBM 650 Electronic Digital Computer was used to process the experimental data, which are tabulated in Table V. The computational program for the computer was written in an interpretive system, designated the F.L.O.P.S. routine, which was developed by the Bell Telephone Laboratories.[27] This same routine was used for the numerical evaluation of Eq. (6) as described in Appendix II.

Table V

G.L.C. EXPERIMENTAL DATA

Run number	Room or WTM temperature (°C)	Column temperature (°C)	Barometer (psia)	Pressure drop (in Hg)	WTM flow rate $ft^3/min \times 10^2$	Air peak time, t_{pa} (min)	Initial time, t_i (min)	Half-height width, t_5 (min)	Final time, t_f (min)	Peak time, t_p (min)	Peak height (mv)
					BENZENE[1]						
1	23.00	97.40	14.44	45.50	5.880	.350	3.160	.750	4.310	3.80	12.53
2	23.00	97.50	14.44	45.47	5.880	.340	3.140	.725	4.310	3.75	12.83
9	22.70	98.10	14.44	40.92	5.340	.380	3.510	.740	4.720	4.20	14.04
10	22.70	98.10	14.44	40.92	5.340	.400	3.560	1.030	5.270	4.41	10.38
11	22.70	98.10	14.44	40.92	5.340	.370	3.490	.800	4.790	4.28	13.23
12	25.00	98.20	14.45	35.85	4.740	.410	4.000	.830	5.350	4.82	14.63
13	25.00	98.10	14.45	35.75	4.710	.420	4.020	.920	5.540	4.92	13.75
14	25.00	98.10	14.45	35.75	4.740	.410	3.970	.870	5.400	4.80	14.11
21	23.00	98.10	14.47	30.75	3.970	.550	4.630	.930	6.160	5.63	15.49
22	23.00	97.90	14.47	30.50	3.980	.525	4.610	.940	6.150	5.63	15.65
23	23.00	97.50	14.47	30.05	4.010	.500	4.710	.950	6.260	5.63	16.17
30	22.78	99.20	14.47	25.50	3.200	.575	5.240	1.100	7.050	6.35	15.14
31	22.78	99.30	14.47	25.50	3.410	.575	5.355	1.025	7.005	6.45	16.19
32	22.78	98.70	14.47	25.35	3.400	.550	5.310	1.050	7.050	6.47	15.81
37	22.78	99.10	14.47	20.47	2.780	.700	6.760	1.450	9.090	8.25	14.97
38	22.78	98.80	14.47	20.15	2.763	.650	6.810	1.250	8.860	8.23	15.99
46	22.78	98.30	14.47	15.10	2.120	1.000	9.350	1.720	12.160	11.30	16.17
47	22.78	98.30	14.47	15.10	2.080	1.000	9.200	1.650	11.850	11.04	15.65
53	22.60	98.60	14.40	10.93	1.504	1.340	13.000	2.350	16.760	15.77	15.71
54	22.60	98.60	14.40	10.96	1.520	1.350	12.850	2.300	16.580	15.60	17.14
58	22.50	98.40	14.33	5.64	.798	2.600	24.500	4.490	31.600	30.00	16.71
62	22.50	102.00	14.33	40.66	5.050	.360	2.850	.650	3.925	3.37	17.17
63	22.50	101.67	14.33	40.60	5.050	.380	2.920	.730	4.160	3.46	15.55
68	22.80	105.73	14.34	29.78	3.886	.480	4.000	.850	5.345	4.73	18.65

Table V (Continued)

Run number	Room or TWM temperature (°C)	Column temperature (°C)	Barometer (psia)	Pressure drop (in Hg)	WTM flow rate $ft^3/min \times 10^2$	Air peak time, t_{pa} (min)	Initial time, t_i (min)	Half-height width, t_5 (min)	Final time, t_f (min)	Peak time, t_p (min)	Peak height (mv)
					BENZENE[1]						
69	22.80	105.77	14.34	30.80	4.010	.485	3.885	.795	5.153	4.61	18.57
70	22.80	105.72	14.34	30.90	4.010	.460	3.865	.880	5.300	4.57	17.25
77	22.80	105.63	14.34	20.30	2.710	.730	5.875	1.100	7.640	6.95	19.83
78	22.80	105.83	14.34	20.35	2.750	.740	5.860	1.095	7.625	6.97	20.39
83	22.50	105.43	14.39	15.40	2.060	1.035	7.855	1.590	10.075	9.33	18.01
84	22.50	105.57	14.39	15.80	2.110	.938	7.650	1.335	9.820	9.05	21.79
85	22.50	105.83	14.47	14.80	1.979	1.000	8.075	1.435	10.370	9.85	21.39
89	22.50	105.80	14.47	10.00	1.351	1.510	12.150	2.055	15.465	14.50	21.91
92	22.50	105.53	14.47	5.20	.699	2.950	23.890	3.870	30.060	28.58	21.41
95	22.61	88.02	14.44	40.00	5.470	.340	4.405	1.060	6.155	5.43	10.57
97	22.61	87.80	14.44	39.80	5.410	.342	4.420	1.003	6.080	5.46	10.97
99	22.61	87.70	14.44	30.50	4.280	.475	5.845	1.260	7.905	7.25	11.81
102	22.44	87.63	14.54	30.30	4.170	.475	5.765	1.230	7.750	7.13	12.05
105	22.44	87.50	14.54	20.50	2.910	.713	8.645	1.645	11.345	10.60	12.11
108	22.44	87.23	14.54	20.60	2.920	.715	8.670	1.685	11.445	10.73	12.19
111	22.44	87.20	14.54	15.20	2.190	.965	11.835	2.330	15.645	14.80	12.43
114	22.44	86.93	14.54	9.80	1.430	1.505	18.520	3.520	24.170	22.95	11.73
116	22.44	86.93	14.54	5.10	.750	2.865	35.795	7.170	47.025	45.13	11.26
					TOLUENE[2]						
3	23.00	97.50	14.44	45.60	5.940	.350	6.250	1.900	9.190	8.40	7.29
4	23.00	97.80	14.44	45.33	5.940	.350	6.210	1.700	8.910	8.25	7.29
5	22.70	97.80	14.44	40.92	5.350	.375	6.900	1.980	10.300	9.40	8.04

Table V (Continued)

Run number	Room or TWM temperature (°C)	Column temperature (°C)	Barometer (psia)	Pressure drop (in Hg)	WTM flow rate ft3/min x 10^2	Air peak time, t_{pa} (min)	Initial time, t_i (min)	Half-height width, t_5 (min)	Final time, t_f (min)	Peak time, t_p (min)	Peak height (mv)
					TOLUENE[2]						
6	22.70	98.20	14.44	40.92	5.350	.375	6.800	1.980	9.950	9.23	8.39
15	25.00	98.10	14.45	35.90	4.720	.430	7.910	2.200	11.500	10.85	8.55
16	25.00	98.40	14.45	35.90	4.720	.400	7.800	1.980	11.120	10.52	8.66
17	25.50	98.40	14.45	35.80	4.720	.440	7.750	2.060	11.220	10.60	8.84
24	23.00	97.30	14.47	29.80	4.020	.475	9.250	2.300	13.110	12.38	8.22
25	23.00	97.40	14.47	30.10	3.980	.475	9.175	2.560	13.450	12.65	9.20
26	23.00	97.90	14.47	30.10	4.010	.500	9.130	2.450	13.120	12.43	9.03
33	22.78	98.50	14.47	25.30	3.400	.550	10.590	2.860	15.330	14.50	9.05
34	22.78	98.60	14.47	25.30	3.400	.600	10.540	2.888	15.260	14.45	9.13
39	22.78	98.70	14.47	20.30	2.750	.720	13.300	3.620	19.230	18.35	9.03
40	22.78	98.80	14.47	20.33	2.745	.700	13.200	3.525	18.940	18.13	8.88
48	22.78	98.33	14.47	15.10	2.080	1.000	17.900	4.900	25.790	24.70	8.68
49	22.78	98.43	14.47	15.10	2.075	1.000	17.900	4.870	25.740	24.55	8.67
55	22.50	98.47	14.33	10.77	1.500	1.360	25.230	7.070	36.350	34.80	8.57
59	22.50	98.20	14.33	5.64	.804	2.580	47.200	11.220	68.250	65.95	8.55
64	22.50	101.53	14.33	40.37	5.000	.375	5.510	1.605	8.105	7.43	10.91
65	22.50	101.23	14.33	39.50	5.025	.375	5.630	1.670	8.285	7.48	10.49
71	22.80	106.17	14.34	30.20	3.918	.500	7.463	1.963	10.705	9.96	11.13
72	22.80	105.65	14.34	30.26	3.976	.480	7.435	2.010	10.720	10.06	11.41
79	22.80	105.77	14.34	20.30	2.700	.730	11.060	2.975	15.905	15.40	11.52
80	22.80	105.60	14.34	20.30	2.700	.760	11.125	2.900	15.870	15.11	11.55
86	22.50	105.73	14.47	15.50	2.070	.985	14.630	3.850	20.780	19.80	11.94
90	22.50	105.57	14.47	10.10	1.355	1.500	22.925	6.140	32.645	31.23	11.46
96	22.61	87.92	14.44	39.78	5.460	.375	9.165	2.670	13.520	12.65	6.46

Table V (Continued)

Run number	Room or TWM temperature (°C)	Column temperature (°C)	Barometer (psia)	Pressure drop (in Hg)	WTM flow rate $ft^3/min \times 10^2$	Air peak time, t_{pa} (min)	Initial time, t_i (min)	Half-height width, t_5 (min)	Final time, t_f (min)	Peak time, t_p (min)	Peak height (mv)
					TOLUENE[2]						
100	22.61	87.67	14.44	30.50	4.265	.463	11.990	3.470	17.605	16.60	6.32
103	22.44	87.53	14.54	30.20	4.190	.485	11.925	3.450	17.530	16.58	6.49
106	22.44	87.33	14.54	20.50	2.940	.720	17.805	5.090	25.995	24.65	6.24
109	22.44	87.03	14.54	15.10	2.170	.960	24.460	7.140	35.645	33.85	6.01
112	22.44	87.13	14.54	10.00	1.460	1.505	37.175	11.110	54.360	51.90	5.77
117*	23.06	100.43	14.41	19.90	2.750	.775	13.375	1.620	16.320	15.23	1.92
118*	23.06	99.90	14.41	19.90	2.720	.775	13.625	1.900	16.850	15.88	3.65
119*	23.06	100.03	14.41	19.90	2.730	.763	13.663	1.980	16.988	16.00	3.91
120*	23.06	99.83	14.41	20.00	2.750	.750	13.525	2.160	17.145	16.13	4.75
121*	23.06	99.93	14.41	20.00	2.760	.768	13.500	2.480	17.665	16.70	6.11
122*	23.06	99.70	14.41	20.00	2.750	.763	13.530	3.115	18.630	17.65	7.36
123*	23.06	99.63	14.41	19.97	2.740	.763	13.535	3.385	19.045	18.03	8.21
					ACETONE[3]						
7#	22.70	98.20	14.44	40.92	5.320	.375	1.350	.680	2.500	1.68	15.29
8#	22.70	98.10	14.44	40.92	5.340	.325	1.240	.290	1.700	1.41	33.99
18#	25.50	98.40	14.45	35.80	4.770	.460	1.590	.300	2.110	1.77	36.43
19#	25.50	98.60	14.45	35.80	4.770	.425	1.490	.550	2.340	1.75	21.59
20#	25.50	98.10	14.45	35.80	4.770	.425	1.440	.300	2.090	1.62	29.49
27●	23.00	98.10	14.47	30.00	3.980	.475	1.700	.290	2.300	1.90	20.01
28●	23.00	98.30	14.47	30.00	3.980	.490	1.730	.325	2.310	1.90	20.29
29	23.00	98.30	14.47	30.00	3.980	.500	1.740	.300	2.310	1.98	16.49
35	22.78	98.70	14.47	25.20	3.390	.600	2.070	.280	2.520	2.27	19.17

Table V (Continued)

Run number	Room or WTM temperature (°C)	Column temperature (°C)	Barometer (psia)	Pressure drop (in Hg)	WTM flow rate $ft^3/min \times 10^2$	Air peak time, t_{pa} (min)	Initial time, t_i (min)	Half-height width, $t_{\frac{1}{2}}$ (min)	Final time, t_f (min)	Peak time, t_p (min)	Peak height (mv)
					ACETONE[3]						
36	22.78	98.80	14.47	25.20	3.340	.550	2.000	.280	2.470	2.22	19.49
41	22.78	98.90	14.47	20.35	2.780	.700	2.500	.325	3.060	2.75	17.65
42	22.78	99.10	14.47	20.35	2.780	.650	2.500	.350	3.120	2.75	19.99
43	22.78	99.10	14.47	20.30	2.745	.657	2.450	.350	3.090	2.75	20.59
44	22.78	98.90	14.47	15.10	2.082	1.000	3.500	.450	4.250	3.87	21.59
45	22.78	98.90	14.47	15.10	2.065	.990	3.400	.440	4.180	3.77	20.49
50	22.60	98.47	14.40	10.70	1.480	1.400	4.925	.590	5.915	5.40	20.23
51	22.60	98.47	14.40	10.80	1.500	1.350	4.930	.600	5.960	5.37	20.35
52	22.60	98.53	14.40	10.80	1.515	1.370	4.830	.600	5.800	5.27	20.43
56	22.50	98.17	14.33	5.60	.789	2.650	9.340	1.030	11.150	10.24	23.91
57	22.50	98.20	14.33	5.64	.798	2.600	9.210	.970	10.910	10.05	22.63
60	22.50	102.17	14.33	41.80	5.100	.375	1.150	.170	1.425	1.22	20.87
61	22.50	102.00	14.33	40.85	5.050	.350	1.100	.180	1.425	1.20	21.87
66	22.80	105.93	14.34	30.00	3.866	.500	1.575	.235	1.985	1.70	20.83
67	22.80	105.80	14.34	29.86	3.876	.480	1.545	.255	2.012	1.70	19.99
73	22.80	105.70	14.34	20.30	2.710	.743	2.350	.300	2.895	2.51	21.46
74	22.80	105.77	14.34	20.35	2.720	.725	2.305	.320	2.820	2.49	23.50
75	22.80	105.63	14.34	20.30	2.690	.750	2.350	.400	3.050	2.56	19.09
76	22.80	105.53	14.34	20.30	2.710	.725	2.305	.330	2.870	2.50	22.65
81	23.80	105.33	14.40	15.25	2.000	1.065	3.182	.495	4.030	3.48	21.95
82	23.80	105.03	14.40	15.40	2.070	1.045	3.105	.405	3.765	3.37	23.07
87	22.50	105.87	14.47	10.10	1.374	1.460	4.620	.540	5.550	4.98	23.43
88	22.50	105.90	14.47	9.85	1.339	1.550	4.835	.535	5.775	5.20	20.97
91	22.50	105.67	14.47	5.20	.702	2.900	9.180	1.000	10.960	9.90	27.43

Table V (Concluded)

Run number	Room or WTM temperature (°C)	Column temperature (°C)	Barometer (psia)	Pressure drop (in Hg)	WTM flow rate $ft^3/min \times 10^2$	Air peak time, t_{pa} (min)	Initial time, t_i (min)	Half-height width, t_5 (min)	Final time, t_f (min)	Peak time, t_p (min)	Peak height (mv)
					ACETONE[3]						
93	22.61	88.47	14.44	39.95	5.320	.363	1.525	.260	1.980	1.71	13.37
94	22.61	88.03	14.44	40.00	5.490	.370	1.530	.233	1.935	1.73	15.75
98	22.61	87.77	14.44	30.50	4.310	.487	2.035	.290	2.525	2.30	15.11
101	22.41	88.00	14.54	30.45	4.170	.475	1.990	.280	2.470	2.23	15.17
104	22.44	87.50	14.54	20.70	2.920	.720	3.000	.395	3.675	3.38	16.99
107	22.44	87.10	14.54	20.60	2.920	.713	3.040	.400	3.725	3.42	15.99
110	22.44	87.28	14.54	15.20	2.160	.975	4.125	.515	4.995	4.65	17.13
113	22.44	87.13	14.54	10.00	1.460	1.455	6.260	.725	7.530	7.05	17.11
115	22.44	86.93	14.54	5.10	.750	2.895	12.500	1.375	14.885	14.08	18.13

Note:

1. Benzene average sample size -- 0.200 ml.
2. Toluene average sample size -- 0.300 ml, except where marked * for sample size variations.
3. Acetone average sample size -- 0.075 ml, except where marked # for 0.200, ml, and ● for 0.100 ml.
4. Column inlet pressure constant at 100 psig for all runs.
5. Liquid stationary phase for all runs -- DC-550 silicone oil.

Mobile-Phase Calculations

The mobile-phase volumetric flow rate, Q, was first corrected for the partial volume of water vapor. This flow rate was then adjusted to column temperature and pressure using the perfect gas law. This gave the column flow rate, Q_{col}, which when divided by the column area gave the superficial velocity, V_o.

An experimental void fraction, α_{calc}, was calculated from the transit time of the air peak through the column after subtracting from the measured air peak time the periods spent in the entry, exit, and expansion-valve sections of the flow path. This column transit time for the air was divided by the superficial column transit time ($= L/V_o$) giving the experimental void fraction.

The modified Reynolds number was computed from the expression

$$Re = \frac{V_o d_p \rho}{\mu},$$

where ρ and μ are the density and viscosity of helium at column conditions.

Diffusivity Calculations

The peak width was found from the difference in final and initial times. An s value for the solute peak was calculated using Eq. (10). Because some of the solute-elution diagrams exhibited a marked assymetry, a second s value was calculated for a symmetrical peak situated between the initial and final times. The peak time for this theoretical peak was

$$t'_p = \frac{(t_f + t_i)}{2},$$

and its s value, s', was calculated from Eq. (11).

The column length was then divided by these s values to give the terms L/s and L/s'. An approximate Peclet number was found from the product of the s value and the ratio of average particle size to column length:

$$Pe \cong s \frac{d_p}{L} .$$

Partition Coefficient Calculation

The partition coefficient based upon the measured peak time was calculated from the expression

$$k = \frac{t_p V_o}{(s\eta)_p L} - \alpha . \tag{16}$$

A partition coefficient for the symmetric peak, k', was also calculated by substituting the theoretical peak time, t'_p, for the measured peak time.

Concentration Calculations

The maximum solute mole fraction in the moving phase, y_{max}, was obtained from the product of peak height, H_p, and the T.C.-cell calibration coefficient, M. The latter was determined by the method reported in Appendix III. The maximum volumetric concentration was calculated from the expression

$$c_{max} = \frac{y_{max} p_o}{R T_{col}} , \tag{17}$$

assuming ideal behavior of the solute in the vapor phase. Here, p_o is the column outlet pressure, and RT_{col} has its usual meaning. The liquid-phase mole fraction, in equilibrium with y_{max}, was calculated from the expression

$$x_{max} = \frac{k c_{max}}{k c_{max} + N} , \tag{18}$$

where N is the number of moles of solvent per unit volume of bed.

An approximate material balance of the solute, ω_{calc}, was calculated from an approximation of the solute-peak area by

$$\omega_{calc} = c_{max} \cdot t_5 \cdot Q_{col} .$$

Miscellaneous Calculations

A reciprocal column temperature was found useful for plotting the partition-coefficient data. The IBM computer also calculated several other quantities that were used for comparison of the data with the work of other authors. These quantities were not tabulated.

Tabulation

The results of the IBM calculations are shown in Table VI A and B. An analysis of these results showed that run number 7 was not reliable. The partition-coefficient vs reciprocal column-temperature plots of runs 60 through 65 showed large deviations from those of all the other runs and were discarded. The acetone runs 7, 8, 18, 19, 20, 27, and 28 used larger sample sizes than the remainder of the runs and were also discarded.

A sample calculation of a typical chromatographic run is shown in Appendix V.

Table VI - A

SUMMARY OF IBM 650 CALCULATIONS FROM G.L.C. DATA[1]

Run number	Column flow rate (ft^3/min x 10^2)	Reciprocal column temperature ($^{o}K)^{-1}$ x 10^5)	Partition coefficient (k')	Partition coefficient (k)	Exit-vapor concentration (lb-moles/ft^3 x 10^4)	Exit-vapor mole fraction	Equilibrium-liquid mole fraction	Elution material balance (lb-moles x 10^6)
				BENZENE				
1	1.000	269.83	9.14	9.32	5.568	.04326	.433	4.178
2	1.000	269.75	9.12	9.19	5.701	.04429	.439	4.136
9	.901	269.32	9.06	9.27	6.379	.04847	.465	4.255
10	.901	269.32	9.85	9.84	4.717	.03584	.411	4.380
11	.901	269.32	9.13	9.47	6.011	.04567	.452	4.335
12	.785	269.25	8.96	9.26	6.821	.05050	.478	4.446
13	.780	269.32	9.13	9.42	6.416	.04747	.468	4.604
14	.784	269.32	8.98	9.22	6.584	.04871	.470	4.496
21	.655	269.32	8.58	8.99	7.411	.05347	.489	4.515
22	.656	269.46	8.57	9.01	7.501	.05402	.491	4.625
23	.659	269.75	8.81	9.06	7.776	.05582	.507	4.872
30	.523	268.52	7.74	8.02	7.410	.05226	.463	4.268
31	.558	268.45	8.35	8.75	7.921	.05589	.498	4.532
32	.555	268.88	8.31	8.75	7.753	.05457	.492	4.522
37	.449	268.60	8.67	9.06	7.506	.05168	.494	4.894
38	.446	268.81	8.47	8.94	8.035	.05520	.506	4.482
46	.338	269.17	8.85	9.34	8.329	.05582	.525	4.844
47	.331	269.17	8.46	8.91	8.061	.05402	.506	4.413
53	.237	268.96	8.55	9.11	8.235	.05423	.514	4.587
54	.239	268.96	8.55	9.11	8.983	.05916	.536	4.949
58	.123	269.10	8.40	9.04	8.966	.05768	.531	4.983
62	.855	266.52	6.89	6.86	7.720	.05927	.444	4.295
63	.855	266.75	7.25	7.07	7.001	.05368	.433	4.369
68	.648	263.90	7.23	7.33	8.773	.06437	.488	4.834

Table VI - A (continued)

Run number	Column flow rate (ft^3/min x 10^2)	Reciprocal column temperature ($^oK)^{-1}$ x 10^5)	Partition coefficient (k')	Partition coefficient (k)	Exit-vapor concentration (lb-moles/ft^3 x 10^4)	Exit-vapor mole fraction	Equilibrium-liquid mole fraction	Elution material balance (lb-moles x 10^6)
				BENZENE				
69	.670	263.87	7.23	7.39	8.691	.06410	.485	4.633
70	.670	263.90	7.36	7.34	8.070	.05954	.471	4.763
77	.442	263.97	7.11	7.34	9.765	.06844	.510	4.752
78	.449	263.83	7.22	7.49	10.033	.07038	.521	4.935
83	.333	264.11	7.11	7.44	9.082	.06216	.492	4.820
84	.342	264.01	7.11	7.39	10.963	.07521	.539	5.010
85	.322	263.83	7.06	7.59	10.812	.07383	.534	4.998
89	.217	263.85	7.14	7.54	11.319	.07562	.548	5.061
92	.111	264.04	7.13	7.61	11.307	.07389	.548	4.871
95	.896	276.83	11.85	12.21	4.961	.03650	.469	4.716
97	.885	277.00	11.61	12.11	5.157	.03788	.474	4.582
99	.685	277.08	11.77	12.46	5.820	.04077	.507	5.029
102	.672	277.13	11.30	11.98	5.951	.04160	.503	4.919
105	.458	277.23	11.40	12.14	6.271	.04181	.518	4.730
108	.459	277.44	11.52	12.34	6.314	.04209	.522	4.893
111	.340	277.46	11.67	12.63	6.602	.04291	.536	5.242
114	.219	277.67	11.68	12.62	6.390	.04050	.529	4.942
116	.114	277.67	11.78	12.91	6.263	.03888	.526	5.122
				TOLUENE				
3	1.011	269.75	20.21	22.03	2.816	.02190	.461	5.412
4	1.011	269.54	19.75	21.59	2.818	.02190	.455	4.846
5	.902	269.54	20.11	22.02	3.180	.02415	.490	5.683

Table VI - A (continued)

Run number	Column flow rate (ft^3/min x 10^2)	Reciprocal column temperature (^oK)$^{-1}$ x 10^5)	Partition coefficient (k')	Partition coefficient (k)	Exit-vapor concentration (lb-moles/ft^3 x 10^4)	Exit-vapor mole fraction	Equilibrium-liquid mole fraction	Elution material balance (lb-moles x 10^6)
				TOLUENE				
6	.903	269.25	19.56	21.60	3.315	.02520	.493	5.931
15	.781	269.32	19.61	21.97	3.468	.02568	.505	5.966
16	.782	269.10	19.08	21.27	3.509	.02601	.501	5.438
17	.781	269.10	19.11	21.42	3.584	.02655	.507	5.767
24	.660	269.90	19.02	21.12	3.445	.02469	.496	5.234
25	.654	269.83	19.12	21.43	3.851	.02764	.525	6.453
26	.660	269.46	18.94	21.22	3.773	.02712	.518	6.104
33	.555	269.03	18.54	20.79	3.864	.02718	.518	6.135
34	.555	268.96	18.45	20.73	3.897	.02742	.519	6.250
39	.444	268.88	18.62	21.07	3.946	.02712	.524	6.345
40	.443	268.81	18.34	20.76	3.879	.02667	.517	6.065
48	.331	269.15	18.67	21.18	3.889	.02607	.522	6.324
49	.331	269.08	18.61	21.00	3.884	.02604	.520	6.263
55	.235	269.05	18.67	21.16	3.910	.02574	.523	6.505
59	.124	269.25	18.53	21.24	3.994	.02568	.526	5.585
64	.845	266.85	14.66	16.05	4.279	.03276	.485	5.809
65	.847	267.07	15.04	16.21	4.136	.03150	.483	5.855
71	.655	263.59	15.16	16.68	4.539	.03342	.508	5.837
72	.663	263.95	15.37	17.10	4.659	.03426	.518	6.217
79	.440	263.87	15.15	17.38	4.933	.03459	.529	6.471
80	.440	263.99	15.15	17.03	4.948	.03468	.530	6.324
86	.337	263.90	15.21	17.08	5.235	.03585	.545	6.800
90	.218	264.01	15.45	17.44	5.151	.03441	.544	6.900
96	.894	276.91	26.55	29.64	2.642	.01941	.513	6.309

Table VI - A (Continued)

Run number	Column flow rate (ft^3/min x 10^2)	Reciprocal column temperature ($^{o}K)^{-1}$ x 10^5)	Partition coefficient (k')	Partition coefficient (k)	Exit-vapor concentration (lb-moles/ft^3 x 10^4)	Exit-vapor mole fraction	Equilibrium-liquid mole fraction	Elution material balance (lb-moles x 10^6)
				TOLUENE				
100	.683	277.10	26.45	29.70	2.710	.01899	.518	6.427
103	.674	277.21	25.99	29.29	2.791	.01950	.521	6.500
106	.463	277.36	26.52	29.89	2.813	.01875	.528	6.631
109	.337	277.60	26.52	29.90	2.781	.01806	.525	6.700
112	.224	277.52	26.90	30.53	2.731	.01734	.524	6.815
117	.443	267.64	16.75	17.20	.839	.00579	.174	.603
118	.438	268.02	17.00	17.75	1.594	.01098	.289	1.328
119	.440	267.93	17.18	17.97	1.707	.01176	.306	1.487
120	.443	268.07	17.33	18.27	2.073	.01428	.350	1.985
121	.444	268.00	17.72	19.04	2.664	.01836	.415	2.940
122	.443	268.16	18.29	20.13	3.211	.02211	.469	4.432
123	.441	268.21	18.49	20.52	3.582	.02466	.499	5.352
				ACETONE				
7	.898	269.25	3.84	3.27	7.287	.05538	.296	4.451
8	.901	269.32	2.64	2.50	16.198	.12308	.392	4.234
18	.789	269.10	3.00	2.84	17.810	.13191	.445	4.217
19	.789	268.96	3.18	2.84	10.551	.07819	.335	4.583
20	.788	269.32	2.84	2.54	14.429	.10679	.381	3.414
27	.655	269.32	2.60	2.43	10.082	.07247	.283	1.916
28	.655	269.17	2.64	2.43	10.217	.07348	.288	2.178
29	.655	269.17	2.65	2.57	8.304	.05973	.248	1.634
35	.553	268.88	2.48	2.45	9.870	.06943	.269	1.530

Table VI - A (Continued)

Run number	Column flow rate (ft^3/min x 10^2)	Reciprocal column temperature (^oK)$^{-1}$ x 10^5)	Partition coefficient (k')	Partition coefficient (k)	Exit-vapor concentration (lb-moles/ft^3 x 10^4)	Exit-vapor mole fraction	Equilibrium-liquid mole fraction	Elution material balance (lb-moles x 10^6)
				ACETONE				
36	.545	268.81	2.34	2.33	10.032	.07059	.261	1.532
41	.449	268.74	2.42	2.39	9.295	.06392	.253	1.357
42	.449	268.60	2.46	2.39	10.521	.07240	.280	1.655
43	.443	268.60	2.37	2.35	10.839	.07457	.279	1.684
44	.332	268.74	2.53	2.52	11.649	.07819	.307	1.743
45	.329	268.74	2.42	2.41	11.055	.07421	.287	1.604
50	.233	269.05	2.46	2.44	11.141	.07326	.291	1.531
51	.236	269.05	2.52	2.48	11.202	.07370	.298	1.587
52	.238	269.01	2.47	2.45	11.244	.07399	.295	1.610
56	.122	269.27	2.43	2.43	13.470	.08659	.330	1.696
57	.123	269.25	2.41	2.40	12.746	.08195	.316	1.529
60	.867	266.40	2.07	1.92	9.783	.07558	.233	1.442
61	.856	266.52	1.98	1.85	10.307	.07920	.234	1.588
66	.645	263.76	2.16	2.02	10.264	.07544	.250	1.557
67	.646	263.85	2.16	2.03	9.861	.07240	.243	1.626
73	.442	263.92	2.18	2.05	11.086	.07772	.267	1.471
74	.444	263.87	2.12	2.04	12.134	.08510	.279	1.725
75	.439	263.97	2.26	2.10	9.864	.06914	.251	1.732
76	.442	264.04	2.14	2.04	11.706	.08202	.274	1.708
81	.322	264.17	2.20	2.09	11.626	.07949	.277	1.856
82	.333	264.38	2.15	2.09	12.220	.08354	.283	1.652
87	.221	263.80	2.09	2.03	12.692	.08485	.285	1.517
88	.215	263.78	2.14	2.08	11.372	.07594	.268	1.312
91	.111	263.94	2.09	2.04	15.192	.09933	.323	1.699

Table VI - A (Concluded)

Run number	Column flow rate (ft^3/min x 10^2)	Reciprocal column temperature (^oK)$^{-1}$ x 10^5)	Partition coefficient (k')	Partition coefficient (k)	Exit-vapor concentration (lb-moles/ft^3 x 10^4)	Exit-vapor mole fraction	Eluilibrium-liquid mole fraction	Elution material balance (lb-moles x 10^6)
				ACETONE				
93	.873	276.49	3.18	3.10	6.577	.04843	.239	1.493
94	.900	276.83	3.26	3.25	7.754	.05705	.275	1.626
98	.690	277.03	3.30	3.33	7.810	.05473	.279	1.564
101	.673	276.85	3.10	3.11	7.846	.05495	.268	1.478
104	.460	277.23	3.19	3.24	9.221	.06154	.307	1.676
107	.459	277.54	3.24	3.29	8.692	.05792	.297	1.598
110	.336	277.40	3.18	3.26	9.543	.06204	.313	1.652
113	.224	277.52	3.22	3.31	9.763	.06197	.321	1.589
115	.114	277.67	3.26	3.37	10.577	.06566	.341	1.658

Note:
1. Data in this table were printed directly from IBM 650 Computer output cards. Since there was no provision for rounding off this data, usually one extra significant figure was tabulated.

Table VI - B

SUMMARY OF IBM 650 CALCULATIONS FROM G.L.C. DATA[1]

Run number	Superficial velocity (ft/min)	Calculated void fraction	Reynolds number	L/s (ft x 10^3)	Peclet number	s'	s	Theoretical peak time difference (min)
				BENZENE				
1	19.72	.655	1.782	21.107	.0649	337	349	.0650
2	19.72	.629	1.782	22.434	.0611	324	328	.0250
9	17.76	.635	1.620	19.128	.0716	370	385	.0850
10	17.76	.683	1.620	34.651	.0395	213	212	- .00499
11	17.76	.611	1.620	21.262	.0644	324	346	.140
12	15.47	.580	1.428	18.079	.0758	383	407	.144
13	15.37	.595	1.419	21.997	.0623	316	335	.140
14	15.47	.580	1.428	20.455	.0670	343	360	.115
21	12.91	.683	1.206	17.020	.0805	397	433	.235
22	12.92	.640	1.209	17.243	.0794	390	427	.250
23	12.99	.601	1.218	17.468	.0784	400	422	.145
30	10.32	.525	.972	18.724	.0732	368	393	.205
31	11.00	.578	1.036	15.082	.0908	448	488	.270
32	10.94	.536	1.033	16.642	.0823	403	443	.295
37	8.86	.561	.845	18.382	.0745	370	401	.324
38	8.79	.495	.840	14.299	.0958	467	515	.395
46	6.66	.624	.644	14.251	.0961	468	517	.545
47	6.53	.607	.632	13.279	.1032	504	555	.515
53	4.67	.569	.455	13.101	.1046	501	562	.890
54	4.72	.584	.460	13.175	.1040	498	559	.885
58	2.43	.580	.240	12.908	.1061	499	571	1.95
62	16.86	.543	1.494	23.381	.0586	317	315	- .0125
63	16.85	.588	1.494	29.600	.0463	260	249	- .0800
68	12.77	.551	1.149	18.635	.0735	386	395	.0575

Table VI - B (Continued)

Run number	Superficial velocity (ft/min)	Calculated void fraction	Reynolds number	L/s (ft x 10^3)	Peclet number	s'	s	Theoretical peak time difference (min)
				BENZENE				
69	13.21	.589	1.186	17.436	.0786	406	422	.0910
70	13.21	.544	1.186	22.674	.0604	326	325	.00750
77	8.71	.583	.801	14.863	.0922	469	496	.192
78	8.85	.608	.813	14.757	.0928	466	499	.232
83	6.57	.643	.612	13.048	.1050	521	565	.365
84	6.74	.578	.626	13.250	.1034	518	556	.315
85	6.34	.581	.591	12.511	.1095	516	589	.627
89	4.28	.598	.403	12.046	.1137	555	612	.692
92	2.19	.598	.208	10.741	.1276	611	686	1.60
95	17.67	.534	1.675	23.938	.0572	291	308	.149
97	17.46	.530	1.657	21.303	.0643	320	346	.210
99	13.51	.590	1.311	18.606	.0736	356	396	.375
102	13.24	.573	1.287	17.822	.0769	370	413	.380
105	9.03	.594	.898	14.952	.0916	438	493	.605
108	9.06	.599	.901	15.414	.0889	420	478	.672
111	6.71	.599	.676	15.273	.0897	416	482	1.06
114	4.33	.604	.441	13.968	.0981	456	527	1.60
116	2.24	.593	.231	14.270	.0960	435	516	3.72
				TOLUENE				
3	19.93	.665	1.800	28.232	.0485	220	261	.680
4	19.93	.666	1.800	24.684	.0555	250	298	.690
5	17.78	.624	1.623	30.151	.0454	204	244	.799

Table VI - B (Continued)

Run number	Superficial velocity (ft/min)	Calculated void fraction	Reynolds number	L/s (ft x 10^3)	Peclet number	s'	s	Theoretical peak time difference (min)
				TOLUENE				
6	17.80	.625	1.623	26.842	.0510	226	274	.854
15	15.41	.618	1.422	25.231	.0543	233	292	1.14
16	15.42	.556	1.422	22.953	.0597	259	321	1.06
17	15.39	.638	1.419	24.697	.0555	239	298	1.11
24	13.01	.558	1.221	22.405	.0611	268	329	1.20
25	12.90	.551	1.209	26.321	.0520	224	280	1.33
26	13.01	.602	1.218	23.747	.0577	248	310	1.30
33	10.94	.536	1.033	24.628	.0556	239	299	1.54
34	10.94	.610	1.033	24.590	.0557	239	299	1.55
39	8.75	.575	.836	24.068	.0569	240	306	2.08
40	8.74	.550	.834	23.101	.0593	250	319	2.06
48	6.53	.607	.632	23.516	.0582	245	313	2.85
49	6.52	.605	.630	23.503	.0583	247	313	2.73
55	4.63	.575	.452	23.532	.0582	245	313	4.01
59	2.45	.580	.242	23.479	.0583	240	314	8.22
64	16.66	.567	1.479	28.113	.0487	220	262	.622
65	16.70	.569	1.486	29.036	.0472	219	253	.522
71	12.91	.595	1.159	24.418	.0561	251	302	.876
72	13.08	.571	1.176	24.574	.0557	244	300	.982
79	8.69	.580	.798	22.811	.0600	247	323	1.91
80	8.68	.615	.798	22.727	.0603	258	324	1.61
86	6.64	.608	.618	22.234	.0616	265	331	2.09
90	4.29	.595	.404	22.325	.0614	261	330	3.44
96	17.62	.616	1.672	27.315	.0501	217	269	1.30

Table VI - B (Continued)

Run number	Superficial velocity (ft/min)	Calculated void fraction	Reynolds number	L/s (ft x 10^3)	Peclet number	s'	s	Theoretical peak time difference (min)
				TOLUENE				
100	13.46	.565	1.306	26.369	.0519	222	279	1.80
103	13.30	.595	1.293	26.338	.0520	220	280	1.85
106	9.12	.611	.907	25.441	.0538	228	289	2.75
109	6.65	.586	.669	25.163	.0544	231	293	3.79
112	4.42	.623	.450	25.268	.0542	226	291	6.13
117	8.74	.639	.831	8.617	.1590	813	855	.382
118	8.64	.628	.822	9.505	.1442	714	775	.642
119	8.67	.617	.825	9.953	.1377	679	740	.674
120	8.73	.608	.831	11.608	.1180	574	635	.795
121	8.77	.633	.834	14.335	.0956	447	514	1.11
122	8.73	.623	.831	19.242	.0712	318	383	1.57
123	8.69	.620	.828	21.524	.0636	279	342	1.74
				ACETONE				
7	17.70	.620	.161	10.799	.0126	89	68	- .245
8	17.76	.503	1.620	24.529	.0558	326	300	- .0600
18	15.55	.690	1.435	19.779	.0693	405	372	- .0750
19	15.56	.617	1.435	54.371	.0252	162	135	- .165
20	15.54	.615	1.435	36.875	.0371	235	200	- .140
27	12.92	.552	1.209	22.983	.0596	355	320	- .100
28	12.92	.579	1.209	21.476	.0638	388	343	- .120
29	12.92	.596	1.209	19.099	.0717	403	386	- .0450
35	10.91	.608	1.030	9.077	.1520	832	817	- .0200

Table VI - B (Continued)

Run number	Superficial velocity (ft/min)	Calculated void fraction	Reynolds number	L/s (ft x 10^3)	Peclet number	s'	s	Theoretical peak time difference (min)
				ACETONE				
36	10.75	.522	1.015	10.283	.1332	723	717	- .0100
41	8.85	.561	.845	9.557	.1434	788	771	- .0300
42	8.86	.501	.845	11.714	.1170	657	629	- .0600
43	8.74	.500	.834	12.482	.1098	599	590	- .0200
44	6.55	.609	.632	8.655	.1583	854	852	- .00500
45	6.50	.593	.627	9.865	.1389	755	747	- .0200
50	4.59	.592	.448	7.746	.1769	959	952	- .0200
51	4.65	.572	.454	8.463	.1619	894	871	- .0700
52	4.70	.594	.458	7.793	.1758	960	946	- .0400
56	2.41	.586	.237	7.200	.1903	1025	1024	- .00500
57	2.43	.580	.240	6.594	.2078	1120	1118	- .0100
60	17.08	.589	1.509	11.614	.1180	701	634	- .0625
61	16.87	.521	1.494	16.765	.0817	482	439	- .0575
66	12.72	.583	1.143	13.405	.1022	603	550	- .0800
67	12.74	.550	1.146	17.429	.0786	463	423	- .0787
73	8.72	.599	.801	10.865	.1261	740	678	- .112
74	8.75	.581	.804	9.819	.1396	792	751	- .0675
75	8.65	.600	.795	17.191	.0797	476	428	- .137
76	8.71	.577	.801	11.771	.1164	671	626	- .0875
81	6.35	.638	.592	13.668	.1002	579	539	- .126
82	6.57	.652	.612	8.839	.1550	866	834	- .0650
87	4.36	.584	.410	8.037	.1705	956	917	- .105
88	4.25	.613	.400	7.531	.1820	1019	979	- .105
91	2.20	.587	.209	7.450	.1839	1024	989	- .170

Table VI - B (Concluded)

Run number	Superficial velocity (ft/min)	Calculated void fraction	Reynolds number	L/s (ft x 10^3)	Peclet number	s'	s	Theoretical peak time difference (min)
				ACETONE				
93	17.20	.567	1.630	16.165	.0847	474	456	- .0345
94	17.73	.610	1.682	12.630	.1085	585	583	- .00250
98	13.61	.619	1.320	10.460	.1310	692	705	.0200
101	13.26	.574	1.287	10.601	.1293	690	695	.00800
104	9.07	.606	.901	9.191	.1491	782	802	.0425
107	9.06	.596	.901	9.245	.1482	780	797	.0375
110	6.62	.596	.666	8.067	.1699	879	914	.0900
113	4.42	.593	.450	7.478	.1832	943	986	.154
115	2.24	.603	.231	6.612	.2072	1054	1115	.387

Note: 1. Data in this table were printed directly from IBM 650 Computer output cards. Since there was no provision for rounding off this data, usually one extra significant figure was tabulated.

VI. DISCUSSION

Definition and Assumptions

The G.L.C. partition coefficient was defined in the theoretical model presented in the section on CHROMATOGRAPHIC THEORY and was assumed to have certain properties. These are briefly summarized here for comparison with experimental observations.

Definition. The partition coefficient is the equilibrium ratio of the solute concentration in the stationary phase to the solute concentration in the mobile phase. The units in use are moles per unit volume of bed as packed in the column, over moles per unit volume of gas in the mobile phase.

Assumptions. The partition coefficient is assumed to be independent of solute concentration (a linear isotherm) and, for a given G.L.C. column, a function of temperature only. This implies that the partition coefficient is not a function of the mobile-phase flow rate.

Temperature dependency. Porter, Deal, and Stross[11] have shown that, from the above definition, the partition coefficient at infinite solute dilution can be expressed

$$k^{o} = \frac{N\,RT}{\lambda^{o}\,p^{o}} \tag{19}$$

where N = moles of stationary solvent per unit volume of bed,

R = universal gas constant,

λ^{o} = activity coefficient of solute in solvent at infinite dilution, and

p^{o} = solute vapor pressure,

and the solute is assumed to be ideal in the vapor phase. Equation (19) was modified to show the temperature dependency of the partition coefficient

$$\frac{\partial \ln k^{o}}{\partial (1/T)} = \frac{\Delta H_v - RT - \overline{\Delta H_s}^{E}}{R} \qquad (20)$$

neglecting the temperature dependency of the molal volume of the solvent. The term ΔH_v is the latent heat of vaporization of the solute in the region of temperature T. The excess partial heat of solution, $\overline{\Delta H_s}^{E}$, is the measure of the nonideality of the solute-solvent system, i.e. $\ln \lambda^{o} = \frac{\overline{\Delta H_s}^{E}}{RT}$.

Experimental Results

Heat effects. Values of the partition coefficient were calculated for each G.L.C. run and their natural logarithms were plotted against the reciprocal of column temperature in Fig. 16. To obtain the apparent heat of solution, the numerator of the right side of Eq. (20), a least-squares line was calculated from the experimental data and is also shown in Fig. 16.

Partition coefficients, k', were also calculated from the theoretical peak times, and represent the partition coefficient of a symmetrical elution peak having the same peak width as the actual experimental peak. A least-squares line was also computed for the k' values of each solute shown in Fig. 16, for comparison.

The apparent heats of solution are obtained from the slopes of the least-squares lines of Fig. 16. From the known heats of vaporization and the approximate mean temperature, the partial excess heats of solution were determined. These values are tabulated in Table VII.

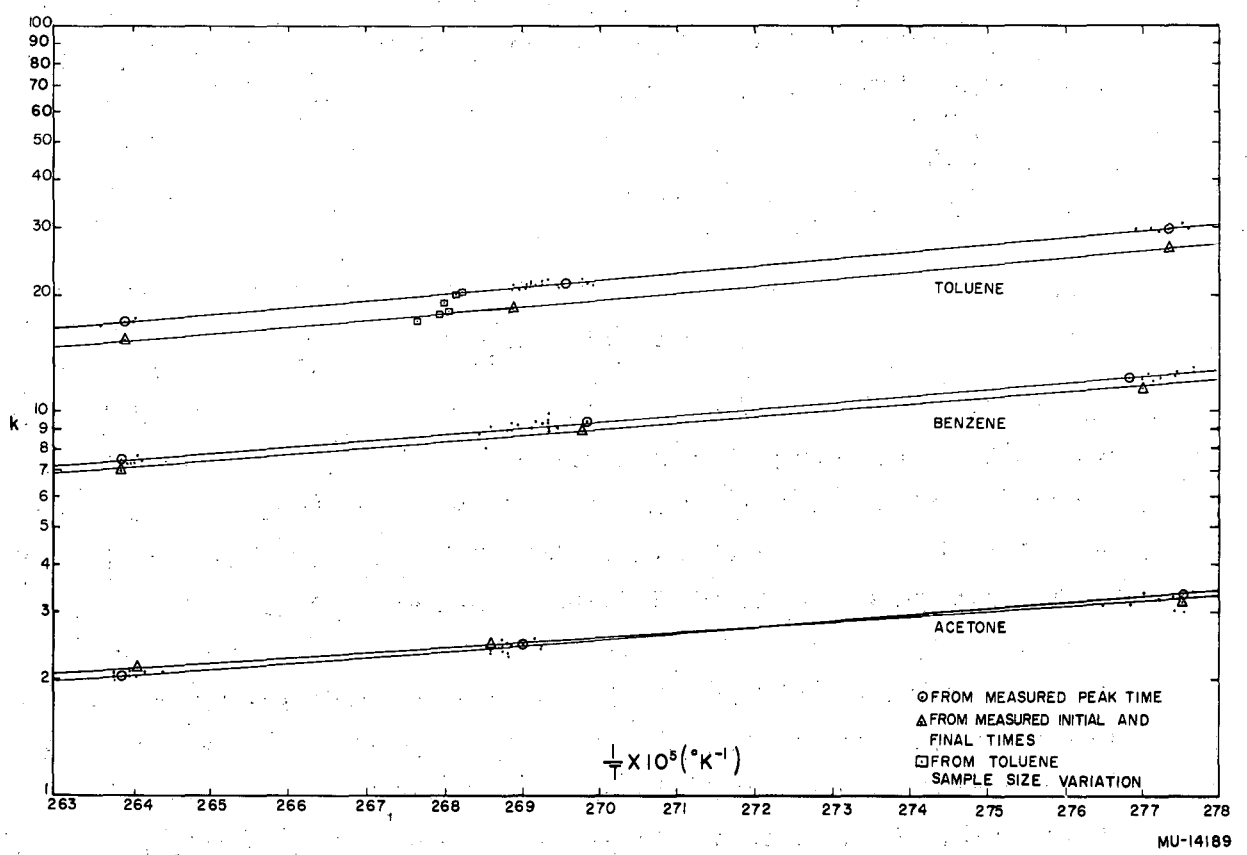

Fig. 16. Partition coefficients as a function of reciprocal column temperature.

Table VII

Apparent heats of solution from G.L.C. measurements using DC-550 silicone fluid with a temperature range of 87°C to 106°C

Solute	$(\Delta H_v - RT - \overline{\Delta H_s^E})_{exp}$ kcal/mole	ΔH_v^* kcal/mole	$(\overline{\Delta H_s^E})_{exp}$ kcal/mole	λ	λ^o
Benzene	7.57	7.21	-1.07	0.24	--
Toluene	8.24	8.13	-0.85	0.32	0.27
Acetone	6.90	6.54	-1.10	0.23	--

* At 100°C

Inspection of Table VII shows that the major heat term for these solutes and solvent is the heat of vaporization. If a value of the partition coefficient at a certain temperature is known, then its value at other temperatures may be estimated from the heat of vaporization.

The activity coefficients, λ, were computed from the partial excess heats of solution. The λ^o shown for toluene was calculated from the data obtained in the runs with sample-size variations. The data were extrapolated to infinite dilution.

Flow dependency. The partition coefficients measured at approximately 88°C were plotted against the Reynolds numbers at which they were observed, and are shown in Fig. 17. The column average temperatures at the beginning and the end of this series of runs are also shown. The slight temperature variation during the period of these runs is believed to be responsible for the minor changes in the partition coefficients.

Solvent variation. All experiments of this work were carried out using a silicone fluid solvent. Selection of the G.L.C. solvent is, as yet, done mostly on an empirical basis although an increasing amount of data on these coefficients for various solutes and solvents is appearing in current writings. Perotti et al. have described a semiempirical method

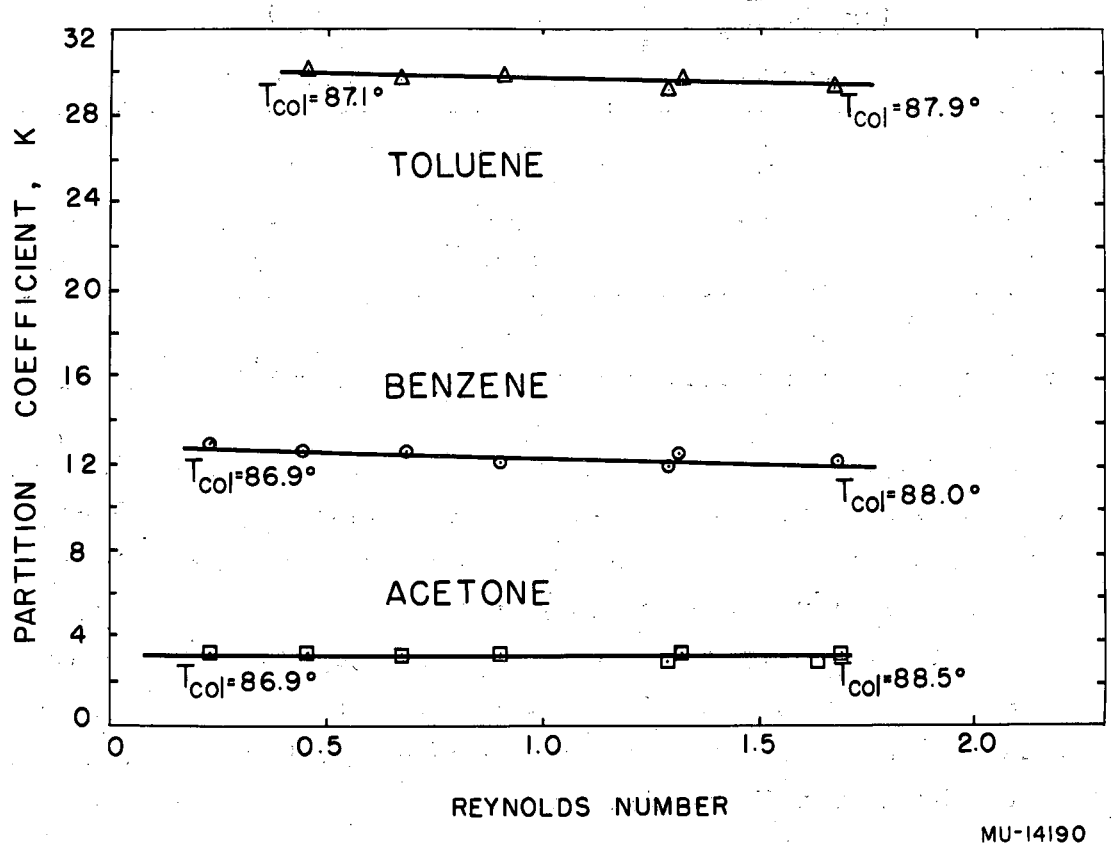

Fig. 17. Partition coefficients as a function of the Reynolds number.

method leading to the prediction of partition coefficients.[28] This method develops an expression for the solute infinite-dilution activity coefficient, λ^{o}, as determined by the chemical natures of the solute and solvent. As yet, this system is not adequately developed for general application to G.L.C. work. Keulmans[5] discusses in some detail the selection of G.L.C. solvents and gives a compilation of many of the solvents in general use.

Sample-Size Variations

During the period of the experimental work, the size of solute sample was observed to influence the measured values of the partition coefficient and the Peclet number. To investigate this effect, a brief study was made of the elution diagrams from runs with different amounts of solute in the column feed charge. Toluene was used for this study because its elution peak showed greater asymmetry than that of the other solutes. The peak asymmetry, attributed to a nonlinear partition coefficient, makes it difficult to arrive at more than qualitative conclusions about the influence of sample size.

Experimental results. Runs numbered 39, 40, and 117 through 123 were used in this study. The elution diagrams of seven of these runs are shown in Fig. 18, where they are superimposed upon a common abscissa. The data collected from these runs are shown in Fig. 19 as a function of the quantity of solute charged to the column. The actual amount of toluene charged to the column was determined by measuring the area of the elution peak with a planimeter and, from the operating parameters and the T.C. cell calibrations, converting this area to the equivalent number of moles of solute. This method was necessary because of the inaccuracy in the measurement of the small volumes (0.035 to 0.300 ml.) of solutes. (With acetone, there was some vaporization of the solute as it was placed on the sample bed because of its fairly low boiling point (56°C) and the relatively high column temperatures.) The maximum variation of the measured amount of solute from the volumetric amount presumed charged was 13% with an average deviation of about 6%.

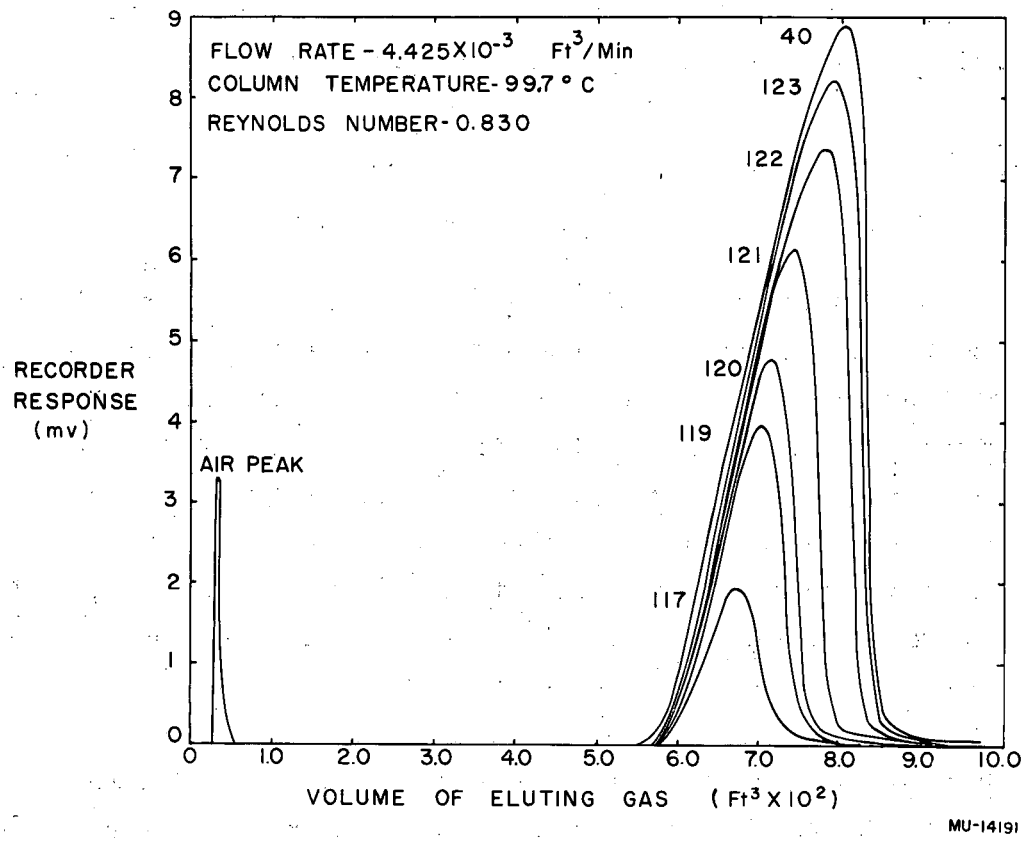

Fig. 18. Superimposed elution diagrams from toluene sample-size variations.

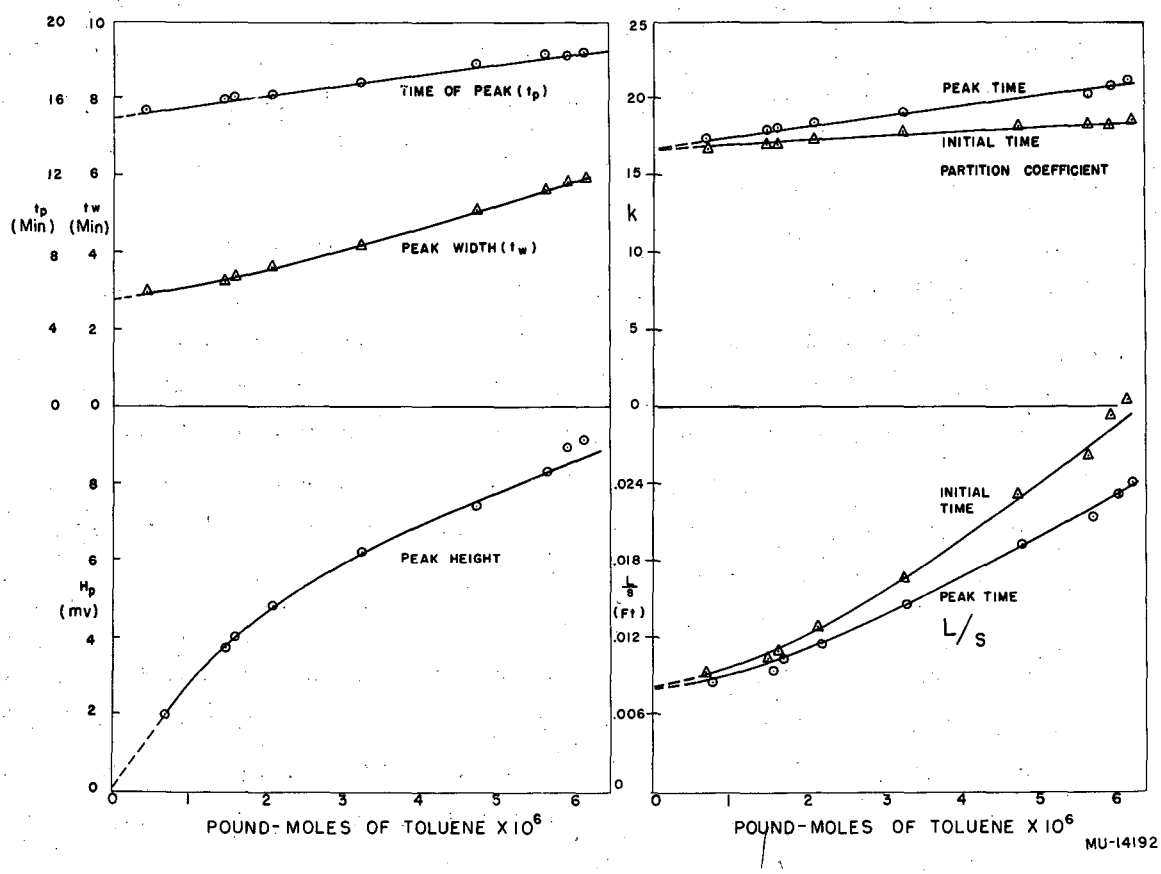

Fig. 19. Data and results of toluene sample-size variations.

Time of peak emergence. The time of the theoretical elution peak emergence is independent of the size of sample for the specified feed conditions. Use of pure solute, charged over a short interval, closely approximated the impulse-feed condition. This approximation is improved by the use of a long column (i.e. $s > 100$). In the toluene study, the time of peak emergence is seen to be a linear function of sample size. The peak time may also be extrapolated to zero sample size, giving the value for infinite dilution (here, $t_p^o = 15$ min).

Peak width. The width of the theoretical elution peak is not affected by the quantity of solute sample. However, in this series of runs, the width increases approximately linearly with sample size except at very small values of the solute sample size. Here, the variation of width appears to deviate from linearity and tends towards a constant value of the peak width that is independent of sample size ($t_w^o = 2.8$ min) as the theory predicts. The influence of sample size on the s parameter is discussed later.

Peak height. The theoretical peak height should be a linear function of sample size. In Fig. 19, we see that this is approximately true for small sample sizes. At higher values of sample size, the peak height does not increase as much. This would be expected from the increase of the peak width.

Partition coefficient. In the theory developed, the partition coefficient is assumed constant. However, in these runs, as the sample size was increased the apparent partition coefficient increased. The computed value of the partition coefficient is related linearly to the peak time. Thus, the partition coefficient shows a linear increase. By extrapolation, the value of the partition coefficient at infinite dilution was found ($k^o = 16.7$). The increase of the partition coefficient, k', based on the initial time and the peak width, is related only to the increase of the peak width because the initial time of all these runs are about the same. Both partition coefficients extrapolate to the same infinite-dilution value.

Infinite-dilution performance. The partition coefficient is truly independent of concentration only in ideal solutions. From the data of Fig. 19, extrapolated to zero sample size, the performance of such a G.L.C. column was estimated. Table VII shows a comparison of column performance at infinite solute dilution and also when charged with a finite amount of solute. The time of peak emergence and peak width both increase by about the same magnitude, but, because of their absolute values, this increase sharply reduces the value of the s parameter.

Table VIII

Comparison of G.L.C. column performance at two feed conditions

Solute, toluene Temperature, 100°C Superficial velocity, 8.7 ft/min	Solvent, DC-550 silicone fluid Reynolds number, 0.835 Helium flowrate, 4.42×10^{-3} ft^3/min	
Quantity of solute feed,	Infinite dilution	5×10^{-6} lb moles
Resolution parameter, s	920	370
L/s	0.008 ft.	0.020 ft.
Time of peak emergence, t_p	15 min.	17.7 min.
Peak width, t_w	2.8 min.	5.2 min.

Static Partition-Coefficient Determinations

Appendix IV describes a static method for determining partition coefficients. This work was performed to verify the order of magnitude of the column-determined coefficients and to check for their variation with concentration. The results of this work, as presented in the appendix, show that the partition coefficients are of the same order of magnitude and that they vary with the quantity of solute present in the two phases.

Longitudinal Diffusivity

Theoretical Definitions and Assumptions

The theory of the chromatographic model postulates that the existence of a longitudinal diffusivity in the column causes the spreading of the solute band. This diffusivity is the sum of the molecular- and eddy-diffusional components. The method of expressing the diffusivity was shown earlier to be

$$\frac{L}{s} = \frac{D}{V} = \frac{D_M}{V} + \frac{d_p}{Pe} , \qquad (21)$$

where $\frac{L}{s}$ has the dimensions of length and is comparable to the theoretical concept of the height of a mixing unit as used by other authors.[12,22] It is, as determined experimentally, equal to one-half the H.E.T.P. employed by Keulmans[6] and van Deemter et al.[12]

Experimental evidence prior to this work indicates that (1) eddy diffusivity is linearly related to the interstitial velocity for high Reynolds numbers; (2) the L/s expression should be independent of the solute, solvent, and mobile phase in the column except when the interstitial velocity is so low that the molecular diffusivity becomes significant compared to the eddy diffusivity; and (3) there should be no effect of temperature or pressure on the L/s term except where the molecular diffusion effect is significant, or where there is a large variation of interstitial velocity along the column because of the high ratio of inlet to outlet pressures.

Experimental Results

The smoothed curves through the L/s values for the three solutes are shown in Fig. 20 as functions of the Reynolds number. Figure 21 shows a comparison of the L/s values computed from the peak time and from the initial times versus the Reynolds number. In Fig. 19, the variation of the L/s value of toluene with sample size is shown.

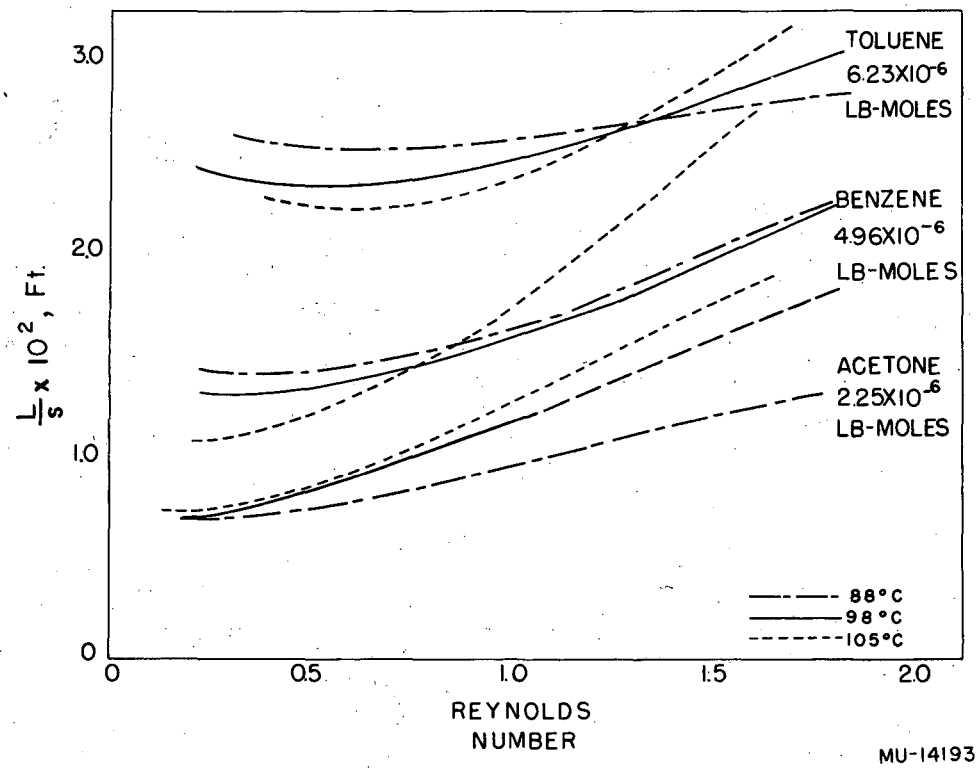

Fig. 20. L/s values as a function of the Reynolds number.

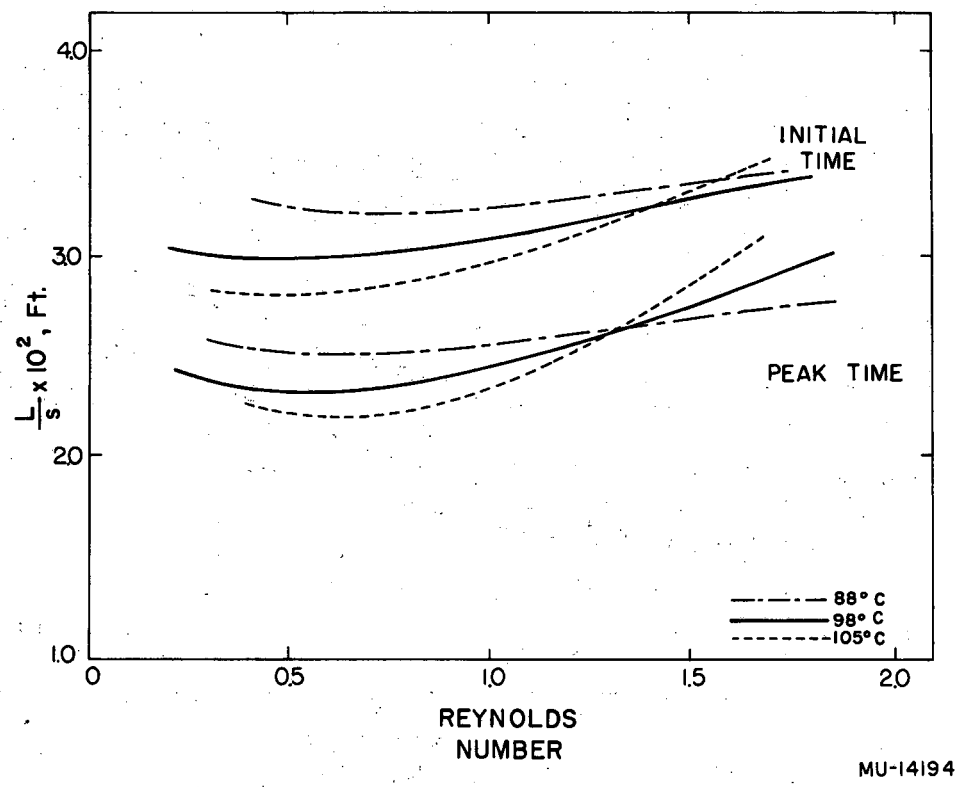

Fig. 21. Comparison of toluene L/s values as a function of the Reynolds number.

Influence of Molecular Diffusivity

Calculation of the molecular diffusivities of the solutes in helium showed them to be on the order of 0.005 ft^2/min (0.075 cm^2/sec) at 100°C and 7.8 atmospheres.[20] The minimum interstitial velocities used in this work were on the order of 3.5 ft/min. Then the maximum contribution of the molecular diffusivity to the L/s value is on the order of 0.0015 ft. Because this is less than one-fifth of the minimum observed values of L/s, the eddy diffusivity will be assumed to contribute the whole of the L/s value in the range of interstitial velocities studies.

Variation of the Eddy Diffusivity with Flow Rates

Study of Fig. 20 shows that the function L/s does not become asymptotic to a constant value with increasing Reynolds numbers as previous experimental evidence and theories would predict. This curve appears to pass through a minimum, or start from a low value, in the Reynolds range of 0.2 to 0.6 and then rise. The function L/s does appear to become asymptotic to some linear function of the Reynolds number at higher velocities. It must be mentioned, however, that in our experiments the Reynolds number did not lie in the highly turbulent region where a constant L/s value would be predicted.

Two possible effects that were not considered in the theoretical model and that may be the cause of or contribute to the variation of the L/s function with the Reynolds number are, first, a finite rate of mass transfer and, second, radial mixing. Both of these effects warrant additional study, which is beyond the scope of our work. However, they will be briefly described and will be considered as tentative explanations for certain observed experimental results.

Finite rate of mass transfer. Our model assumes a condition of continuous equilibrium between the two phases, which infers an infinite rate of mass

transfer. As mentioned earlier, van Deemter et al.[12] developed an expression for the H.E.T.P. involving terms for molecular and eddy diffision and also a third term for the resistance to mass transfer. The third term is

$$\frac{4}{\pi^2} \quad \frac{k\,\alpha_L/\alpha}{1 + (k\,\alpha_L/\alpha)^2} \quad \frac{d_f^2}{D_L} \quad V \quad , \tag{22}$$

where α_L = fractional volume of the solvent

d_f = an estimated solvent film thickness assuming the liquid uniformly dispersed on the solid

D_L = solute diffusivity in the solvent.

Radial mixing. Spreading of the solute band by radial mixing in a tube has been proposed by Taylor[29] and further discussed by Aris.[30] Under laminar flow conditions, the velocity profile across a tubular section is not uniform and the interaction of this profile with molecular diffusivity produces a radial mixing effect that has been called Taylor diffusion. The effective diffusivity, D_T, for this mechanism has been shown to be

$$D_T = \frac{a^2\,V_o^2}{48\,D_M} \tag{23}$$

for laminar flow in a tube of radius a. Originally, Taylor set certain restrictions on the length of the tube and the flow velocity for which Eq. (23) is valid. Aris has since shown that these restrictions are not necessary.

Application of this radial mixing to laminar flow conditions in the column provides a second means of accounting for the increase of the L/s value with increasing interstitial velocity.

Temperature Effects

Although no temperature influence on the L/s values is predicted, each solute's L/s curve exhibits a temperature sensitivity. In all cases the values of L/s rise more rapidly with higher temperatures. The factors that influence this variation are difficult to determine. One factor is the decrease of the partition coefficient resulting from increased temperature. The obvious nonlinear isotherm has a direct effect on peak width and hence on the L/s values. If a finite rate of mass transfer is considered, the decrease in the partition coefficient tends to increase the numerator of Eq. (22) while the same temperature rise will give a very marked increase in the solute diffusivity in the solvent, D_L, thereby increasing the denominator of Eq. (22). The use of the Taylor diffusivity term would predict a decrease in the L/s value because the gas diffusivity, D_M, in the denominator would increase with a temperature increase.

Sample-Size Influence

The L/s value calculated from the runs with sample-size variation are shown in Fig. 19 plotted as a function of the quantity of solute charged to the column. Above 1.6×10^{-6} lb moles of solute charged to the column, the L/s lengths increase almost linearly. Below this quantity of charge, the L/s lengths are less dependent on sample size and reach a limiting value for infinite dilution ($L/s^{o} = 0.008$ ft). When this limiting value is compared with the L/s value of acetone at the same Reynolds number in Fig. 20, the infinite dilution value for toluene is some 25% less than the acetone value. With the limited data that are available for sample-size variations, the dependence of the L/s value (as determined by our linear isotherm model) can only be said to be a function of the number of moles charged to the column. Because the variation in peak width is related to the asymmetry of the peak, a quantitative relationship between the L/s lengths of the solutes cannot be predicted.

Causes of band spreading at constant Reynolds number. The probable causes of the increase of peak width and the L/s value with increasing sample size are:

1. The nonlinearity of the partition coefficient as discussed earlier.

2. The longer period of time required to feed the solute charge from the bed section in the sample injection valve -- the desorption of this bed section. The effect of the bed section with larger sample sizes and higher partition coefficients is that the column is not charged impulsively but is charged over a finite period with a concentration of solute varying with the time of the charging period. This prolonged charging was enhanced by the period of equilibration of the solute prior to charging.

The placement of the thermocouples in the column resulted in the measurement of the change of bed temperature as the peak passed the thermocouple location. As the peak approached the thermocouple, the temperature would rise, because of the solute condensation. This effect was most easily noted with the broad toluene peaks at low flow rates. As the peak moved past the thermocouple, the bed would cool from solute evaporation, sometimes to temperatures lower than the ambient temperature of the bed. In run No. 59, as an extreme example, the peak time was about 66 min and the peak width, 21 min at the end of the column. The first thermocouple, some 5 in. into the bed, indicated a peak width of roughly 10 min which finished passing the thermocouple only some 12 min after charging.

Particle size. The influence of particle size on the eddy-diffusion term was not studied in this work. All experimental work was done with a bed having a 30 to 60 mesh size of particles. With these particles, the maximum value of the Peclet number was 0.2 for the acetone runs at a low Reynolds number, assuming a mean particle diameter for this calculation. If the small effect of the molecular diffusivity is considered, the Peclet number is somewhat larger, approximately 0.25. If the method

of van Deemter et al.[12] were applied -- by extrapolation of the asymptote of the L/s curve at higher Reynolds numbers back to Re = 0 giving the d_p/Pe quantity -- the Peclet number would be on the order of 0.7. This value is in fairly good agreement with those they obtained.

VII. CONCLUSION

A mathematical model of an elution chromatographic column has been proposed which will facilitate the design of industrial chromatographic equipment. Using either published or batch data on the partition coefficients of solute-solvent systems and the standard flow properties of packed beds, the theory can be used to predict:

1. The operating conditions of chromatographic columns for a specified solute purity, or

2. The solute purities for given-column operating conditions.

Validity of the Model

In its present form, the theory predicts a greater column separation ability than is actually observed, sometimes by a factor of 2 or more. For most accurate column predictions, two conditions must prevail:

1. The qauntities of the individual solutes of the feed charge must be small -- an empirical figure is approximately 2.5×10^{-3} moles solute/ft^2 column cross section.

2. The superficial velocity of the mobile phase must be low -- approximately 1.0 to 6.0 ft/min. The numerical values of the feed charge given will depend on the value of the resolution parameter -- the s-value -- and the value of the partition coefficient. The larger these parameters, the greater is the solute capacity of a given column.

Testing of the Model

The model was tested with a 7.4-ft G.L.C. column using silicone oil as the stationary solvent. The results of this work are summarized and the deviations from the theoretical predictions are noted.

Partition coefficients. The effective partition coefficients of benzene, toluene, and acetone were calculated from their respective chromatograms. It was found that these calculated values were insensitive to variations of the velocity of the mobile phase, and that they varied with the temperature in a regular way. Moreover, it was observed that the calculated partition coefficients also varied with the amount of solute charged to the column. This is due chiefly to the nonlinearity of the equilibrium isotherm, whereas it will be remembered that the mathematical model assumed that the partition coefficient is independent of solute concentration.

Independent determinations of the partition coefficients by a static-equilibrium technique yielded values that were consistently lower than those measured in the column. Both methods showed, in the case of toluene, a fairly similar variation of the isotherms with increased concentrations. The reasons for the differences in the values of the partition coefficients determined by these two methods are not known.

Flow properties. The values of the longitudinal diffusion were measured for the various solutes in a column packed with 30 to 60 mesh particles impregnated with 40 parts of silicone fluid per 100 parts of pulverized fire brick. The measured values of the longitudinal diffusivity, expressed as the Peclet group, varied widely, from 0.01 to 0.20. There was a regular variation of this group with the velocity of the mobile phase. Higher velocities produced lower Peclet numbers. The Peclet numbers reported in the literature were invariably measured at much higher Reynolds numbers and were found to be practically independent of flow rate, temperature, and solute concentration.

Future Work

This work can be extended in several promising directions. New mathematical models should be developed and then checked experimentally to determine the influence of the following factors on the performance of the G.L.C. column:

1. The existence of significant mass-transfer resistance between the mobile and stationary phases.

2. The nonlinearity of the equilibrium isotherms.

3. Diffusion in the liquid-solvent phase absorbed by the packing.

4. The particle size and the fractional void volume.

5. The effect of adsorption of the solutes by the carrier solid.

6. The influence of high column pressures on the solutes in the mobile phase.

In addition, further experimental work should consider the charging mechanism and its influence on the peak shape. The method for controlling the column temperature should be improved.

ACKNOWLEDGMENTS

I wish to express my gratitude to Professors Charles R. Wilke and Andreas Acrivos for their invaluable aid, advice, direction, and encouragement, and to Professor Harold A. Johnson for his review of the text.

I thank Mr. Eugene Fenech for his direction and assistance in the use of the IBM 650 computer.

The continued help of Mr. Gardner Young has greatly aided in the development of the experimental equipment.

Mr. Robert Brown and Mr. Robert Hamilton have constantly encouraged me through the difficult periods of this project.

Mrs. Patricia Howard has enhanced this report in her typing of the manuscript.

This work was performed under the auspices of the United States Atomic Energy Commission.

APPENDICES

Appendix I. Properties of Experimental Materials

Chemicals

Benzene. Baker and Adamson, reagent grade, General Chemical Division

Molecular weight	78.11
Specific gravity	0.879 (20°C)
Boiling point	80.1°C
Thermal conductivity, vapor	$9.1 \times 10^{-3} \frac{\text{Btu}}{\text{hr-ft}^2(^\circ\text{F/ft})}$ at 200°F
Molecular diffusivity* in helium	4.825×10^{-3} ft^2/min

Toluene. Baker and Adamson, reagent grade, General Chemical Division

Molecular weight	92.13
Specific gravity	0.8669 (20°C)
Boiling point	110.6°C
Thermal conductivity, vapor	$11.5 \times 10^{-3} \frac{\text{Btu}}{\text{hr-ft}^2(^\circ\text{F/ft})}$ at 200°F
Molecular diffusivity* in helium	3.76×10^{-3} ft^2/min

Acetone. Baker and Adamson, reagent grade, General Chemical Division

Molecular weight	58.08
Specific gravity	0.788 (25°C)
Boiling point	56.1°C
Thermal conductivity, vapor	$9.9 \times 10^{-3} \frac{\text{Btu}}{\text{hr-ft}^2(^\circ\text{F/ft})}$ at 200°F
Molecular diffusivity* in helium	4.59×10^{-3} ft^2/min

---

* Evaluated at 100°C, 7.8 atmospheres from Wilke and Lee.[21]

Helium. Grade AA - U.S. Navy

Molecular weight	4.0
Density (at $0^{\circ}C$, 760 mm Hg)	0.01114 lbs/ft^3
Thermal conductivity	$97.7 \times 10^{-3} \frac{Btu}{hr\text{-}ft^2(^{\circ}F/ft)}$ at $200^{\circ}F$

Silicone Oil. DC-550 fluid -- Dow-Corning Corporation

Lot number	BB-147
Molecular weight (calculated)	1756
Specific gravity	1.07
Chemical composition	Methyl-phenyl silicone
Viscosity at $100^{\circ}C$	18 cp.

Column Packing. C-22 insulation brick, Johns Manville Corporation

Original form - Fired, diatomaceous bricks

Final form - Mixture of sized particles

U.S. Standard Mesh 30 to 60 (0.0098 in. to 0.0234 in.)

Appendix II. Solution of the Differential Equation of the Chromatographic Model

The differential equation for the chromatographic model,

$$D \frac{\partial^2 c}{\partial z^2} = V \frac{\partial c}{\partial z} + \frac{\partial c}{\partial \tau}, \qquad (24)^*$$

has been derived from material balance over a small transverse section of the column. The boundary conditions of the model are,

$$\text{at } z = 0, \quad \delta(\tau) = Vc - D\frac{\partial c}{\partial z} \quad \text{for } \tau > 0, \qquad (25a)$$

$$\text{at } z = L, \quad \frac{\partial c}{\partial z} = 0 \quad \text{for } \tau > 0, \qquad (25b)$$

$$\text{and when } \tau = 0, \; c = 0. \qquad (25c)$$

Using the substitution

$$c \equiv \psi \exp\left(\frac{Vz}{2D} - \frac{V^2\tau}{4D}\right),$$

we may write equation (24) as

$$D \frac{\partial^2 \psi}{\partial z^2} = \frac{\partial \psi}{\partial \tau}, \qquad (26)$$

and equation 25 at $z = 0$, for $\tau > 0$

$$\delta(\tau) = \left[\frac{V}{2}\psi - D\frac{\partial \psi}{\partial z}\right] \exp\left[-\frac{V^2\tau}{4D}\right], \qquad (27a)$$

and at $z = L$, for $\tau > 0$

$$\frac{\partial \psi}{\partial z} + \frac{V}{2D}\psi = 0, \qquad (27b)$$

$$\text{and when } \tau = 0, \quad \psi = 0. \qquad (27c)$$

---

* Also designated as Eq. (2) on page 15.

Now this system of equations will be solved by the method of the Laplace transformation. The definition of the transforms will be taken as:

$$Y(z) = \int_0^\infty e^{-p\tau} \psi(z,\tau)d\tau$$

Equations (26) and (27) are then written

$$D \frac{d^2Y}{dz^2} = pY, \tag{28}$$

and at $z = 0$,

$$\frac{V}{2} Y - D \frac{dY}{dz} = 1, \tag{29a}$$

and at $z = L$,

$$\frac{dY}{dz} + \frac{V}{2D} Y = 0. \tag{29b}$$

The general solution of Eq. (28) may be written directly as

$$Y = a_1 e^{(p/D)^{1/2}z} + a_2 e^{-(p/D)^{1/2}z}. \tag{30}$$

Then at $z = 0$, we have

$$\frac{V}{2} (a_1 + a_2) - \sqrt{pD}\,(a_1 - a_2) = 1, \tag{31a}$$

and at $z = L$,

$$\frac{V}{2} \left(a_1 e^{(p/D)^{1/2}L} + a_2 e^{-(p/D)^{1/2}L}\right) + \sqrt{pD} \left(a_1 e^{(p/D)^{1/2}L} - a_2 e^{-(p/D)^{1/2}L}\right) = 0. \tag{31b}$$

It follows by rearrangement that

$$a_1 = \frac{\sqrt{pD} - \frac{V}{2}}{-(\frac{V}{2} - \sqrt{pD})^2 + (\frac{V}{2} + \sqrt{pD})^2 \; e^{2(p/D)^{1/2}L}},$$

and

$$a_2 = \frac{\sqrt{pD} + \frac{V}{2}}{(\frac{V}{2} + \sqrt{pD})^2 - (\frac{V}{2} - \sqrt{pD})^2 \; e^{-2(p/D)^{1/2}L}}.$$

At z = L, the solution to the differential equation (28) is

$$Y = \frac{(\sqrt{pD} - \frac{V}{2})\ e^{(p/D)^{1/2}L} + (\sqrt{pD} + \frac{V}{2})\ e^{(p/D)^{1/2}L}}{-(\frac{V}{2} - \sqrt{pD})^2 + (\frac{V}{2} + \sqrt{pD})^2\ e^{2(p/D)^{1/2}L}}, \tag{32}$$

which may also be written

$$Y = \frac{\dfrac{2\sqrt{pD}\ e^{-(p/D)^{1/2}L}}{(\frac{V}{2} + \sqrt{pD})^2}}{\left(\dfrac{\frac{V}{2} - \sqrt{pD}}{\frac{V}{2} + \sqrt{pD}}\right)^2 e^{-2(p/D)^{1/2}L}}. \tag{32a}$$

In this form, the denominator may be expanded in the manner of the series

$$\frac{1}{1 - x^2} = 1 + x^2 + x^4 + \ldots\ldots$$

giving

$$Y = \frac{2\sqrt{pD}}{(\frac{V}{2} + \sqrt{pD})^2}\ e^{-(p/D)^{1/2}L}\left[1 + \left(\frac{\frac{V}{2} - \sqrt{pD}}{\frac{V}{2} + \sqrt{pD}}\right)^2 e^{-2(p/D)^{1/2}L} + \ldots\right]. \tag{33}$$

It is apparent that, as $L \longrightarrow \infty$, all terms beyond the first of the series are negligible, so, to a first approximation, L may be assumed large and the second and subsequent terms of the expansion neglected.

To obtain the inverse of Eq. (33), the equation may now be written

$$Y = \frac{2}{\sqrt{D}}\ \frac{p^{1/2}}{(\beta_1 + p^{1/2})^2}\ e^{-\beta_2 p^{1/2}} = \frac{2}{\sqrt{D}}\ p\left[\frac{1}{p^{1/2}\ (\beta_1 + p^{1/2})^2}\ e^{-\beta_2 p^{1/2}}\right], \tag{34}$$

where, be definition, $\beta_1 = \dfrac{V}{2\sqrt{D}}$

and $\beta_2 = \dfrac{L}{\sqrt{D}}$.

The inverse transform of the portion of the equation in brackets is found to be:[31]

$$f(\tau) = 2\pi^{-1/2}\tau^{1/2}e^{-\beta_2^2/4\tau} - (2\beta_1\tau + \beta_2)\, e^{(\beta_1\beta_2+\beta_1^2\tau)}\operatorname{erfc}\left(\frac{\beta_2}{2\tau^{1/2}} + \beta_1\tau^{1/2}\right), \tag{35}$$

and at $\tau = 0$, $f(\tau) = 0 = f(0)$.

The term erfc (x) denotes the counter error function, which is,

$$\operatorname{erfc}(x) = 1 - \operatorname{erf}(x).$$

The inversion is completed by

$$\mathcal{L}^{-1}y = \frac{2}{\sqrt{D}}\left[\frac{d\,f(\tau)}{d\,\tau} + f(0)\right],$$

where

$$\frac{d\,f(\tau)}{d\,\tau} = \frac{2}{\sqrt{\pi}}\left(\beta_1^2\,\tau^{1/2} + \frac{1}{2\tau^{1/2}}\right)e^{-\beta_2^2/4\tau}$$

$$- \left(2\beta_1^3\,\tau + 2\beta_1 + \beta_1^2\beta_2\right)\left[e^{(\beta_1\beta_2 + \beta_1^2\,\tau)}\operatorname{erfc}\left(\frac{\beta_2}{2\tau^{1/2}} + \beta_1\tau^{1/2}\right)\right] \tag{36}$$

and $f(0) = 0$.

After we substitute the original nomenclature, the solution of the differential equation is

$$C = \frac{2}{\sqrt{D}}\left[\frac{2}{\sqrt{\pi\,\tau}}\left(\frac{V^2\,\tau}{4D} + 1/2\right)e^{-(L-V\tau)^2/4D\tau}\right.$$

$$\left. - \frac{1}{\sqrt{D}}\left(\frac{V^3\tau}{4D} + V + \frac{V^2L}{4D}\right)\quad e^{VL/D}\operatorname{erfc}\frac{L + V\tau}{2\sqrt{D\tau}}\right]. \tag{37}$$

This solution can be written in a dimensionless form by substitution of the parameters

$$s \equiv \frac{VL}{D} \qquad \text{and} \qquad \eta \equiv \frac{D}{L^2}\tau = \frac{D\,t}{L^2\gamma} .$$

Then at z = L the solution is, in the dimensionless form,

$$CL = \frac{4}{\sqrt{\pi\eta}} \left(\frac{s^2\eta}{4\eta} + \frac{1}{2} \right) e^{-(1-s\eta)^2/4\eta}$$

$$- 2\left(\frac{s^3\eta}{4} + s + \frac{s^2}{4} \right) e^{s} \operatorname{erfc}\left(\frac{1 + s\eta}{2\sqrt{\eta}} \right) . \qquad (38)$$

The left side of Eq. (38) is dimensionless when the original assumptions of unit column area and unit molar feed are incorporated.

Numerical Evaluation

For ease of computation, it is better to consider the quantity ($s\eta$) as the independent variable. For calculation of a concentration-time curve at the outlet of the chromatogram (z = L), a value of s is set and then $s\eta$ is varied from 0.0 through 1.0 to the point where CL becomes insignificant. The calculation of time-concentration curves is done readily because the equation contains only well-tabulated functions. However, since the solution is actually the small difference between two much larger numbers, high accuracy of calculation is required to give useable answers.

For this work is was desired to have a large family of time-concentration curves available for comparison with experimental results. The equation was programmed for solution by an IBM 650 computer. Machine computation required modification of Eq. (38) in order to calculate values for the counter-error function. The asymptotic expansion of the counter-error function is:

$$\operatorname{erfc}(x) = \pi^{-1/2} e^{-x^2} \left[\frac{1}{x} - \frac{1}{2x^3} + \frac{1\cdot 3}{2^2 x^5} - \frac{1\cdot 3\cdot 5}{2^3 x^7} + \cdots\cdots \right] .$$

Then Eq. (38) becomes

$$CL = \frac{2}{\sqrt{\pi\,\eta}}\, e^{-\frac{(1 - s\eta)^2}{4\eta}} \left\{ \frac{2}{\sqrt{\pi}} \left(\frac{s^2\eta}{4} + \frac{1}{2} \right) - \left[\frac{s^3\eta}{4} + s + \frac{s^2}{4} \right] \left[\frac{2\sqrt{\eta}}{1 + s\eta} - \frac{(2\sqrt{\eta})^3}{2\,(1+s\eta)^3} + \ldots\ldots \right] \right\} . \tag{39}$$

The program for solution of the IBM 650 computer was easily written in the system prepared by members of the Bell Telephone Laboratories.[27] This is an interpretive system which transforms the IBM 650 computer into a three-address, floating-decimal, general-purpose computer. The program system is generally known as the F.L.O.P.S. routine.

In the compurational program, it must be remembered that the expansion used for erfc (x) is an asymptotic formula that is valid for large values of x ($x > 4$). Time-concentration calculations with $s = 15$ required full use of the 30 terms of the expansion whose coefficients were included as program constants. The program was so designed that it would indicate if all terms of the expansion were calculated. This would occur when no term of the expansion was less than 10^{-7}.

Time-concentration curves for values of $s\eta < 15$ were computed with desk calculator and tables of the functions.[32,33] Selected curves for s calues ranging from 3.5 to 900 are shown in Figs. 1 and 2. In Table IX the CL values are given for various $s\eta$ values for the families of curves shown in Figs. 1 and 2. Also shown are the value of the maximum ordinate and its location on the $s\eta$-axis.

Table IX

A. Computed values of the CL ordinate of Equation (38) for various values of the s parameter (3.75 to 37.5)

$s\eta$	s = 3.75	7.5	15	25	37.5
0.1	0	0	0	0	0
0.2	0.17	0.01	0	0	0
0.3	0.53	0.16	0.01	0	0
0.4	0.80	0.48	0.12	0.02	0
0.5	0.93	0.79	0.43	0.16	0.04
0.6	0.94	0.99	0.83	0.55	0.29
0.7	0.89	1.06	1.14	1.06	0.87
0.8	0.81	1.03	1.29	1.45	1.51
0.9	0.72	0.94	1.27	1.57	1.84
1.0	0.63	0.85	1.13	1.44	1.75
1.1	0.54	0.70	0.95	1.18	1.39
1.2	0.46	0.59	0.75	0.88	0.97
1.3	0.39	0.48	0.58	0.62	0.61
1.4	0.34	0.39	0.43	0.41	0.35
1.5	0.29	0.32	0.32	0.26	0.19
1.6	0.24	0.26	0.23	0.16	0.10
1.7	0.20	0.20	0.16	0.10	0.05
1.8	0.17	0.16	0.11	0.06	0.02
1.9	0.15	0.12	0.08	0.03	0.01
2.0	0.12	0.10	0.05	0.02	0
2.5	0.05	0.03	0.01	0	0
Maximum point					
CL	0.945	1.06	1.30	1.57	1.86
$s\eta$	0.56	0.72	0.83	0.895	0.929

Table IX

B. Computed values of the CL ordinates of Equation (38) for various values of the s parameter (100 to 2000)

$s\eta$	s = 100	200	500	900	2000
0.65	0.05	0	0	0	0
0.70	0.01	0	0	0	0
0.75	0.53	0.09	0	0	0
0.80	1.12	0.45	0.02	0	0
0.85	1.85	1.35	0.29	0.03	0
0.90	2.51	2.68	1.84	0.81	0.06
0.925	2.73	3.31	3.31	2.42	0.72
0.95	2.87	3.78	4.90	5.05	3.65
0.975	2.90	4.02	6.05	7.61	9.51
1.00	2.84	4.00	6.31	8.47	12.62
1.025	2.69	3.74	5.64	7.07	8.96
1.05	2.48	3.30	4.36	4.60	3.57
1.075	2.23	2.76	2.94	2.36	0.87
1.10	1.95	2.20	1.75	0.95	0.12
1.15	1.40	1.21	0.44	0.08	0
1.20	0.93	0.57	0.07	0	0
1.25	0.57	0.23	0.01	0	0
1.30	0.33	0.08	0	0	0
1.35	0.18	0.03	0	0	0
1.40	0.10	0.01	0	0	0
1.45	0.05	0	0	0	0
1.50	0.02	0	0	0	0
1.55	0.01	0	0	0	0
Maximum point					
CL	2.90	4.04	6.34	8.49	12.64
$s\eta$	0.972	0.985	0.994	0.997	0.9985

Appendix III. Thermal-Conductivity-Cell Calibration

Purpose

A calibration of the thermal conductivity (T.C.) cell was conducted for the three solutes in the G.L.C. experimental prorgam in order to be able to calculate the concentrations of the solute in the column effluent.

Equipment and Procedure

The apparatus for this calibration was fitted into the G.L.C. experimental facilities so that the same gas flow and temperature controllers, pressure gage, recorder, and T.C. cell circuitry of the G.L.C. experiments could be used. The equipment consisted basically of a saturator, a vapor heater, and the T.C. cell and its recorder.

Helium at a constant pressure was brought from the control panel to the reference side of the T.C. cell. Zeroing of the bridge circuit was obtained by bypassing the helium directly to the sample side of the T.C. cell.

From the reference side of the T.C. cell, the gas flowed to the base of a thermostated saturator which was made of a 48-in. section of 1-in. industrial-glass tubing. The tube was packed with 1/4-in. ceramic saddles and filled to approximately 2/3 of capacity with the solute being calibrated. Saturator temperature was regulated by the Micro-Max temperature indicator-controller. This controlled the passage of current to the nichrome ribbon heater wrapped along the length of the saturator. The saturator was enclosed in a 4-ft section of 4-in. glass tubing for insulation.

The top of the saturator was fitted with the following:

1. An iron-constantan thermocouple, connected to the temperature controller, which measured the temperature between the two glass tubes.

2. A copper-constantan thermocouple which measured the temperature of the solute-helium vapor leaving the saturator.

3. A pressure connection to the 100-psi gage at the control panel which indicated the saturator pressure.

4. An expansion valve, heated with an electrical tape, for control of the saturator pressure and the vapor flow rate.

The vapor, after expansion, went through an 8 ft. coil of 1/4-in.-O.D. copper tubing immersed in an oil bath at 100°C. Then the vapor passed through the sample side of the T.C. cell. The T.C.-cell temperature was approximately 100°C, the normal temperature for the cell during the experimental work.

A range of solute concentrations in the helium gas was obtained by varying the saturator temperature and pressure. Mole fractions of the solute were calculated from its vapor pressure at the saturator temperature, and the total column pressure. The solutes and helium were assumed to behave as perfect gases.

Results and Discussion

The results of the T.C. calibration are shown in Fig. 22 in the form of the recorder response in mv plotted against the mole fraction of the solute. The slopes of these curves were used in the IBM calculations of the G.L.C. data. The T.C. cell was designed to be fairly insensitive to variations in the gas flow. In the calibration of acetone, a 7-fold increase in the volumetric flow rate resulted in approximately a 10% decrease in the recorder response.

The experimental data and calculated results are shown in Table X.

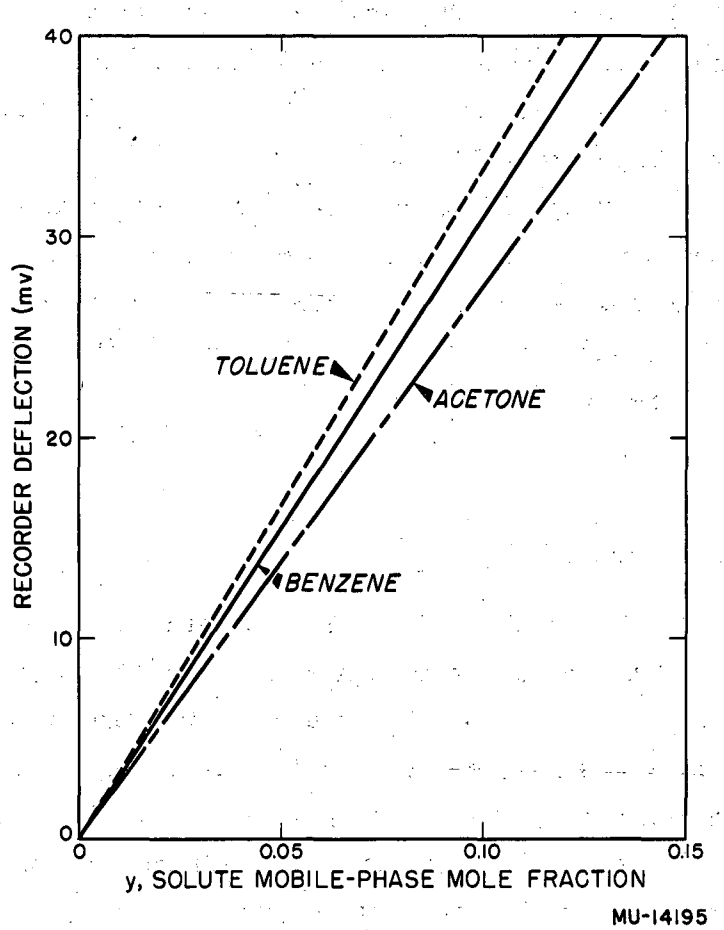

Fig. 22. T.C.-cell circuit response to solute mobile-phase concentration.

Table X

Thermal-conductivity-cell calibration data and calculated results

Run	Barometer (psia)	Saturator Temp. (°C)	Saturator Press (psig)	WTM flow $ft^3/min \times 10^2$	y mole fraction	Recorder response (mv)
			Benzene			
H-1	14.37	27.25	10.0	0.42	0.083	25.40
H-2	"	26.50	15.0	0.42	0.067	21.16
H-3	"	26.75	20.0	0.60	0.058	18.00
H-4	"	26.75	25.0	0.67	0.051	15.64
H-5	14.40	27.00	35.0	0.85	0.041	12.36
H-6	"	26.75	50.0	1.08	0.031	9.56
H-7	"	26.50	60.0	1.23	0.027	8.34
H-8	"	26.50	75.0	1.42	0.022	6.88
H-9	"	26.25	90.0	1.562	0.019	5.84
			Toluene			
J-1	14.38	44.25	5.1	0.54	0.072	23.36
J-1a	"	46.7	5.0	1.75	0.080	24.12
J-1b	"	51.1	5.1	2.78	0.097	25.08
J-2	"	43.3	15.1	0.52	0.045	16.52
J-2a	"	52.5	15.32	1.67	0.068	15.32
J-2b	"	42.4	15.1	3.33	0.043	13.96
J-3	"	39.25	50.1	0.58	0.017	6.34
J-3a	"	40.75	50.0	1.58	0.018	5.90
J-3b	"	43.3	50.2	3.00	0.021	6.28

(continued)

Table X (continued)

Run	Barometer (psia)	Saturator Temp. (°C)	Saturator Press. (psig)	WTM flow $ft^3/min \times 10^2$	y mole fraction	Recorder response (mv)
			Acetone			
I-1	14.45	28.25	5.1	0.44	0.251	83.0
I-2	"	27.75	10.1	0.52	0.195	62.9
I-3	"	27.25	14.9	0.66	0.160	50.0
I-4	"	27.0	20.1	0.74	0.134	41.4
I-5	"	27.0	30.1	0.92	0.104	30.85
I-6	"	27.0	40.0	1.18	0.085	23.8
I-7	"	27.5	50.35	1.38	0.073	19.86
I-8	"	27.0	60.25	1.56	0.062	17.28
I-9	"	27.25	70.3	1.68	0.055	15.01
I-10	"	27.25	79.9	1.90	0.050	13.35
I-11	"	26.75	90.0	2.05	0.044	12.0
I-12	"	27.0	100.0	2.30	0.041	10.88
I-12a	"	26.25	99.8	0.58	0.040	11.64
I-12b	"	26.13	100.0	1.31	0.039	11.38
I-12c	"	27.38	99.8	4.37	0.041	10.68
I-13a	"	26.75	50.0	3.79	0.072	19.44
I-13b	"	27.50	50.0	1.98	0.073	20.12
I-13c	"	26.75	50.1	0.78	0.072	20.87

Appendix IV. Equilibrium Coefficient Measurements

Introduction

Design of G.L.C. or other gas-liquid contacting equipment requires a knowledge of, or a means of predicting, the solute equilibrium relationship between the two phases. For solute-solvent systems where both are volatile, standard vapor-liquid equilibrium stills are the general source of this data.

However, in G.L.C. the differences in volatilities between solute and solvent is great and often there is no appreciable solvent vapor pressure. Therefore, normal vapor-liquid techniques will not furnish the desired data. A dynamic method for determination of G.L.C. equilibrium coefficients has been described by Porter, Deal, and Stross.[11]

A static method of determining the equilibrium relationships of G.L.C. solute-solvent systems was developed for this work. Basically, it involves the measurement of the solute vapor pressure over a solute-solvent mixture of known concentration.

Equipment

The overall arrangement of the equilibrium apparatus is shown in Fig. 23. Though installed on the G.L.C. equipment rack, the equilibrium equipment used only the helium-gas supply and the 6-point recorder of the G.L.C. apparatus.

Major components of the equilibrium equipment are: the equilibrium vessel, the pressure transducer, the manometer, and the pressure-vacuum manifold. Auxiliary components are the vacuum pump, cold trap, D.C. voltage supply, and the associated electrical circuits connected to the 6-point, 10-mv recorder.

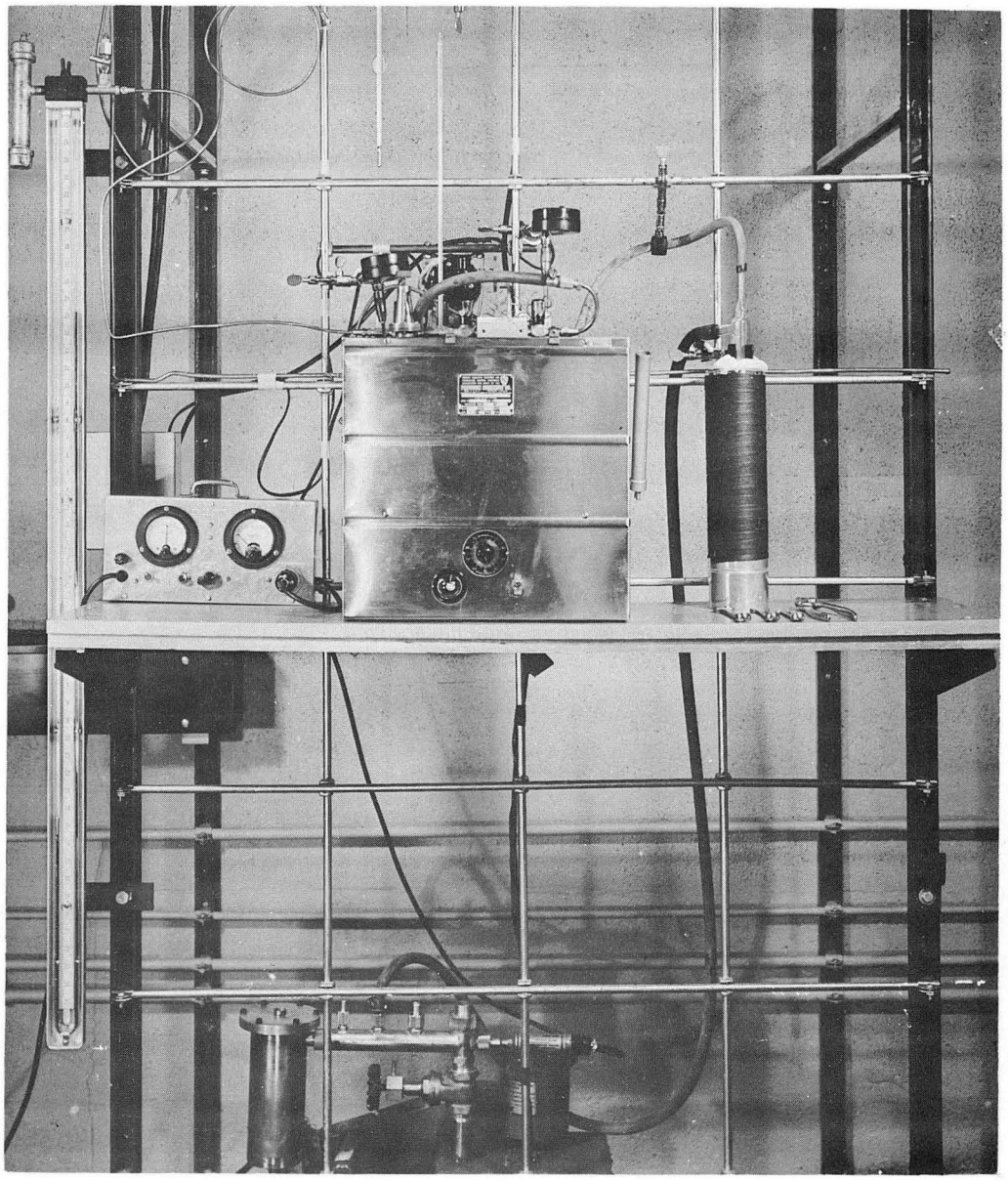

ZN-1786

Fig. 23. Equipment arrangement for equilibrium determinations.

Equilibrium vessel. The equilibrium vessel, Fig. 24, was constructed of 1-in.-I.D. brass tubing (0.030-in. wall thickness), 4.75 in. long and closed at the bottom. A 3/16-in. flange, fitted with an O ring, was soldered to the top and a short length of 1/4-in.-O.D. copper tubing, with standard flare fitting, was attached just below the flange for connection with the pressure transducer.

The closure for this vessel was constructed in two pieces. The first was the sealing flange, fitted with the crushing rod. This 1/4-in. steel rod passed through the 1/8-in. brass sealing flange into the vessel. A 1/2-in. brass "Sylphon" seal is attached at one end to the sealing flange and at the other, to a disc soldered on the crushing rod. This seal makes the vessel vacuum tight while still allowing movement of the crushing rod. A spring clip was threaded on the base of the crushing rod to hold the solute-filled amplues.

The second part of the closure unit was the mount for the screw fitting that was used to position the crusher rod. It was constructed of brass with a steel screw and collar. The collar was slotted to fit over the crushing rod.

All three pieces were assembled together with six 5-40 screws.

Pressure transducer. The Giannini pressure transducer (model 47155)*, used for these experiments, utilized a pressure capsule that operated the wiper of a precision potentiometer in direct proportion to the applied pressure. The transducer was designed for absolute pressure measurement between 0 to 100 psi. Though the instrument's range far exceeded the range of pressures measured in these experiments, proper use of the dc voltage applied to the transducer gave full-scale deflection of the recorder for absolute pressures of one atmosphere. The transducer would reproduce a given pressure with a ± 20 mm Hg accuracy.

Associated with this transducer were the necessary electrical components to furnish the desired output to the recorder. These units

---

* G. M. Giannini and Co., Inc., East Orange, N. J.

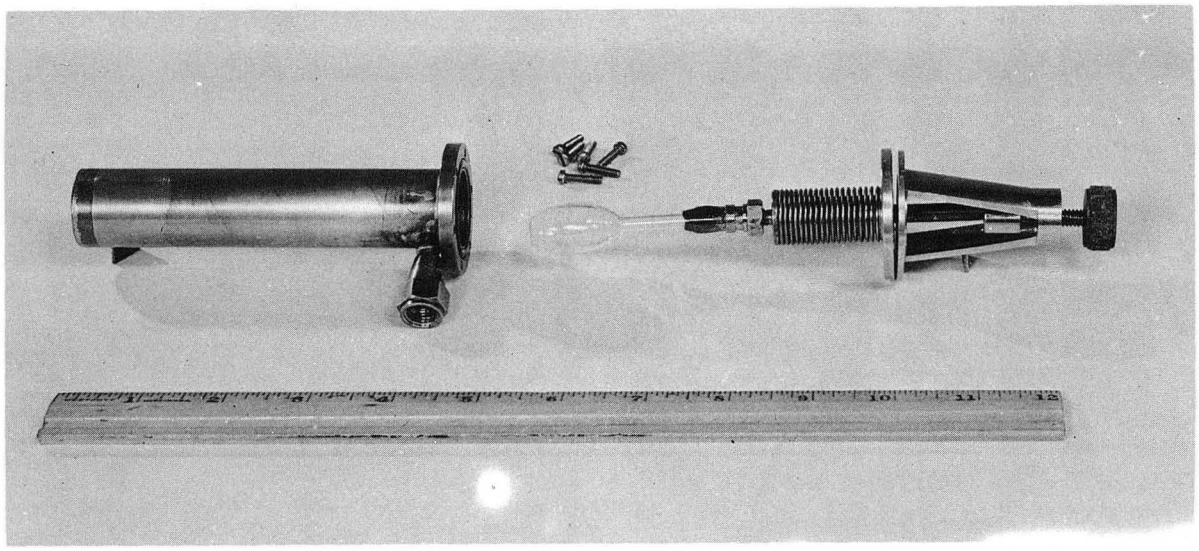

ZN-1779

Fig. 24. Exploded view of equilibrium vessel fitted with ampule.

consisted of a stabilized dc power supply, a voltage-divider circuit, and a 10-mv Leeds and Northrup recorder.

Mercury manometer. A 50-in. Merium U-tube manometer filled with mercury was used for calibrating the transducer. The manometer was connected to the transducer through the pressure-vacuum manifold, and could be isolated from the manifold by a needle valve.

Pressure-vacuum manifold. This unit was machined from brass bar stock to accommodate 3 needle valves and a fitting for connection to the pressure transducer. As mentioned before, one valve opened the manifold to the U-tube manometer. The other two valves were connected with the helium supply (at a pressure of approximately 15 psig) and the the vacuum system. The latter consisted of a Kinney vacuum pump connected to the manifold through a liquid-air cold trap. The transducer was connected to the manifold by a length of rubber vacuum tubing.

Procedure

Ampule preparation. Prior to the equilibrium measurements, it was necessary to prepare ampules filled with varying amounts of the solutes. Glass tubing, 6-mm in diameter, was blown into ampules with volumes of 1/2 ml to 6 ml. After cleaning and drying, each ampule was weighed, filled with solute, sealed off under vacuum after being chilled with liquid air, and given a final weighing to determine the amount of solute added.

Transducer calibration. The pressure transducer was calibrated before each series of equilibrium runs were performed. This was done by adjusting the dc-supply voltage to a valve that would give full-scale deflection of the recorder. The pressure in the transducer had been set by use of the pressure and vacuum controls to a value somewhat higher than expected in the runs. The parometer and U-tube manometer readings were used to measure the absolute pressure in the transducer. Then, the transducer was

evacuated in stepwise pressure increments down to the lowest pressure obtainable with the vacuum pump. At each step, pressure and recorder readings were taken and these data were then plotted to give a calibration chart of recorder deflection against absolute pressure.

Equilibrium determinations. The equilibrium determinations were performed in the following manner:

1. An amount of silicone oil solvent was placed in the equilibrium vessel, and its weight was determined by weighing before and after filling. The approximate amount of oil used was determined by the solute-solvent ratio desired for the run and also certain volumetric limits on the quantity of oil.

2. The ampule was placed in the spring clip of the crushing rod and the clip was, in turn, positioned on the thread end of the rod to give slight clearance from the bottom of the vessel. The three units of the equilibrium vessel were assembled and then attached to the transducer, Fig. 25. The whole assembly (Fig. 26) was placed in a stirred oil bath at 100 °C. It was supported in the bath by a yoke mount that permitted oscillation of the unit by an eccentric rocker. Rocking rate was 180 c.p.m.

3. The pressure in the vessel and transducer was lowered to approximately 100 mm absolute while the temperature reached an equilibrium. Then the units were evacuated to the minimum pressure obtainable and isolated from the rest of the system by the needle valve on the manifold side of the transducer.

4. The valve between the transducer and the equilibrium vessel was then closed and the ampule crushed. Equilibration of the solute and solvent oil was allowed to take place for a period of time estimated to be sufficient on the basis of the quantity of material present. The greater the weight fraction of solute, the longer the time allowed for equilibration.

5. The valve between the transducer and the equilibrium vessel was then opened. Further time was allowed for the pressure to rise and reach a constant value, which was the recorded final pressure.

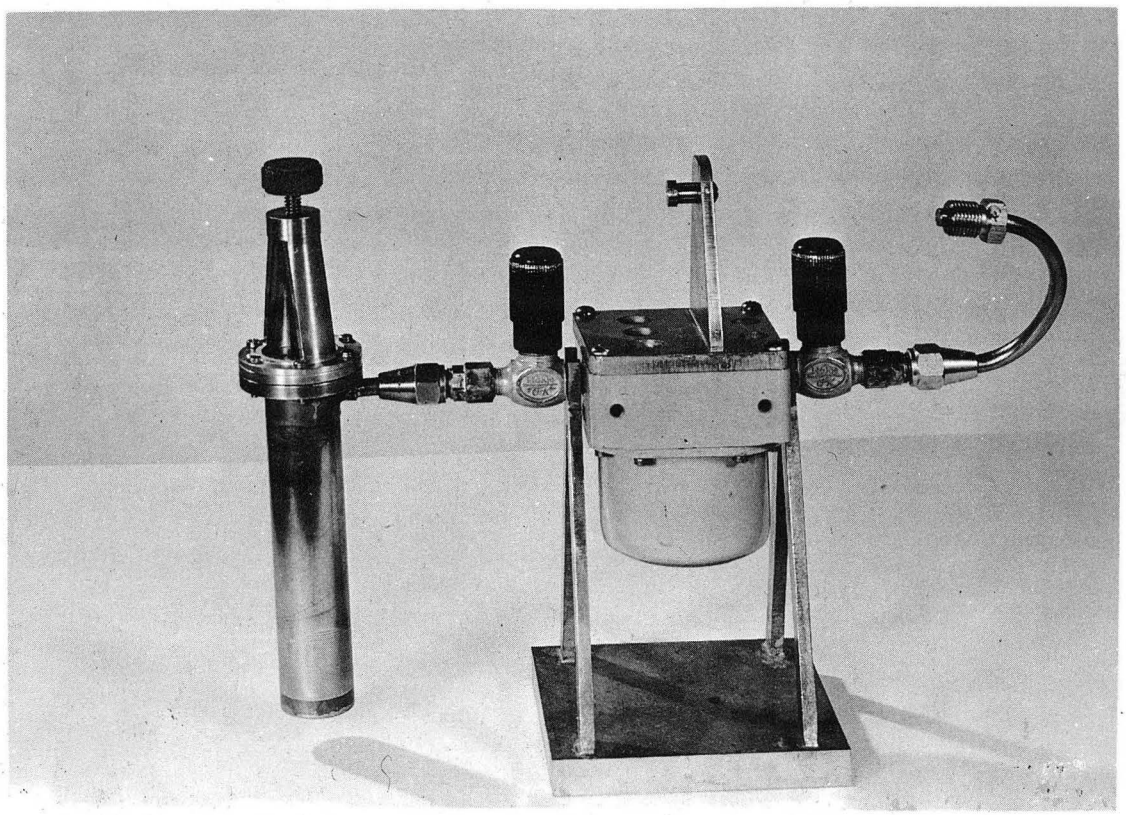

ZN-1782

Fig. 25. Equilibrium vessel and pressure transducer assembled and mounted in rocker yoke.

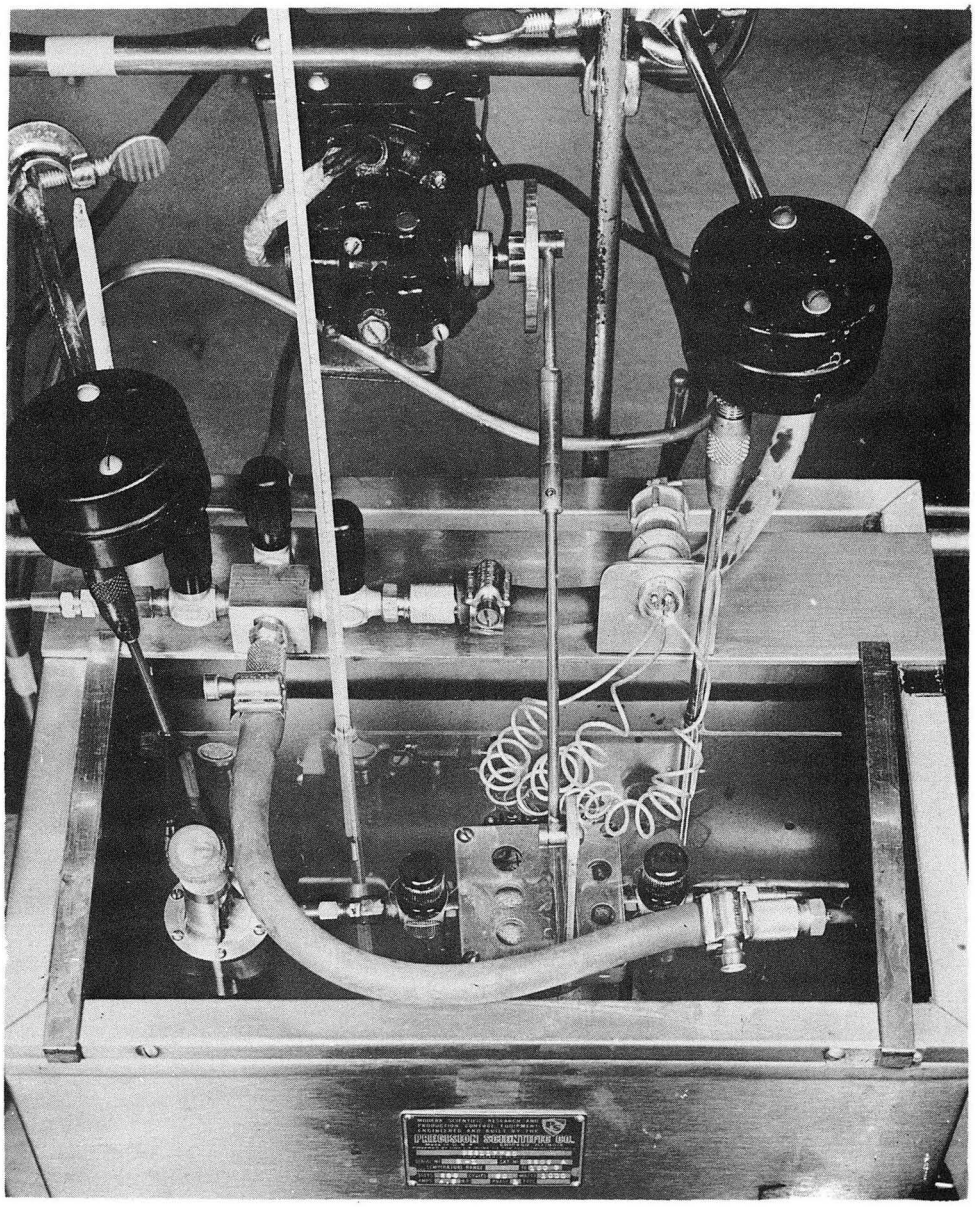

ZN-1784

Fig. 26. Detail of assembled equilibrium apparatus immersed in the constant-temperature oil bath.

6. The assembly was removed from the oil bath and vented to atmospheric pressure. The equilibrium vessel was detached from the transducer, emptied of the solute and oil, and then cleaned and dried in preparation for the next determination.

Discussion

Experimental results. The data from the equilibrium determinations are shown in Table XI. Fig. 27 is a plot of the molar ratios of the solute and solvent liquid against the observed pressure rise. With the high k values of toluene, relatively small amounts of the solute were vaporized. With acetone and, to a lesser degree, benzene, the amount of solute vaporized was a significant percentage of the total amount of solute present. The volume of the equilibrium vessel and the transducer was measured and found to be 162 ml. The volumes of the liquids were estimated from their densities and then subtracted from the volume of the two vessels. The perfect gas law was applied to calculate the amount of solute vaporized. The amount of solute remaining in the liquid was figured by differences and the solute-solvent molar ratio, n', was then calculated. The equivalent G.L.C. liquid-phase concentration, n, was found by multiplying the solute-solvent molar ratio by the moles of solvent per ft^3 of column packing, N. The vapor concentration, c, was calculated using the perfect gas law and the measured pressure.

The values of n and c are shown in Fig. 28 on a logarithmic plot. Benzene exhibits an almost linear relation between the two concentrations. Both toluene and acetone show that the liquid phase concentration increases faster than the vapor concentration. G.L.C. data obtained from the sample-size variations with toluene are also plotted in Fig. 28. The c values of these runs were calculated from the maximum mobile phase concentration at the solute peak. The n values were calculated from the c values and the partition coefficients, k. Points from benzene and acetone data are also shown. These points are the average of data from several runs as indicated in Table XI.

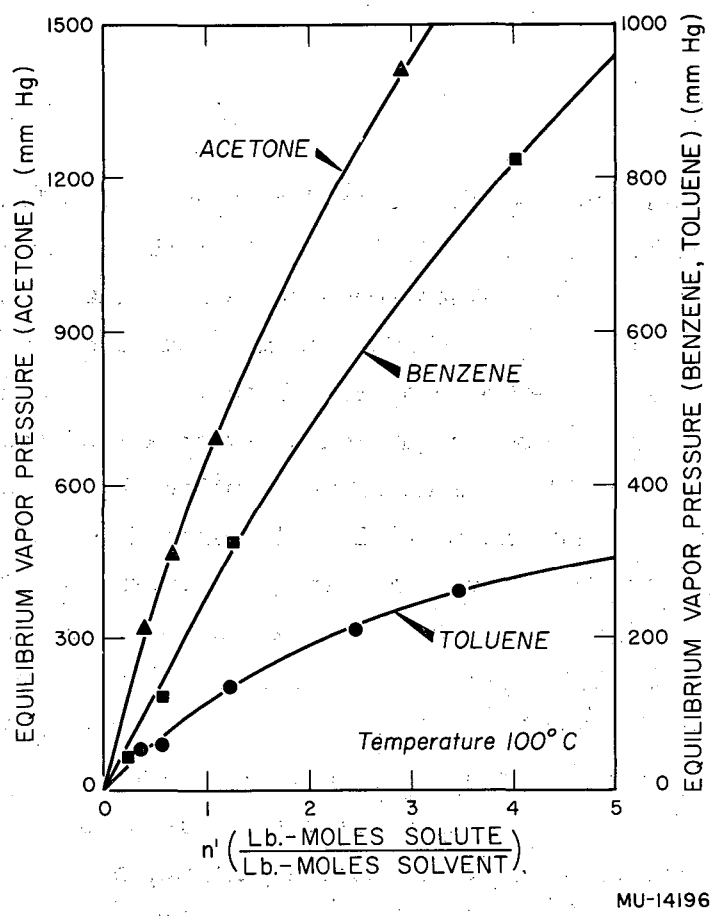

Fig. 27. Solute equilibrium vapor pressure as a function of liquid-phase concentration.

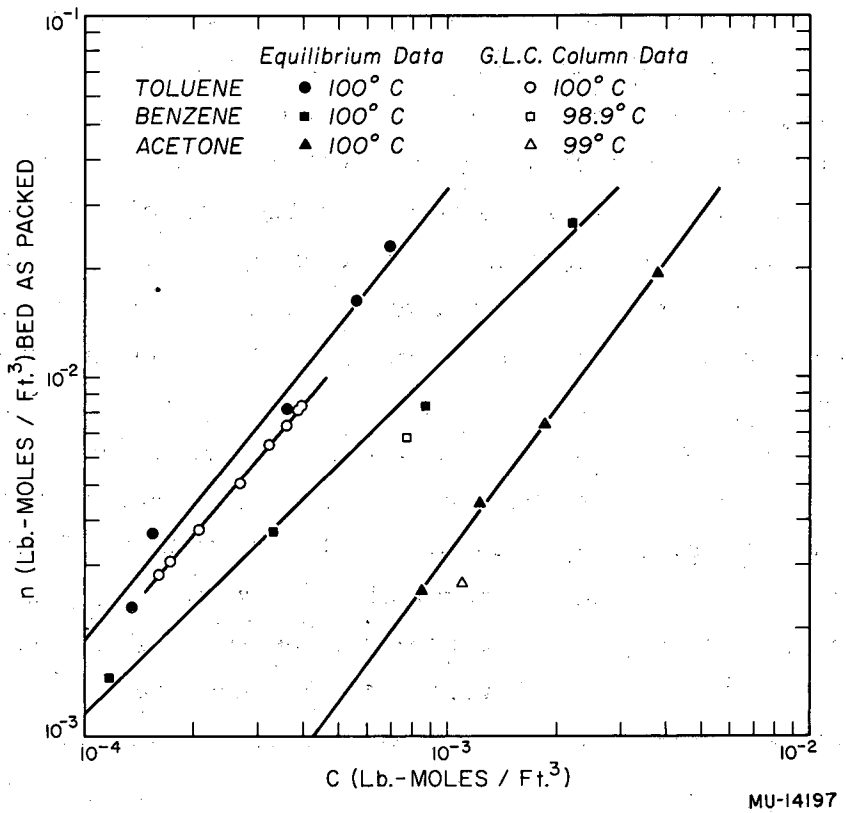

Fig. 28. Mobile-phase concentration as a function of liquid-phase concentration.

Errors. The sources of errors in these measurements were of the following nature:

1. Weighing errors resulting from contamination of the outer surfaces of the glassware and equilibrium vessel during the filling operations. Use of proper techniques minimize these effects.

2. The violent rupture of the ampule in the evacuated equilibrium vessel caused splashing of the solvent oil into the bellows folds of the sylphon seal, and, to some extent, into the 1/4-in.-O.D. tubing that connects the vessel to the transducer. Some oil was lost to the transducer when the valve between the two units was opened. In run K-4, the ampule was unintentionally crushed with the valve between the equilibrium vessel and transducer open. The errors resulting from these circumstances are unpredictable and can be minimized by long equilibration times and improved methods of introducing the solute into the solvent.

3. Transducer-calibration and reproducibility errors are the third possible types of errors. Use of a transducer with a smaller pressure range, i.e. 0 to 15 or 0 to 30 psia, would give more accurate data. In the toluene determinations (except M-5), the transducer voltage was set to give a pressure-voltage ratio of 200 mm Hg/mv at the recorder. Benzene runs were made with approximately 75 mm/mv, and the ratio was varied for the acetone run to accommodate the high volatility of the solute.

Conclusion

The partition coefficients determined by these static-equilibrium measurements differ from the G.L.C. column values by as much as 40%. Toluene determinations show that the equilibrium coefficients have the same variation with concentration as those calculated from the column elution diagrams.

Table XI

Equilibrium experimental data at 100°C

Run designation	Solute weight gms	Solvent weight gms	Equilibrium distributions (gm-moles x 10^{-2}) Solute liquid	Solute vapor	Solvent liquid	Solute/Solvent = n' in liquid	n Solute lb-moles ($ft^3 x 10^{-3}$)	Observed pressure rise (mm Hg)	c Solute lb-moles ($ft^3 x 10^{-3}$)	k
					Toluene					
K-4	0.4902	25.7170	5.03	0.29	14.6	0.345	2.29	50.2	0.135	17.0
K-1	0.7973	26.3790	8.33	0.33	15.0	0.555	3.69	57.0	0.153	24.1
K-2	1.6784	25.1010	17.42	0.78	14.3	1.22	8.12	134	0.36	22.6
K-3	3.3806	25.4828	35.5	1.2	14.5	2.45	16.3	207	0.556	29.3
M-5	4.1560	22.0227	43.6	1.5	12.6	3.46	23.0	258	0.693	33.2
Column Data (Runs 117 to 123, 39, 40) shown on Fig. 28.										
					Benzene					
L-1	0.2420	22.4120	2.84	0.26	12.8	0.22	1.46	43.4	0.117	12.5
L-2	0.4596	16.1748	5.14	0.76	9.2	0.56	3.72	123	0.33	11.3
L-3	0.8544	11.1845	8.8	2.10	6.37	1.26	8.38	322.5	0.867	9.7
L-4	4.1776	21.2454	48.6	4.8	12.1	4.02	26.7	822	2.21	12.1
Column Data (Runs 31, 37)							6.8		0.77	8.9
					Acetone					
M-1	0.4391	26.7498	5.76	1.8	15.2	0.38	2.53	316	0.85	2.98
M-2	0.6256	21.0860	8.0	2.8	12.0	0.67	4.45	465	1.25	3.56
M-3	0.6631	10.8655	6.9	4.5	6.2	1.11	7.40	690	1.85	4.00
M-4	2.9265	25.5447	42.4	8.0	14.5	2.92	19.4	1410	3.79	5.12
Column Data (Runs 42 to 45 averaged)							2.67		1.10	2.42

Appendix V. Sample Calculation for Run Number 116

Experimental Data

Room temperature	22.4°C
Column temperature	86.9°C
Barometric pressure	14.54 psia
Column pressure drop	5.10 in. Hg
Wet test meter flow rate, Q	7.5×10^{-3} cfm
Air peak time, t_{pa}	2.865 min
Initial time, t_i	35.795 min
Peak width at one-half peak height, t_5	7.17 min
Final time, t_f	47.025 min
Solute peak time, t_p	45.13 min
Maximum peak height, H_p	11.27 mv

Calculation Constants

Column inlet pressure	100 psig
Water-vapor correction	0.973 ft^3 dry gas/ft^3 saturated vapor
Column area	5.07×10^{-4} ft^2
Column length	7.375 ft
Ratio--column area/entry area	0.372
Length, entry section	0.708 ft
Ratio--column area/valve area	2.58
Length, valve section	0.271 ft
Area, exhaust section	1.97×10^{-4} ft^2
Length, exhaust section	1.04 ft
Void-volume fraction	0.644
Helium density, 0°C and 1 atmos	1.114×10^{-2} lbs/ft^3
Particle size, d_p	1.37×10^{-3} ft
Helium viscosity, 88°C	8.67×10^{-4} lb/ft-min
Helium viscosity, 98°C	8.75×10^{-4} lb/ft-min
Helium viscosity, 105°C	8.91×10^{-4} lb/ft-min
Stationary solvent density, N	6.65×10^{-3} lb-moles/ft^3 of bed

T.C. cell coefficient, M, benzene	3.45×10^{-3} mole fraction/mv
T.C. cell coefficient, M, toluene	3.00×10^{-3} mole fraction/mv
T.C. cell coefficient, M, acetone	3.62×10^{-3} mole fraction/mv
Sample size, benzene, 0.2 ml	4.96×10^{-6} lb-mole
Sample size, toluene, 0.3 ml	6.23×10^{-6} lb-mole
Sample size, acetone, 0.2 ml	6.00×10^{-6} lb-mole
Sample size, acetone, 0.1 ml	3.00×10^{-6} lb-mole
Sample size, acetone, 0.075 ml	2.255×10^{-6} lb-mole
Gas constant, R	19.314 psia-ft^3/lb-mole-$^\circ$K

Column Flow Rate

$$Q_{col} = Q \text{ (water vapor correction)} \frac{p_{bar}}{\frac{p_i + p_o}{2}} \cdot \frac{T_{col}}{T_{wtm}}$$

$$= 7.5 \times 10^{-3} \times 0.972 \times \frac{14.54}{113.29} \times \frac{360.1}{295.6}$$

$$= 1.14 \times 10^{-3} \text{ ft}^3/\text{min}$$

Superficial Velocity

$$V_o = \frac{Q_{col}}{A} = \frac{1.14 \times 10^{-3}}{5.07 \times 10^{-4}} = 2.25 \text{ ft/min}$$

Calculated Void Fraction

$$t_{entry} = \frac{L_{entry}}{V_o} \frac{A_{entry}}{A} = \frac{0.708}{2.25} \times \frac{1}{0.372} = 0.847 \text{ min}$$

$$t_{valve} = \frac{L_{valve}}{V_o} \frac{A_{valve}}{A} = \frac{0.271 \times 1}{2.25 \times 2.58} = 0.0468 \text{ min}$$

$$t_{exit} = \frac{A_{exit} \quad L_{exit} \quad T_{wtm}}{Q \text{ (water-vapor correction) } t_{col}}$$

$$= \frac{1.96 \times 10^{-4} \times 1.04 \times 295.6}{7.5 \times 10^{-3} \times 0.972 \times 360.1}$$

$$= 0.023 \text{ min}$$

$$t_o = \frac{L}{V_o} = \frac{7.375}{2.25} = 3.28 \text{ min}$$

$$t_{col} = t_{pa} - (t_{entry} + t_{valve} + t_{exit})$$

$$= 2.87 - 0.917$$

$$= 1.95 \text{ min}$$

$$\alpha_{calc} = \frac{t_{cal}}{t_o} = \frac{1.95}{3.28} = 0.594$$

<u>Solute Peak Characteristics</u>

$$t_w = t_f - t_i = 47.0 - 35.8 = 11.2 \text{ min}$$

$$s = 32\left(\frac{t_p}{t_w}\right)^2 = 32\left(\frac{45.1}{11.2}\right)^2 = 517$$

$$s' = 32\left(\frac{t_i}{t_w} + 1/2\right)^2 = 32\left(\frac{35.8}{11.2} + 1/2\right)^2 = 435$$

$$t'_p = \left(\frac{t_i}{t_w} + 1/2\right) t_w = 3.69 \times 11.2 = 41.4 \text{ min}$$

$$Pe = s\frac{d_p}{L} = 517 \quad \frac{1.37 \times 10^{-3}}{7.375} = 0.096$$

$$\Delta t = t_p - t'_p = 45.1 - 41.4 = +3.7 \text{ min}$$

$$\frac{L}{s} = \frac{7.375}{517} = 0.0143 \text{ ft}$$

Partition Coefficient

$$(s\eta)_p = \frac{1}{s}\left(\frac{4.3187708}{s} - 2.9925346\right) + 1.000072$$

$$= 0.993$$

$$(t_p)_{col} = t_p - (t_{entry} + t_{valve} + t_{exit})$$

$$= 44.2 \text{ min}$$

$$k = \frac{(t_p)_{col}}{(s\eta)_p} \frac{V_o}{L} - \alpha$$

$$= \frac{4.42 \times 2.25}{0.993 \times 7.375} - 0.644$$

$$= 12.9$$

$$k' = \frac{(t_p)'_{col}}{(s\eta)'_p} \frac{V_o}{L}$$

$$= 11.8$$

Column Exit Concentrations

$$y = H_p M = 11.27 \times 3.45 \times 10^{-3}$$

$$= 0.0389$$

$$C = \frac{y\ p_o}{R\ T_{col}} = \frac{.0389 \times 112}{19.31 \times 360}$$

$$= 6.26 \times 10^{-4}\ \frac{\text{lb-moles}}{\text{ft}^3}$$

$$x = \frac{n}{n + N} = \frac{kC}{kC + N} = \frac{12.9 \times 6.26 \times 10^{-4}}{12.9 \times 6.26 \times 10^{-4} + 6.65 \times 10^{-3}}$$

$$= 0.548^*$$

Approximate Solute Material Balance

$$\omega = C\ t_5\ Q_{col} = 6.26 \times 10^{-4} \times 7.17 \times 1.14 \times 10^{-3}$$

$$= 5.12 \times 10^{-6}\ \text{lb-moles}$$

$$Re = \frac{\rho_{col}\ d_p\ V_o}{\mu_{col}}$$

$$= \frac{6.51 \times 10^{-2} \times 1.37 \times 10^{-3} \times 2.25}{8.67 \times 10^{-4}}$$

$$= 0.232\ .$$

---

* The values of x shown in Table VI were calculated from k' values rather than k values, as shown here.

Appendix VI. G.L.C. Design Problem

Introduction

The purpose of this problem is to show the application of theoretical and experimental results to the design of a large G.L.C. column for an industrial situation. A preliminary cost estimate is also given for the G.L.C. unit and its necessary accessories to show the economic potential of such a unit.

The Separation Problem. In most petroleum refineries, the use of catalytic reformers has increased the quantities of aromatic compounds produced from crude stocks in addition to the general production of higher octane fractions. These aromatics often are more valuable as petrochemical intermediates than they are as gasoline additives or solvents. Various methods have been used for separation of these aromatic fractions into relatively pure components. However, as the molecular structures increase in size, the number of isomers of a particular molecular weight increase. Such is the case with the xylenes and ethylbenzene, all with the same formula C_8H_{10}. The resolution of a refinery cut with a distillation range of 135° to 145°C into its components will be considered. This cut will be processed by a G.L.C. unit to separate it into the following fractions.

Paraffins and naphthenes (15% by volume*). These hydrocarbons will be recycled to the refinery or marketed as solvents. Though n-nonane has a boiling point of 150.8°C, it will be used as the "typical" component of the paraffin fraction.

Ethylbenzene (12% by volume*). This material will be separated for use in organic syntheses, such as the manufacture of styrene.

Mixed meta and para xylenes (45% and 20% by volume, respectively*). This fraction will be sent for further refinement by a fractional-crystallization plant into isomers of high purity. They cannot be readily separated with G.L.C. or distillation equipment.

Ortho xylene (8% by volume*). This material may be used in phthalic anhydride manufacture or in other appropriate organic syntheses.

---

*Figures in parentheses show the feed composition.

Discard fraction. In the G. L. C. separation, a small portion (2% by volume) of the meta and para xylene fraction will be discarded because of its high content of ethyl benzene. This will upgrade the purity of the meta-para xylene cut.

Physical properties. Some physical properties of these chemicals are shown in Table XII.

Basic Design Considerations

A G.L.C. unit will be designed for the processing of 400 lbs per hour of feed stock. Over a period of one year's operation, with 90% running time, the G.L.C. unit will produce about 3 million pounds of finished products with an estimated value of approximately $1,000,000.

Solvent Selection. The solvent selected for this separation is a polyethylene glycol polymer with a molecular weight of 400 ± 20 (P.E.G. 400). Aromatic hydrocarbons have a much higher solubility in P.E.G. 400 than do saturated paraffins and naphthenes. This property makes it possible to remove the paraffinic components after passing them through a short length of G.L.C. column.

Partition Coefficients. Experimental data on partition coefficients are taken from the work of Adlard.[34] The partition coefficients are reported in terms of the solute concentration per unit volume of solvent and now are modified to be expressed in terms of the solute concentration per unit volume of bed. Conversion is made using the solvent liquid-volume fraction. Adlard does not give data for either ethylbenzene or nonane. The values used were obtained by interpolation between m-xylene and toluene for ethylbenzene and between n-octane and n-decane for n-nonane. The solute-solvent data are summarized in Table XIII for the column operating at a temperature of 100°C.

Packing Selection and Characteristics. The column packing, 20 to 40 mesh crushed fire brick, will be impregnated with the P.E.G. 400 at a ratio of 40 parts of P.E.G. 400 solvent to 100 parts of the solid fire brick by weight. The estimated characteristics of this packing are also shown in Table XIII.

Table XII

Some physical properties of the aromatic feed

(Boiling range 135° to 145°C)

Physical properties	Solute				
	Ethyl benzene	Meta-xylene	Para-xylene	Ortho-xylene	n-Nonane
Chemical formula	$C_6H_5C_2H_5$	$C_6H_4(CH_3)_2$	$C_6H_4(CH_3)_2$	$C_6H_4(CH_3)_2$	C_9H_{20}
Molecular weight	106.16	106.16	106.16	106.16	128.25
Density (gms/ml $\frac{20°}{4°}$)	0.8669	0.86417	0.86105	0.8802	0.7176
Melting point (°C)	-93.9	-53.6	+13.2	-29	-53.7
Boiling point (°C)	136.15	139.104	138.351	144.41	150.798
Specific heat (pcu/lb-°C) at 100°C	0.518	0.455	0.462	0.465	0.568
Heat of vaporization (pcu/lb)	145.7	147.6	146.1	149.1	124
Vapor pressure at 100°C (mm Hg)	256	240	232	198	165
Relative volatility between components*	1.07	1.035	1.17	1.20	

*(See Table XIII for G.L.C. relative volatilities.)

Table XIII

Operating data and packing characteristics for an industrial G.L.C. separation

Column temperature	100°C
Stationary solvent phase	Polyethylene glycol with a molecular weight of approximately 400 (P.E.G. 400)
Mobile phase	Hydrogen gas

Solutes and their partition coefficients (modified by definition).

Solute	B.P. (°C)	k	Relative volatilities
n-nonane	150.8*	4.05	
			4.56
ethylbenzene	136.2*	18.5	
			1.168
m-, p-xylene	139.1-138.4	21.6	
			1.294
o-xylene	144.4	28.0	

Column packing (assuming a 1 foot length of column of 1 ft^2 cross-sectional area.)

Material	Crushed firebrick (C-22 Insulation Brick)
Size range	20 to 40 mesh (U.S. sieve series)
Average particle size	0.0175 in.
Weight of solid support	24.7 lbs
True density of support	131 lbs/ft^3
True volume of support	0.19 ft^3
Weight of solvent (40/100)	9.9 lbs
Density of solvent at 100°C (estimated)	70 lbs/ft^3
True volume of solvent	0.14 ft^3
Mobile-phase volume (by difference)	0.67 ft^3

*Interpolated data.

Pressure Drop. The pressure drop of the mobile phase as it passes through the packed column may be calculated from the expression of Keulmans,[5]

$$p_i^2 = p_o^2 + \frac{2 V_o L p_o \mu}{\alpha K g_c}, \qquad (40)$$

where p_i and p_o are inlet and outlet pressures of the column, V_o is the superficial velocity of the mobile phase, L is the column length, μ is the mobile-phase viscosity, α is the void-volume fraction, K is the permeability coefficient, and g_c is the gravitational dimensional constant. Keulmans reports the permeability coefficients for this material.[5]

Operating Pressures. The theoretical model assumes a uniform velocity along the length of the column. Short columns allow low ratios of inlet to outlet pressures with low inlet pressures and have a relatively small velocity variation along the column length. As the column length is increased, the pressure drop increases for a desired flow rate, and it is necessary to raise the absolute value of the column inlet pressure to maintain the same ratio of inlet to outlet pressure and the same velocity gradient. This ratio was set at approximately 2 in this design.

Mobile-Phase Selection. The pressure drop through the column is related to the velocity of the mobile phase by the viscosity term in the numerator of Eq. (40). Because of the small particle size, the pressure drop is a major consideration. In the design of the G.L.C. unit, hydrogen gas was chosen because of its low viscosity and ready availability at most refineries.

Solute Feed Rate. The G.L.C. column operates as a batch-type process in which a certain amount of material is charged to the column and is processed for a period of time before another amount is charged. The feed rate to the column is determined by the partition coefficients, the mobile-phase interstitial velocity and the relative volatilities of the solutes. The quantity of feed per charge is dependent on the amount of stationary solvent phase per unit column area, the column cross-sectional area, and for a specified purity of product, the relative volatility of the components that are most difficult to separate.

Column Length. The resolution between ethylbenzene and m-, p-xylene is the most difficult separation to be accomplished by the G.L.C. column. The relative volatibility of these two components is 1.168. From the work of Glueckauf[10] we can determine the number of theoretical chromatographic plates required to effect a separation that will give no greater than 0.1% impurity in either solute. The required number of plates is approximately 1500. In the body of this work, we saw that the s number of a column is, by definition, twice the number of theoretical plates (where $s > 100$). For the desired separation between the ethylbenzene and the m-, p-xylene peaks, the column should have an s value of approximately 3000.

In the theoretical model, we assumed that the column length for a desired s value is

$$L = s \left(\frac{\alpha D_m}{V_o} + \frac{d_p}{Pe} \right) . \tag{41}$$

Because the molecular diffusivity is quite small when compared with the superficial velocity, the first term in the brackets of Eq. (41) is usually negligible. The Peclet number (as calculated from the eddy diffusivity) is then the factor that would determine the column length for a desired separation (with a given packing material, i.e., average particle diameter).

In the experimental work done with the small G.L.C. column, the values of the Peclet number varied from 0.05 to 0.15. This variation was not predicted by theory. The Peclet number was dependent on the interstitial velocity, the quantity of solute sample charged, and, to a slight extent, on the temperature of column operation.

An empirical expression was developed from the toluene data of the small G.L.C. column. The toluene data should give a fairly good description of the xylene performance because it is based on the velocity variation of the L/s values at 88°C (well below its normal boiling point) and the sample-size variation. The larger the variation of the L/s value over a given range of the velocity, the smaller is the partition coefficient. The xylenes and ethyl benzene have partition coefficients in the same order of magnitude as the toluene partition coefficient. The limited data on sample-size variation show that this variation seems to be independent of the solute.

The empirical expression is:

$$L = s\ (1.68 \times 10^{-2}\ V^{0.15} + 1.81\ \omega_o^{0.64} - 2.5 \times 10^{-2}) \quad (42)$$

where V = interstitial velocity (ft/min) and

$$\omega_o = \frac{\text{lb moles (solute)/ft}^2 \text{ column area}}{\text{lbs (solvent)/ft}^3 \text{ of column as packed}} .$$

The units of ω_o were selected to be generally applicable to combinations of solutes and solvents in columns of various diameters with various solvent-volume fractions.

Equation (42) is based upon the data for a single solute charge. It is assumed that each solute will act independently of the others when a mixture of solutes is charged to the column.

Equation (42) shows that the L/s value for any one solute is significantly influenced by the quantity of solute charged and is influenced to a much lesser degree by this mobile-phase velocity. The minimum values of V and ω_o for toluene were 14.3 ft/min and $2.5 \times 10^{-4}\ \frac{\text{lb moles ft}}{\text{lb}}$. Below these values both exponents tend toward zero. No data were taken to determine the upper limits of applicability of Eq. (42). As the value of V increases, there should be no significant change in the exponent of the first term of Eq. (42) as long as the ratio of inlet and outlet pressure is kept low. As the sample size is increased, the solute peak will probably become saturated (flat-topped). Saturation will increase the exponent of the ω_o term.

The column length is determined approximately by application of Eq. (41). The value of the Peclet number used is 0.0425 (based on the extrapolation of the toluene data at 88°C out to a Reynolds number of 3.8 (V_o = 40 ft/min). Thus we have

$$L = 3000\ \left(\frac{0.67 \times 3.3 \times 10^{-3}\ \text{ft}^2/\text{min}}{40\ \text{ft/min}} + \frac{.0175\ \text{in.}}{12\ \text{in/ft} \times 0.0425}\right)$$

$$= 3000\ (5.53 \times 10^{-5} + 3.43 \times 10^{-2})\ \text{ft}$$

$$= 103\ \text{ft.} \cong 100\ \text{ft.}$$

The molecular diffusivity used for the calculation is for xylenes and hydrogen at approximately 225 psia and 100°C. The superficial velocity

of 40 ft/min was chosen to be a compromise between a low velocity having a low pressure drop with a long elution time and a high velocity having a high pressure drop and a short elution time.

Individual Solute L/s Values. As noted above, the data on the small G.L.C. column showed considerable variation of the L/s value with size of sample. The arbitrary size of feed charge chosen was 1 mole of feed per ft^2 of solvent cross section. For a column with 1-ft^2 cross-sectional area, the feed charge would be 0.14 mole (because the solvent cross-sectional area is 0.14 ft^2). Equation (42) may be used to compute the L/s values of the different components of the feed to determine the effective s number for each component. Table XIV shows the results of these calculations.

The Predicted Elution Diagram. The s value for each solute (from Table XIV) and the partition coefficients (from Table XIII) provide sufficient data for prediction of the column elution diagram by the use of the theoretical expressions of Appendix II.

Peak Heights. Relative peak heights are calculated by ratios derived from Eq. (15):

$$\frac{C_1}{C_2} = \frac{(\omega_o)_1 \; (\alpha + k)_2 \; \sqrt{s_1}}{(\omega_o)_2 \; (\alpha + k)_1 \sqrt{s_2}} \quad . \tag{43}$$

For the aromatic solutes, the meta-, para-xylene peak was assumed to be the reference peak. The ethylbenzene peak height is 0.35 times that of the reference and the o-xylene peak 0.17 times the reference peak height. The paraffin peak is approximately 1.65 times as high as the reference peak.

Time Base. If we assume that the solute peaks will be symmetrical, then the peak maximum will occur when the value of $s\,\eta \cong 1$. With the average superficial velocity set at 40 ft/min, the times of the peak maximum can be calculated and the elution diagram drawn. Figure 29 shows the elution diagram for the aromatic portion of the feul charge at the outlet of the

Table XIV

Effective L/s values for separation of solutes in an aromatic fraction using Eq. (42).[a]

	Mole fraction in feed	Moles charged per ft^2 column area	ω_o $\left(\frac{\text{Moles solute}/ft^2}{\text{lbs solvent}/ft^3}\right)$	L/s (ft)	s
Feed	1.00	0.14	14.3×10^{-3}	(0.1271)	(785)
Ethyl benzene	0.12	0.0168	1.72×10^{-3}	0.0378	2650
m-xylene	0.45	0.0630	9.2×10^{-3}	0.0966	1034
p-xylene	0.20	0.0280			
o-xylene	0.08	0.0112	1.13×10^{-3}	0.0296	3380
paraffin (n-nonane)	≈ 0.15	0.0210	2.12×10^{-3}	0.0423	2360

[a] Interstitial velocity, V = 60 ft/min, (V_o = 40 ft/min, α = 0.67).
Gross solute charge ≅ 0.14 mole/ft^2 column area.
Solvent density ≅ 9.9 lbs/ft^3 bed as packed.

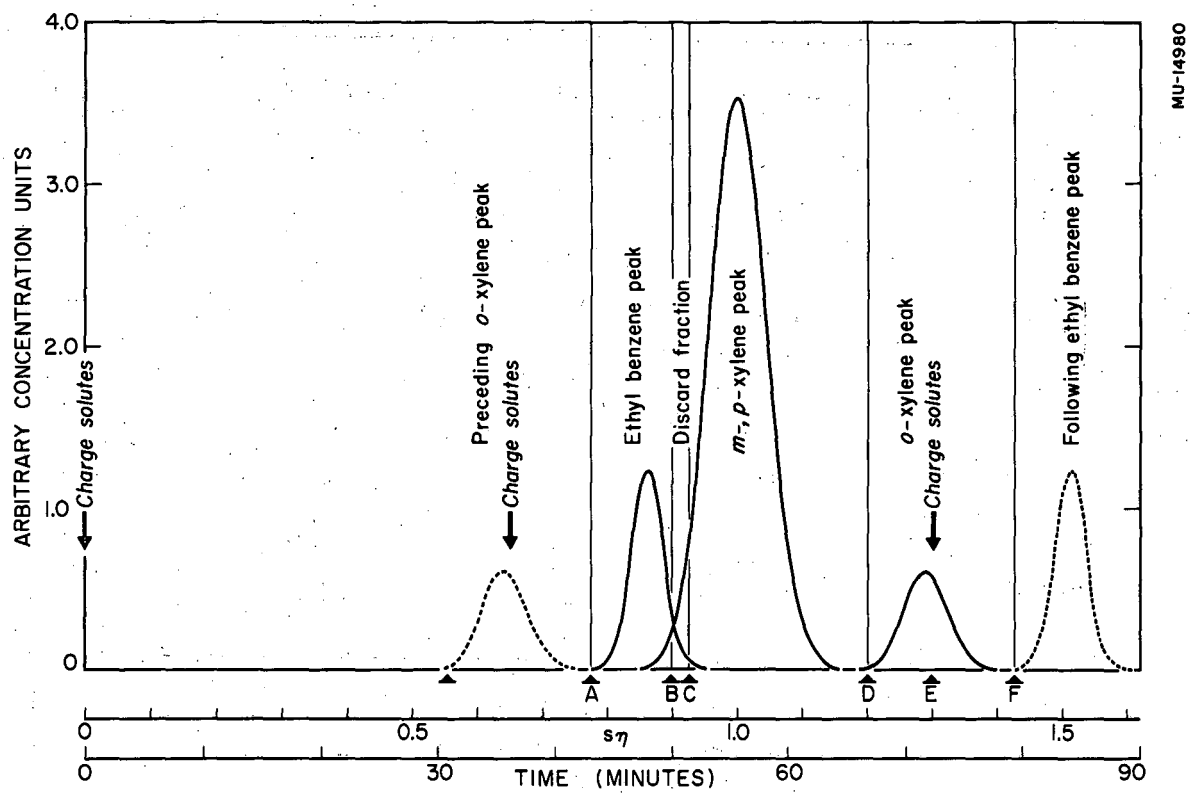

Fig. 29. G.L.C.-column elution cycle (at the exit of aromatic section B-4).

column (L = 100 ft). The paraffins are not shown on this figure because they will be removed at the point L = 10 ft. The abscissa is shown in both the s η units for the m-, p-xylene peak and in minutes for the specified mobile-phase velocity.

The Operating Cycle. The normal operating cycle of this G.L.C. unit is shown in Table XV where the zero time is arbitrarily taken at a time of charging the column. Study of Table XV shows that there will be more than one charge in the column at one time. The frequency of charging is determined by the time required to elute the aromatic components of any charge from the column.

Paraffin Separation. Because of the small partition coefficient (and the resulting high relative volatility) of the paraffin fraction, a short initial column section of 10 ft length is used for resolution of the paraffins from the aromatics. A by-pass is provided to supply the mobile phase to the major column sections during this resolution period. The final time for the paraffin fraction is predicted to be approximately 1.35 minutes after charging. The initial time of emergence of both the ethylbenzene and the m-, p-xylene peaks is at 3.85 minutes. Because of these large time differences, the paraffins will be sharply separated from the aromatics.

Column Diameter. The feed rate to the column was arbitrarily set at 0.14 moles/ft^2 column. This is an over-all high loading of the column, but if each solute is treated separately, only the m-, p-xylene fraction has a high specific loading. The charging ratio of the specific components are shown in Table XIV. From the time-base data of the elution diagram, the span of the aromatic elution is about 36 minutes. There will be about 1.66 charges/hour. This is equivalent to 25 lb/hr for each square foot of column. The total area requirement for the processing of 400 lbs/hr is then 16 ft^2. This area is realized by a column approximately 4.5 ft in diameter.

Table XV

Operating cycle of G.L.C. column as shown in Fig. 29.

(Times are based on a superficial velocity of 40 ft/min. Equipment designations refer to Fig. 30.)

Time (min)	s η[a]	Event
0	0	Solutes charged - Flow of mobile phase of first column section (B-1) goes to paraffin adsorber (F-1).
3	0.054	Flow of first-column section (B-1) shifted to second column section (B-2). Mobile phase by-pass closes.
36.2	0.65	Solutes charged, first-column section (B-1) flow shifted to paraffin adsorber (F-1), and by-pass is on.
39.2	0.705	Flow of first-column section (B-1) returned to second-column section (B-2). Mobile-phase by-pass is off.
43	0.775	Ethylbenzene appears at column exit, effluent is shifted to ethylbenzene adsorber (F-2) (Point A, Fig. 29).
50	0.90	Minimum between ethylbenzene and m-, p-xylene peaks. Flow shifts to discard channel. (Point B).
51.5	0.925	Effluent flow shifted to m-, p-xylene adsorber (F-3) (Point C).
67	1.20	Effluent flow shifted to o-xylene adsorber (F-4) (Point D).
72.4	1.30	Solutes charged. First column section (B-1) flow shifted to paraffin adsorber (F-1). By-pass is on. (Point E.).
75.4	1.35	Flow of first column section (B-1) returned to second column section (B-2). Flow through by-pass is off.
79.2	1.425	Column effluent switched to ethylbenzene adsorber (F-2) (Point F).

[a] s η values are for m-, p-xylene peak.

Plant and Equipment Design

General Plant Layout. The schematic of this G.L.C. plant is shown in Fig. 30. The plant consists of four basic systems; the column, the solute-recovery system, the mobile-phase recycle system, and the timing-unit system. The inputs of the plant are the feed stream, process steam, an inert purge gas, make-up hydrogen and utilities. The outputs of the plant are the product streams, discard from the recycle-gas cleaner (F-5), and a small amount of waste hydrogen.

Equipment Detail. The design detail of the plant's equipment is, at best, only approximate for this problem. Certain comments on the assumptions used in sizing the equipment and estimating the economic factors must be noted for clarity and are given below. The specifications of the individual units along with estimated costs are given in Table XVI.

The G.L.C. Column. Because of the low structural strength of the fire brick packing, the column design incorporates frequent mesh supports for the packing. These supports are spaced about every 4 feet, and each carries more than a ton of packing. Normal materials of construction and techniques are employed. Special emphasis on the tightness of the system is necessary because of the hydrogen mobile phase.

Interstage Compressors. For these units (C-2 and 3), two-stage, axial-flow or centrifugal compressors are adequate. The compression ratio is approximately 2:1. Interstage cooling is advisable.

Timing Unit. The control of the process timing is incorporated in the master timing unit (TU-1). This unit uses the information from the sensing unit (S.U.) on the column effluent. A differentiation circuit with time comparison operates the feed, paraffin by-pass, and solute selector valves through the auxiliary timing units (TU-2, TU-3). An elution program is built into the master timing unit (TU-1). The control of the feeding and paraffin-stripping function is delegated to the auxiliary timing units.

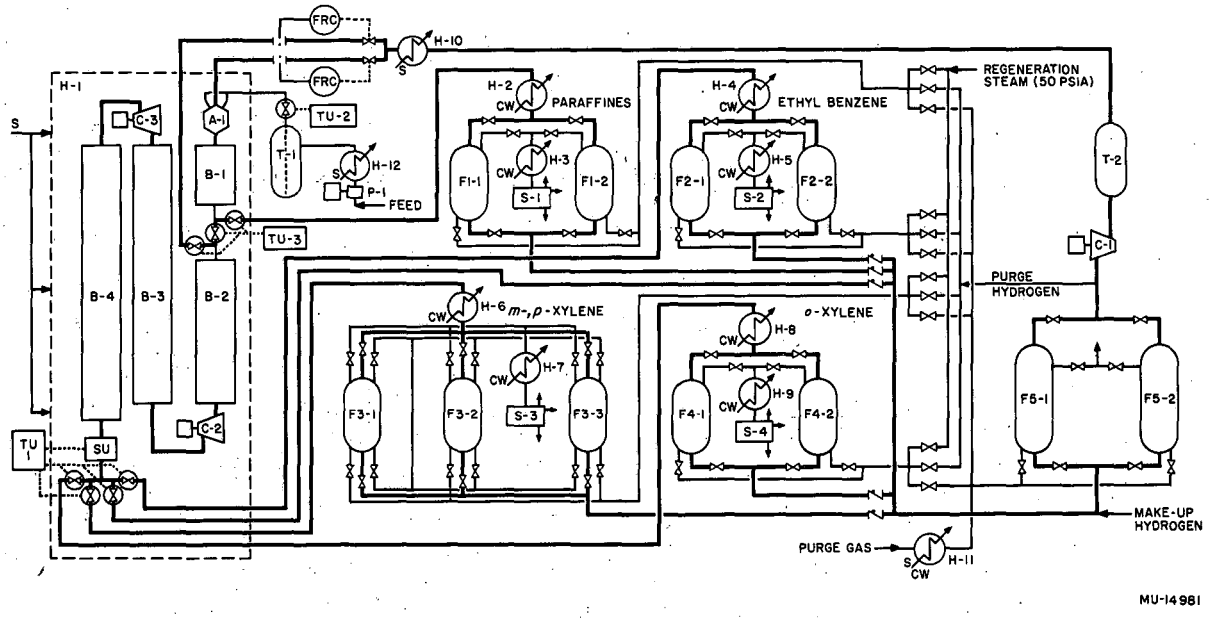

Fig. 30. G.L.C. processing-plant flow design.

Adsorption Units. The solutes are adsorbed from the hydrogen mobile phase by fixed beds of activated charcoal. Specific adsorption data for the solutes being processed were not available so that data available for benzene was used. The adsorption units for paraffin, ethylbenzene, and o-xylene are of an identical design based on an adsorptive capacity equal to, or greater than, that assumed to be required for 24-hour adsorption operation. Each of these systems has two adsorbers preceded by a gas cooler. Valves are located in the system for isolation, steam regeneration, and purging of the adsorbers. The regeneration time is 12 hours for these units.

The m-, p-xylene adsorbers handle the major amount of solute. This system uses three adsorbers in all with two in series operation and the third in regeneration. Each unit serves as a secondary adsorber for 12 hours and a primary adsorber for the succeeding 12 hours. It is then regenerated during a 6-hr period, allowed to cool, and purged before being returned to service.

The adsorption system for each solute is fitted with a regeneration condenser and a phase separator to recover the product. After regeneration and cooling with purge gas, the units are purged with hydrogen before being put back on stream.

Recycle Gas Cleaner. The circulating hydrogen stream passes through a cleaner prior to recompression. These cleaning units were designed for purification and dehydration of the hydrogen stream with charcoal and silica gel, respectively. The on-stream period of operation of each of these units should be 24 hours. The units are regenerated by passage of a hot inert gas through the unit. Regeneration should take approximately 12 hours.

Recycle Gas Compressor. The recycle gas cleaner also serves as a buffer vessel for the recycle gas compressor. This unit receives the hydrogen at approximately 100 psia and compresses it to 325 psia, using 3 stages of compression and interstage cooling. The high-pressure gas is fed to a high-pressure receiver (T-2) which absorbs the fluctuations from the compressor. In the calculation of the power requirements of the compressors, an over-all driver-compressor efficiency of 50% was assumed.

Column Feed Unit. The feed stream received from the refinery is assumed to pass through intermediate storage to the positive-displacement feed pump (P-1). This pump delivers the feed to the heater (H-12), where it is heated well above the normal boiling point and hence to the high-pressure receiver (T-1). Either superheated steam or electrical heaters may be used in feed heater (H-12) to maintain the desired feed temperature, which is about 350°F. The feed pressure of 400 psia (or higher as necessary) injects the feed into the mobile phase through suitable nozzles when the feed valve is opened. The combination of pressure and temperature gives rapid vaporization of the fuel. Mobile-phase flow to the column is closely regulated for good control of elution times.

Heat Exchangers. Standard heaters, coolers, and condensers may be used for this plant. The two exceptions are the feed heater (H-12) and the column heater (H-1). The latter is a large tank approximately 11 ft in diameter that is fed with steam condensing at atmospheric pressure. Approximate design data for the equipment of this plant are shown in Table XVI.

Plant Economics.

A preliminary cost estimate of the G.L.C. plant has been prepared using the method of Chilton.[35] In his paper he gives various figures for the installed cost of equipment based on the Engineering News Record (E.N.R.) index of 400. Also, a method of estimating other construction and engineering costs is discussed. Means of estimating the production cost of the product and miscellaneous capital requirements are given. Finally, an estimation of the upgrading of the feed stream value has been prepared from current price data available on these materials.

Installed Process Equipment Costs. The estimates of the installed cost of the various plant components are shown in Table XVI. Costs are based on an E.N.R. index of 400. Basic costs are from Chilton's graphs. Various multiplying factors (cost factors) have been estimated where the basic unit

Table XVI

EQUIPMENT DATA AND ESTIMATED COSTS

Feed injector and G.L.C. columns (E.N.R. index = 400)

Code	Description	p_i (psia)	p_o (psia)	Diam. (ft)	Length (ft)	Volume (ft^3)	Basic cost ($1000)	Cost Factor	Final cost ($1000)	Remarks
A-1	Feed injection unit	(ℓ) 350 (g) 300	300 300	3	4.5	~28	1.2	4	4.8	High operating pressure and special injector fittings.
B-1	Paraffin stripper column	300	250	4.5	10	160	2.5	2	9.8	
B-2	Aromatic column 1	250	140	4.5	23	368	5.75	1.5	19.67	Packing cost equals $30/ft^3 in place. Tower requires special baffles for packing. Final cost includes installed packing.
B-3	Aromatic column 2	300	140	4.5	33	528	8.25	1.5	28.24	
B-4	Aromatic column 3	300	133	4.5	34	544	8.5	1.5	29.10	

(continued)

Table XVI (continued)

Compressors											
Code	Description	p_i (psia)	p_o (psia)	t_i (°C)	t_o (°C)	Mass flow (lbs/hr)	Inlet volume (ft^3/min)	Stages	Driver rating (Hp)	Cost ($1000)	Remarks
C-1	Primary gas compressor	100	325	22	73	2535	1202	3	1200	80	All are centrifugal compressors, with overall compressor and driver efficiency - assumed to be 50%.
C-2	First inter-stage compressor 1	140	300	100	151	2681	1007	2	885	65	
C-3	Second inter-stage compressor 2	140	300	100	151	2681	1007	2	885	65	

(continued)

Table XVI (continued)

Adsorbers

Code	Description	p_i (psia)	p_o (psia)	Diam. (ft)	Length (ft)	Vessel volume (gal)	Charcoal weight (lbs)	Bed cost ($1000)	Vessel cost ($1000)	Total cost ($1000)	Remarks
F 1 1 & 2	Paraffin adsorbers (2)	125	120	4.5	10.5	900	3600	3.60	2.7	12.6	Total cost includes the adsorbent bed (at $1/lb) installed for all units.
F 2 1 & 2	Ethylbenzene adsorbers (2)	125	120	4.5	10.5	900	3600	3.6	2.7	12.6	
F 3 1,2,&3	m-, p-xylene adsorbers (3)	125	115	6.0	12.0	1875	7500	7.5	4.0	34.5	
F 4 1 & 2	o-xylene adsorbers (2)	125	120	4.5	10.5	900	3600	3.6	2.7	12.6	
F 5 1 & 2	Recycle-gas purifiers (2)	110	105	3.5	25	1800	1200/1200	2.4	3.8	12.4	Charcoal bed / Silica-gel bed

(continued)

Table XVI (continued)

Exchangers

Code	Description	Hot-side inlet temp. (°C)	Hot-side outlet temp. (°C)	Cold-side inlet temp. (°C)	Cold-side outlet temp. (°C)	Hot-side stream (lbs/hr)	Cold-side stream	U Δ t $\frac{PCU}{hr\text{-}ft^2}$	Transfer Area (ft^2)	Cost ($1000)	Remarks
H-2	Preadsorber cooler, paraffins	100	30	20	31	254	water, 8.8 gpm	222	218	2.0	All units are steel shell and tube exchangers.
H-3	Paraffin recovery condenser	138	38	20	31	480	water, 47 gpm	2220	106	1.25	Recovery is at a rate twice as great as the rate of adsorption.
H-4	Preadsorber cooler, ethylbenzene	100	30	20	31	498	water, 20 gpm	222	495	3.2	
H-5	Ethylbenzene recovery condenser	138	38	20	31	417	water, 38 gpm	2220	95	1.2	Same as noted for H-3.
H-6	Preadsorber cooler, m-, p-xylenes	100	30	20	31	1242	water, 45 gpm	222	1110	5.0	
H-7	m-, p-xylenes recovery condenser	138	38	20	31	2024	water, 182 gpm	2220	450	3.0	Same as noted for H-3.
H-8	Preadsorber cooler, o-xylene	100	30	20	31	842	water 38 gpm	222	883	4.3	

(continued)

Table XVI (continued)

Exchangers

Code	Description	Hot-side inlet temp. (°C)	Hot-side outlet temp. (°C)	Cold-side inlet temp. (°C)	Cold-side outlet temp. (°C)	Hot-side stream (lbs/hr)	Cold-side stream	$U \Delta t$ PCU/hr-ft^2	Transfer Area (ft^2)	Cost ($1000)	Remarks
H-9	o-xylene-recovery condenser	138	38	20	31	256	Water, 23 gpm	2220	57	0.9	Same as noted for H-3.
H-10	Mobile-gas-phase heater	138	138 (50 psia)	72	110	Steam 625	Hydrogen 2535 lbs/hr.	222	1450	5.5	
H-11	Purge-gas heater	205	182 (150 psia)	25	160	Steam 39	inert gas 600 lbs per hr.	222	91	1.2	For reactivation of recycle gas purifiers (F-5).
H-12	Feed heater	370	370	20	350	42 kw	feed, 400 lbs per hr.	1111	71.4	1.05	Use electrical heaters in fluid stream.

Exchangers

Code	Description	Diam. (ft)	Length (ft)	Volume (ft^3)	Pressure (psia)	Heat Source	Steam consumption (lbs/hr)	Basic cost ($1000)	Cost ($1000)	Remarks
H-1	Column heater	11	40	3800	14.7	Condensing steam	100	5.0	10.0	$U \Delta t \cong 22$ PCU/hr-ft^2. Outer side insulated. Assumed cost factor is 2.

(continued)

Table XVI (continued)

Feed Pump

Code	Description	p_i (psia)	p_o (psia)	Fluid temp. (°C)	Mass rate (lbs/hr)	Volume rate (gpm)	Driver power (Hp)	Over-all efficiency %	Cost ($1000)	Remarks
P-1	Feed pump	14.7	350	25	400	≈ 1	0.35	40	0.8	Price is based upon a 1-Hp unit.

High-Pressure Vessels

Code	Description	Operating pressure (psia)	Shape	Length (ft)	Diam. (ft)	Volume (gal)	Basic cost ($1000)	Cost factor	Cost ($1000)	Remarks
T-1	Feed reservoir	350	Cylinder with pressure ends	5	3	250	1.3	2.0	2.6	
T-2	High-pressure buffer tanks	325	Cylinder with pressure ends	10.5	3	560	2.0	2.0	4.0	

(continued)

Table XVI (continued)

Continuous Decanters

Code	Description	Pressure (psia)	Temp. (°C)	Maximum Liquid input lbs/hr	Maximum Liquid input gal/min	Diameter (ft)	Height (ft)	Volume (gal)	Cost ($1000)	Remarks
S-1	Decanter, paraffin product	14.7	38	240	0.5	2	4.5	100	0.5	
S-2	Decanter, ethylbenzene product	14.7	38	208.3	0.45	2	4.5	100	0.5	Because of the special decanter fittings, a cost factor of twice the basic tank cost is used.
S-3	Decanter, m-, p-xylene product	14.7	38	1012	2.1	3	7.5	400	1.10	
S-4	Decanter, o-xylene product	14.7	38	128	~0.1	2	4.5	100	0.5	

(continued)

Table XVI (continued)

Timing Units			
Code	Description	Remarks	Cost
TU-1	Main-system timer	Operates in conjunction with mobile-phase sensing unit and solute-fraction valves.	The cost of these units and other plant instruments are lumped together in an instrumentation cost in Table XVII.
TU-2	Feed auxiliary control	Controlled by TU-1 and opens the main feed valve at regular intervals.	
TU-3	Elution by-pass control	Controlled by TU-2; modifies the flow path of the first column section (B-1) for 3 minutes after each charging.	

would require modification. The factors are used to compute the final cost of each item. The summation of these costs at the current E.N.R. index, the installed process-equipment cost, is given in Table XVII.

Total Physical Cost. Chilton bases the costs of process piping, instrumentation, manufacturing buildings, auxiliary facilities, and outside lines each as a fraction of the installed process-equipment cost. The percentages are determined by the nature and complexity of the plant and process and the amount of auxiliary equipment that is required. These percentages were estimated within the ranges specified by Chilton. The total of these costs and the installed process-equipment costs is the total physical cost. These costs are summarized in Table XVII.

Total Plant Costs. The cost of engineering, construction, contingencies, and the relative size factor of the plant are estimated as percentages of the total physical cost. The summation of these costs along with the total physical cost gives the total plant cost. This summation is also shown in Table XVII.

Production Costs. Table XVIII gives the cost of production per pound of combined product. The factors used in this estimate are also outlined by Chilton. The use of activated charcoal is assumed to be 5 lbs per ton of total product processed. The stationary-solvent useage is estimated to be 1% of the total solvent requirement (17,000 lbs) for every 200 solute charges. The solid-support useage is considered to be negligible compared to its total quantity (43,000 lbs).

Product Value. The estimate of the final-product value is based on current prices of these materials. Table XIX summarizes the product upgrading. The applicability of these figures depends on the demand for these products at the high purities obtainable with a G.L.C. column.

Table XVII

Plant cost summary (dollars)
incorporating the current ENR index (735)

Installed process equipment costs (I.P.E.C.)		
Feed unit and column	168,300	
Compressors	386,000	
Adsorbers	29,200	
Exchangers	52,600	
Column heater	18,400	
Feed pump	1,470	
Pressure vessels	12,130	
Decanters	4,780	
Total I.P.E.C.	672,880	
Additional facility costs (A.F.C.)		
Process piping (50% I.P.E.C.)	336,400	
Instrumentation (15% I.P.E.C.)	100,900	
Buildings (10% I.P.E.C.)	67,300	
Auxiliary facilities (5% I.P.E.C.)	33,600	
Outside lines (5% I.P.E.C.)	33,600	
Total A.F.C.	571,800	
Total physical cost (T.P.C.)		1,244,680
Construction expenses, etc.		
Engineering and construction (35% T.P.C.)	435,600	
Contingencies (30% T.P.C.)	373,400	
Size factor (20% T.P.C.)	248,900	
Total construction expenses	1,057,900	1,057,900
Total plant cost.		2,302,580

Table XVIII

Estimated cost of production per pound of final products

Item	Unit cost (dollars)	Cost/lb product (dollars)
Raw material feed	0.040/lb	0.0408
Activated-charcoal replacement	0.30/lb	0.0008
Column-solvent replacement	0.235/lb	0.0012
Operating labor (2 men at 2.50/hr)	5.00/hr	0.0127
Supplies (10% off labor cost)	0.50/hr	0.0013
Utilities		
Cooling water	0.06/1000 gal	0.0017
Steam	0.75/1000 lbs	0.0038
Power	0.01/kw-hr	0.0575
Annual maintenance labor (5% of total physical cost)	62,234/yr	0.0202
Annual maintenance materials (5% of total physical cost)	62,234/yr	0.0202
Laboratory expense (20% of operating labor)	1.00/hr	0.0025
Insurance, taxes, and depreciation (Annual, 10% of total physical cost)	124,500/yr	0.0402
Overhead (75% of labor cost)	3.75/hr	0.0096
Process improvement research (3% of sales)		0.0099
Total production cost per lb products.		0.2224

Table XIX

Estimated product values and income
based on 400 lbs of feed processed per hour

	Ethyl-benzene	m-, p-xylenes	Ortho-xylene	Paraffins and naphthenes	Discard stream
Quantity of solute per lb of feed (lb)	0.12	0.65	0.08	0.15	--
Yield of each stream per lb of feed (lb)	0.1208	0.6303	0.08	0.15	0.019
Estimated product purity (%)	95	99.8	100	100 (non aromatic)	76.5 ethyl benzene
Estimated product value per lb feed (dollars)	0.25	0.25	1.50	0.10	0.05
Gross product value per lb of feed (dollars)	0.0302	0.1576	0.1200	0.0150	---

Total gross product value -----0.3228 per lb of feed-----

or 0.3294 per lb of product produced.

Annual production = 3,090,528 lbs per year (at 0.9 time factor of operations)

Monthly production = 257,544 lbs per average month

Economic Summary. A summary of the cost estimate is given in Table XX. On the basis of 90% time in operation, the plant shows a rate of return on the capital investment of approximately 13%. This figure is low. Further considerations of a G.L.C. unit for industrial operation requires either processing of a product with higher unit value or modification of the basic process to give greater through put or lower operating cost. Reduction of the compressor requirements would markedly affect the cost of plant and operations. An increase of the production rate would increase the rate of return on the investment. The most promising means of obtaining a favorable rate of return would be from the processing of materials whose values are markedly increased by the high purities obtainable with G.L.C. equipment.

A further application of G.L.C. that might be considered is its use for paraffin-aromatic separations where the relative volatility is large. This operation could use many columns in parallel and could use more rapid methods of recovery of the solutes than adsorption. Short column lengths and rapid cycling could effectively separate a much larger amount of material than is the case in the problem studied here.

Table XX

Capital investment requirements of the G.L.C. plant and estimated payout period

Total plant cost (From Table XVII)	$2,302,580
Finished product inventory (One month's production cost)	$ 57,278
Accounts receivable (One month's production at selling price)	$ 84,835
Operating expenses (One month's production cost)	$ 57,278
Total capital requirement	$2,501,971
Gross profit per pound of product	$0.1070
Annual gross profit	$330,686
Gross rate of return on capital	13.3%
Payout period	7.5 years

NOMENCLATURE

Symbol	Definition	Units
	Arabic letters	
a	Column or tube diameter	ft
c	Solute concentration in mobile phase	lb moles/ft^3
d_f	Solvent film thickness, Eq. (21), p. 87	ft
d_p	Arithmetic mean particle size	ft
k	Partition coefficient equals n/c	--
n	Solute concentration in stationary phase	lb moles/ft^3 bed as packed
p	Pressure	psi
Δp	Pressure differential across the column	psi
t	Time	min
t_p	Time of emergence of solute maximum concentration	min
t_{pa}	Time of emergence of air maximum concentration	min
t_w	Time-base width of solute or air peak	min
t_5	Time-base width of solute or air peak at 1/2-peak height	min
x	Solute mole-fraction in stationary phase	--
y	Solute mole-fraction in mobile phase	--
z	Distance into bed from column inlet	ft
A	Cross-sectional area of bed	ft^2
C	Solute mobile-phase concentration at L	lb moles/ft^3
D	Effective solute longitudinal diffusivity	ft^2/min

Symbol	Definition	Units
D_L	Solute diffusivity in stationary phase	ft^2/min
D_M	Solute diffusivity in mobile phase	ft^2/min
D_T	Taylor diffusivity, Eq. (23)	ft^2/min
E	Solute eddy diffusivity in the mobile phase	ft^2/min
H_p	Solute peak height	mv
$\overline{\Delta H_s}^E$	Excess partial heat of solution	Btu/lb mole
H_v	Latent heat of vaporization	Btu/lb mole
L	Length of bed	ft
M	Slope of thermal-conductivity-cell calibration curve	mole fraction/mv
N	Solvent molar volume in packing	lb moles/ft^3 of bed as packed
p^o	Solute partial pressure	psi
Q	Mobile phase flow rate	ft^3/min
R	Gas constant	$\frac{ft^3 - psi}{lb\ mole\ ^oK}$
T	Temperature	^oK
V	Interstitial velocity	ft/min
V_o	Superficial velocity	ft/min

Greek letters

α	Void volume fraction	--
α_L	Solvent volume fraction	--
γ	$(1 + k/\alpha)$	--
δ (t)	Impulsive feed function	lb moles/min

Symbol	Definition	Units
λ	Activity coefficient	--
μ	Viscosity of mobile phase	lbs/ft-min
ρ	Density of mobile phase	lbs/ft^3
τ	Modified time, equals t/γ	min
ω	Solute feed charge	lb-moles

Dimensionless groups

s	Column-flow parameter	VL/D
$s\eta$	Modified time parameter	$\frac{t\,V_o}{(\alpha+k)L}$
Pe	Peclet number	Vd_p/E
Re	Modified Reynolds number	$\frac{V_o d_p \rho}{\mu}$
η	Column time parameter	$\frac{t}{\gamma}\frac{D}{L^2}$

Subscripts and superscripts

calc	Calculated values
col	Quantity measured at column conditions of temperature and pressure
f	Final conditions or point
i	Initial conditions or point
m	Midpoint condition
max	Maximum condition
o	Outlet or exit condition

Symbol	Definition	Units
A	Acetone	
B	Benzene	
T	Toluene	
'	Prime symbols indicate values predicted by the chromatographic theory, i.e. t'_p, s', etc.	

LIST OF TABLES

Table I. Features and common uses of gas-liquid partition-chromatography equipment 6

Table II. Properties of DC-550 -- C-22 firebrick packing. . . . 31

Table III. Solute, temperature, and flow-rate distribution of G.L.C. experimental runs 48

Table IV. Miscellaneous experimental data. 52

Table V. G.L.C. experimental data 56

Table VI. Summary of IBM 650 calculations from G.L.C. data . . 65

Table VII. Apparent heats of solution from G.L.C. measurements . 80

Table VIII. Comparison of G.L.C. column performance at two feed conditions. 86

Table IX. Computed values of the CL ordinate of Eq. (38) for various values of the s parameter 107

Table X. Thermal-conductivity-cell calibration data and calculated results 112

Table XI. Equilibrium experimental data 126

Table XII. Some physical properties of the aromatic feed . . . 134

Table XIII. Operating data and packing characteristics for an industrial G.L.C. separation. 135

Table XIV. Effective L/s values for separation of solutes in an aromatic fraction using Eq. (42). 140

Table XV. Operating cycles of G.L.C. column as shown in Fig. 29. 143

Table XVI. Equipment data and estimated costs. 148

Table XVII. Plant cost summary (dollars) incorporating the current ENR index (735) 157

Table XVIII. Estimated cost of production per pound of final product. 158

Table XIX. Estimated product values and income based on 400 lbs. of feed processed per hour 159

Table XX. Capital investment requirements of the G.L.C. plant and estimated payout period 161

LIST OF FIGURES

Fig. 1. Theoretical elution diagrams for low values of the s-parameter. 18

Fig. 2. Theoretical elution diagrams for high values of the s-parameter. 19

Fig. 3. Theoretical elution diagrams (normalized) for low values of the s-parameter 20

Fig. 4. Theoretical elution diagrams (normalized) for high values of the s-parameter 21

Fig. 5. Over-all G.L.C. equipment schematic diagram 25

Fig. 6. G.L.C. equipment arrangement 26

Fig. 7. Construction detail of G.L.C. column 27

Fig. 8. Sample-injection valve and upper column assembly . . . 28

Fig. 9. Internal thermocouple construction for G.L.C. column . . 29

Fig. 10. Sample-injection valve 33

Fig. 11. Thermal conductivity cell and controlled temperature box 36

Fig. 12. Internal construction of the T.C. cell. 37

Fig. 13. Thermal-conductivity cell schematic diagram 38

Fig. 14. Operational arrangement of sample-injection valve, expansion valve, and T.C. cell. (Fiberglass insulation removed.) 42

Fig. 15. Method of elution-peak characterization 49

Fig. 15a. Superimposed experimental and theoretical elution diagrams. 51

Fig. 16. Partition coefficients as a function of reciprocal column temperature 79

Fig. 17. Partition coefficients as a function of the Reynolds number. 81

Fig. 18. Superimposed elution diagrams from toluene sample-size variations. 83

Fig. 19. Data and results of toluene sample-size variations 84

Fig. 20. L/s values as a function of the Reynolds number 88

Fig. 21. Comparison of toluene L/s values as a function of the Reynolds number 89

Fig. 22. T.C.-cell circuit response to solute mobile-phase concentration 111

Fig. 23. Equipment arrangement for equilibrium determinations . . 115

Fig. 24. Exploded view of equilibrium vessel fitted with ampule. . 117

Fig. 25. Equilibrium vessel and pressure transducer assembled and mounted in rocker yoke 120

Fig. 26. Detail of assembled equilibrium apparatus immersed in the constant-temperature oil bath. 121

Fig. 27. Solute equilibrium vapor pressure as a function of liquid-phase concentration 123

Fig. 28. Mobile-phase concentration as a function of liquid-phase concentration 124

Fig. 29. G.L.C.-column elution cycle. 141

Fig. 30. G.L.C. processing-plant flow design 145

BIBLIOGRAPHY

1. M. Tswett, Ber. deut. botan. Ges. 24, 316, 384 (1906).

2. Kuhn, Winterstein, and Lederer, Hoppe-Seyler's Z. physiol. Chem. 197, 141 (1931).

3. A. Tiselius, Arkiv. Kemi, Mineral. Geol. 14B, No. 22, 5 pp. (1940); ibid. 16A, No. 18, 11 pp. (1943).

4. N. C. Turner, Nat. Petrol. News 35, R-234 (1943).

5. A. I. M. Keulmans, Gas Chromatography (Reinhold, New York, 1957).

6. A. J. P. Martin and R. L. M. Synge, Biochem. J. (London) 35, 1358 (1941).

7. A. T. James and A. J. P. Martin, Biochem. J. (London) 50, 679 (1952).

8. D. H. Desty, Vapor-Phase Chromatography (Butterworths, London, 1957).

9. J. J. Walthall, Fundamentals of Gas Chromatography, Technical Bulletin 57-4, 1957, Western Petroleum Refiner's Association, Tulsa, Oklahoma.

10. E. Glueckauf, Trans. Farad. Soc. 51, 34 (1955).

11. Porter, Deal, and Stross, J. Am. Chem. Soc. 78, 2999 (1956).

12. Van Deemter, Zuiderweg, and Klinkenberg, Chem. Eng. Sci. 5, 271 (1956).

13. J. N. Wilson, J. Am. Chem. Soc. 62, 1583 (1940).

14. D. DeVault, J. Am. Chem. Soc. 65, 532 (1943).

15. L. Lapidus and N. R. Amundson, J. Phys. Chem. 56, 984 (1952).

16. J. C. Giddings and H. Eyring, J. Phys. Chem. 59, 416 (1955).

17. H. C. Thomas, Ann. N. Y. Acad. Sci. 49, 161 (1948).

18. Kasten, Lapidus, and Amundson, J. Phys. Chem. 56, 683 (1952).

19. S. Goldstein, Proc. Roy. Soc. (London) A219, 151, 171 (1953).

20. N. K. Hister and T. Vermeulen, Chem. Eng. Progr. 48, 505 (1952).

21. C. R. Wilke and C. Y. Lee, Ind. Eng. Chem. 47, 1253 (1955).

22. A. Klinkenberg and F. Sjenitzer, Chem. Eng. Sci. 5, 258 (1956).

23. P. V. Danckwerts, Chem. Eng. Sci. 2, 1 (1953).

24. J. F. Wehner and R. H. Wilhelm, Chem. Eng. Sci. 6, 89 (1956).

25. E. M. Fredericks and F. R. Brooks, Anal. Chem. 28, 297 (1956).

26. Dimbat, Porter, and Stross, Anal. Chem. 28, 290 (1956).

27. V. M. Wolontis, A Complete Floating-Decimal Interpretive System for the IBM 650 Magnetic Drum Calculator, IBM Technical Newsletter 11, March 1956.

28. Pierotti, Deal, Derr, and Porter, J. Am. Chem. Soc. 78, 2989 (1956).

29. G. Taylor, Proc. Roy. Soc. (London) A219, 186 (1953); ibid. A225, 473 (1955).

30. R. Aris, Proc. Roy. Soc. (London) A235, 67 (1956).

31. H. Bateman, Tables of Integral Transforms, Bateman Manuscript Project, C. I. T., (McGraw-Hill, New York, 1954), Vol. I, p. 297, Eq. 19.

32. Tables of the Exponential Function, e^x, Ed. 2, (U. S. Government Printing Office, Washington, D. C. 1947).

33. Mathematical tables project, Table of Probability Functions, Vol. I, Ed. 2, (U. S. Government Printing Office, Washington, D. C. 1947).

34. E. R. Adlard, Evaluation of Polyglycols as Stationary Phase for Gas-Liquid Partition Chromatography, in Vapor-Phase Chromatography, D. H. Desty, Ed. (Butterworths, London, 1957). See also A. I. Keulmans, Gas Chromatography, (Reinhold, New York, 1957), p. 177.

35. Cecil H. Chilton, Chem. Eng. 56, 97 (June 1949).